Sheffield Hallam University

A Sheffield Hallam University thesis

Internet of Medical Things – Integrated, Ultrasound-based Respiration Monitoring System for Incubators

Tareq Abdulqader

A thesis submitted in partial fulfilment of the requirements of
Sheffield Hallam University
for the degree of Doctor of Philosophy

November 2020

Declaration

I hereby declare that:

1. I have not been enrolled for another award of the University, or other academic or professional organisation, whilst undertaking my research degree.

2. None of the material contained in the thesis has been used in any other submission for an academic award.

3. I am aware of and understand the University's policy on plagiarism and certify that this thesis is my own work. The use of all published or other sources of material consulted have been properly and fully acknowledged.

4. The work undertaken towards the thesis has been conducted in accordance with the SHU Principles of Integrity in Research and the SHU Research Ethics Policy.

5. The word count of the thesis is 34,624.

Name	Tareq Abdulqader BEng IEng MIET
Date	November 2020
Award	PhD
Faculty	ACES Faculty
Director of Studies	Professor Reza Saatchi

Signature: _TAREQ ABDULQADER_

Abstract

The study's aim was to develop a non-contact, ultrasound (US) based respiration rate and respiratory signal monitor suitable for babies in incubators. Respiration rate indicates average number of breaths per minute and is higher in young children than adults. It is an important indicator of health deterioration in critically ill patients. The current incubators do not have an integrated respiration monitor due to complexities in its adaptation. Monitoring respiratory signal assists in diagnosing respiration rated problems such as central Apnoea that can affect infants. US sensors are suitable for integration into incubators as US is a harmless and cost-effective technology.

US beam is focused on the chest or abdomen. Chest or abdomen movements, caused by respiration process, result in variations in their distance to the US transceiver located at a distance of about 0.5 m. These variations are recorded by measuring the time of flight from transmitting the signal and its reflection from the monitored surface. Measurement of this delay over a time interval enables a respiration signal to be produced from which respiration rate and pauses in breathing are determined.

To assess the accuracy of the developed device, a platform with a moving surface was devised. The magnitude and frequency of its surface movement were accurately controlled by its signal generator. The US sensor was mounted above this surface at a distance of 0.5 m. This US signal was wirelessly transmitted to a microprocessor board to digitise. The recorded signal that simulated a respiratory signal was subsequently stored and displayed on a computer or an LCD screen. The results showed that US could be used to measure respiration rate accurately. To cater for possible movement of the infant in the incubator, four US sensors were adapted. These monitored the movements from different angles. An algorithm to interpret the output from the four US sensors was devised and evaluated. The algorithm interpreted which US sensor best detected the chest movements.

An IoMT system was devised that incorporated NodeMcu to capture signals from the US sensor. The detected data were transmitted to the ThingSpeak channel and processed in real-time by ThingSpeak's add-on Matlab© feature. The data were processed on the cloud and then the results were displayed in real-time on a computer screen. The respiration rate and respiration signal could be observed remotely on portable devices e.g. mobile phones and tablets. These features allow caretakers to have access to the data at any time and be alerted to respiratory complications.

A method to interpret the recorded US signals to determine respiration patterns, e.g. intermittent pauses, were implemented by utilising Matlab© and ThingSpeak Server. The method successfully detected respiratory pauses by identifying lack of chest movements. The approach can be useful in diagnosing central apnoea. In central apnoea, respiratory pauses are accompanied by cessation of chest or abdominal movements. The devised system will require clinical trials and integration into an incubator by conforming to the medical devices directives. The study demonstrated the integration of IoMT-US for measuring respiration rate and respiratory signal. The US produced respiration rate readings compared well with the actual signal generator's settings of the platform that simulated chest movements.

Acknowledgement

Table of Contents

List of Figures

List of Tables

Equations

List of Abbreviations

AHB	-	Advanced High-Performance Bus
AOP	-	Apnoea of prematurity
ASDA	-	American Sleep Disorders Association
CCD	-	Charge - Coupled Device
CPAP	-	Continuous positive airway pressure
ECG	-	Electrocardiogram
EDR	-	Electrocardiogram Derived Respiration
EEG	-	Electroencephalogram
EOG	-	Electrooculography
ESP	-	Espressif Smart Connectivity Platform
FDA	-	Food and Drug Administration, USA
FFT	-	Fast Fourier Transform
FG	-	Fibre Grating
GND	-	Ground
HCI	-	Human Computer Interface
HIPAA	-	Health Insurance Portability and Accountability Act
HITECH	-	Health Information Technology for Economic and Clinical Health Act
HR	-	Heart Rate
IoMT	-	Internet of Medical Things
IoT	-	Internet of Things
LCD	-	Liquid Crystal Display
LED	-	Light Emitting Diode
M2M	-	Machine-To-Machine Communication
MDDS	-	Medical Device Data Systems
NICU	-	Neonatal Intensive Care Unit
NTC	-	Negative Temperature Coefficient
OSA	-	Obstructive Sleep Apnoea
PR	-	Pulse Rate
PSG	-	Polysomnography
PWM	-	Pulse Width Modulation
REM	-	Rapid Eye Movement
RFID	-	Radio-Frequency Identification
RR	-	Respiratory Rate
RVSM	-	Radar Vital Signs Monitor
SAS	-	Sleep Apnoea Syndrome
SMT	-	Surface Mounted Technology
SSL	-	Secure Sockets Layer
SVM	-	Support Vector Machine
TLS	-	Transport Layer Security
TOA	-	Time of arrival

US	-	Ultrasonic
WAN	-	Wide Area Network
WLAN	-	Wireless Local Area Network
WPAN	-	Wireless Personal Area Network

List of Symbols Used in Formulae

p	-	Density of the medium
d	-	Diameter of the transducer $= = 2r$
f	-	Frequency
L	-	Distance of the object
r	-	Radius of the transducer
R_1, R_2	-	Resistances
r_A	-	Respiration Actual
r_C	-	Respiration Calculated
t	-	Time elapsed between the emission and the reception of the ultrasound pulse
v	-	Propagation velocity of ultrasound through the medium or speed of wave
V_{out}	-	Output Voltage
V_{ref}	-	Reference Voltage
Z	-	Acoustic Impedance
α	-	Signal angle to object
λ	-	Wavelength of the ultrasound beam
θ	-	Unknown measure of an angle

Chapter 1: Introduction

1.1 RATIONALE

The purpose of the study is to design and evaluate an internet of things (IoT) integrated ultrasound (US) respiration monitoring device suitable for integration into incubators used in hospitals to monitor babies. The device was intended to measure both respiration rate and to detect pauses in breathing due to central apnoea. There is currently no instrument as part of incubators to measure respiration rate, even though respiration rate is a very important indicator of medical wellbeing. In central apnoea, pauses in breathing during sleep, result in cessation of chest movements. Integration of a respiration monitor as part of incubator will allow continuous monitoring of the baby's respiration. This provides a reassurance about the baby's medical condition as well as alerting the medical staff in emergency. It is also valuable for monitoring a number of respiratory conditions such as central apnoea where intermittent pauses in breathing occur during sleep (EQA, 2005).

Parkes (2011) states that respiratory rate is a highly sensitive marker of patients' medical conditions. It gives early signs of deterioration in respiration. Its assessment can help health practitioners detect subtle changes in patients' physiology and reduce the risk of multi-organ damage, arrest, or death.

Several devices are available in the market that can monitor breathing of infants during sleep. However, these devices are contact based, i.e. the sensing unit needs to be attached to the patient's body. Contact sensors can cause stress due to the discomfort they can create that in turn can alter the respiration rate. The respiration monitor in this study is a noncontact system.

US based technology for implementing the required respiration monitoring is appropriate as it is completely harmless, can be implemented in a cost-effective manner and can provide a practical solution to the problem. As infants do not move significantly in an incubator, the US wave can focus on the chest or abdomen. The movements of the chest or abdomen cause their distances to the US sensor to vary over time. These distance variations are measured by determining the time of flight of the US signal from the transmitter/receiver (transceiver) to the body and its reflection back to the sensor.

Continuous measurement of these time variations results in a respiration signal from which respiration rate and pauses in breathing are determined.

To evaluate and test the device, a laboratory setup of US sensors was used to measure US signal that was reflected from different surfaces. This signal was produced by a set up that involved a sinewave generator driving a platform. The platform surface would move vertically in relation to the signal amplitude and frequency. The reason for using this set up was to avoid experimenting on babies in a hospital setting when the method was being developed. Furthermore, the approach allowed comparison of US based measured respiration rate with the actual rate set by the signal generator's frequency to be carried out. This experiment and results on different surfaces and within 15 degrees' angle are explained in chapters 4, 5 and 6.

It would be advantageous for clinicians to monitor infants' respiration rate remotely to intervene in a timely manner in cases where the baby's health is at risk. A laboratory system that integrated IoT or IoMT (Internet of Medical Things) in Neonatal Intensive Care Unit (NICU) and transmitted the collected and analysed data over the cloud to remote locations and through mobile device is discussed in chapter 8. The US signals were detected using NodeMcu IoT platform device. The US signals were processed, analysed using MATLAB$^{©}$, and transmitted over the cloud to remote locations using ThingSpeak IoT platform.

1.2 ORGANISATION OF THE REPORT

The report is organised into six chapters. The background study to conduct this study, literature reviewed, physics of US, respiration and apnoea, and breathing pattern analysis in infants are discussed in the first 2 chapters of the report. Chapter 3 describes the theory behind the hardware devices used in the study such as the US sensors and other sensors, power supply, optimum sensing angle, and the Internet of Things (IoT) technologies that shall be used for wireless transmission of monitored output.

Single and multiple US sensors were used for measurements. A non-contact based US respiration rate monitoring device, with a single distance measuring US sensor can be integrated into infant incubators. This setup was used to measure signals received from a flat surface and a fabric surface which are explained in chapters 4 and 5. A

modification in this setup to measure respiration of the target within 15 degrees' inclination is explained in chapter 6. Chapter 7 describes the laboratory experiment performed using multiple US sensors, to detect signals from platform that simulates chest movements. The monitored respiratory rate should be sent to clinicians in remote locations. A laboratory study to transmit US sensor detected signals over the cloud to remote locations using IoT devices and through a mobile application is discussed in chapter 8. The conclusions of the study and future developments are discussed in chapter 9.

The conclusions cover the observations derived from chapters 4, 5, 6, 7, and 8. The subsequent reference and appendix sections are common to the whole report. The hardware devices used for conducting the project, software code used, and other relevant details are explained in the appendices.

1.3 AIMS AND OBJECTIVES

1.3.1 AIM

To develop and evaluate an IoMT integrated US respiration monitor suitable for babies in incubators.

1.3.2 OBJECTIVES

i. Develop a non-contact US based respiration monitoring system and evaluate its performance on manikins or on a computer controlled artificial lungs system. This should adapt measurement of respiration rate and apuses in breathing due to central apnoea.

ii. Evaluate effectiveness the developed system in different scenarios. This evaluation should be based on devising a suitable platform that simulate baby's chest movements.

iii. Investigate how multi US sensors can be integrated to improve accuracy of tracking chest movements.

iv. Investigate how US sensors can be used to detect pauses in respiration and explore validity of the method in detecting central apnoea.

<blockquote>
v.   Devise Internet of Medical Things (IoMT) techniques to wirelessly transmit respiratory data to the cloud, store and process them on the cloud and make the results available to clinicians remotely.
</blockquote>

1.4 BACKGROUND

Current respiration measurement techniques like nasal prongs, nasal thermistor, Strain Gauge, ECG derived etc., are contact based. Nasal prongs are the gold standard but are poorly tolerated as they are placed inside the nostril. Others are more tolerated but because they are contact based, they can cause discomfort or can be removed by the patient during an overnight recording. This project aimed at developing a non-contact method to monitor infants' respiration rate and pausing in breathing during sleep (caused by central apnoea), using ultrasound (US) sensors.

The US transceiver used in this study detected chest and abdominal movements caused by respiration by transmitting a high frequency sound wave to the baby's chest or abdomen and compared the transmitted signal with the signal reflected from the baby. When the subject breathes out, the chest moves in, and its distance to the sensor increases. Opposite occurs when air is inhaled. These changes are detected when the transmitted and reflected signals' time of flight are measured.

1.5 PROPOSED SOLUTION AND STUDY'S CONTRIBUITIONS

The proposed system will capture the US signal, process it and extract the respiration rate information from it. Data will then be transferred to a central cloud server using IoMT devices. The captured data will be processed in the cloud server with an aid of online MATLAB$^©$ application, analysed and dashboards and reports will be created.

Many methods are available to monitor infants' respiration, but most of them are contact based. The proposed system is non-contact based and can be placed inside an incubator. Multiple sensors will be used to get near-accurate results of the respiration rate. This system intended to be placed within an incubator and hence there will be less interference.

The study's contributions to be presented in the subsequent chapters are summarised as:

- Development of a suitable platform that simulated baby's chest movement to allow evaluations to be accurately carried out.
- Devising and evaluation of an US sensor-based approach to measure respiration rate.
- Comparison of single and multiple US in measuring respiration signal
- Investigating the efficacy of US technology to detect pauses in breathing due to central apnoea.
- Devising solutions to transmit data over the cloud and mobile applications to clinicians in remote locations. IoT platforms (NodeMcu ESP8266 and ThingSpeak) were used to attain this purpose. Integrated MATLAB$^{©}$ processing was devised to provide dashboards and reporting features to view the results visually.

Chapter 2: Literature Review

In this chapter, the literature related to this study is reviewed.

2.1 RESPIRATION RATE MEASUREMENT - CONTACT METHODS

Respiration rate measurement can be grouped into contact and non-contact forms. Some of these methods are explained in the following sections

2.1.1 CONTACT METHODS

2.1.1.1 AIRFLOW BASED METHODS

The nasal prongs airflow sensor is a contact based device used to measure the respiratory airflow (Cooking-Hacks, 2013). Figure 1 demonstrates the method of physical attachment. The device consists of a flexible thread which fits behind the ears, and a set of two prongs which are placed in the nostrils. Respiratory airflow is detected and measured by the prongs connected to an air pressure meter. A problem with airflow based system is that it introduces discomfort and thus some children do not tolerate it. Nasal prong is accurate; it is the gold standard for respiratory airflow measurement.
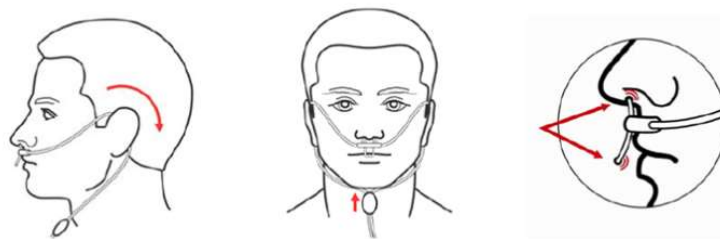
Figure 1: Illustration of Nasal Prongs Airflow (Cooking-Hacks, 2013)

2.1.1.2 ELECTROCARDIOGRAM (ECG) DERIVED RESPIRATION RATE

Electrocardiogram Derived Respiration (EDR) signal is a technique that is based on a process known as 'Sinus Arrhythmia' (study of the rhythm, i.e. sequence and frequency of the heart). The device consists of the ECG electrodes that are attached to the subject. Respiration has a modulating effect on the ECG. The electrodes measure the fluctuations in ECG from which the respiration rate is derived (Al-Khalidi, Saatchi, Burke et al., 2011).

EDR is believed to be based on small ECG morphology changes during the respiratory cycle which is caused by heart movement relative to the electrodes and the change in lung volume (Al-Khalidi, Saatchi, Burke et al., 2011).

2.1.1.3 STRAIN GAUGE METHOD

Strain Gauge procedure is used to measure respiration rate. It consists of two bands, one placed around the rib cage, i.e. the thoracic band, and the other placed over the abdomen at the level of the umbilicus, i.e. abdomen band. The reason for using two bands is that there is an uncertainty as to whether respiration causes chest or abdomen movement. Typically, the signals from these two bands are averaged. The bands typically contain a conducting material which can be either a wire or a foil arranged in a manner that is extendible or deformable such that the conductivity can be maintained when force is applied, i.e. an increase in area of the conductor due to respiration results in an increase in the resistance of the conductor (band). The method involves a classification algorithm of second order autoregressive modelling and zero cross algorithm, to separate respiratory signals as apnoea, respiration, or respiration with motion (Bayes De Luna, N. Batchvarov and Malik, 2005).

2.1.2 NON-CONTACT METHODS

2.1.2.1 RADAR BASED RESPIRATION RATE MONITORING

Radar Vital Signs Monitor (RVSM) is a system that was established to monitor Olympic athletes at distances exceeding 10 m. The system was based on the Doppler phenomenon, detecting breathing-induced movements of the chest. The RVSM method of monitoring respiration rate has the limitation of motion artefact, which leads to corruption of breathing signals (Al-Khalidi, Saatchi, Burke et al., 2011).

2.1.2.2. THERMAL SENSOR AND THERMAL IMAGING BASED METHODS

Thermal imaging is contactless. The sensor is used to detect the change in skin surface temperature around the nose and mouth generated by respiration. Studies were carried out to develop this technique, e.g. (Al-Khalidi, Saatchi, Burke et al., 2011). Thermal imaging data were analysed and corrected concurrently by the use of a computer. Tracking methods were developed to deal with body movement during recording. However, if the face moves out of the camera's field of view, the method fails (Al-Khalidi, Saatchi, Burke et al., 2011).

2.1.2.3 OPTICAL BASED RESPIRATION RATE MONITORING

This is a non-invasive visual sensing method to detect the respiration pattern that uses a fibre grating (FG) vision sensor and processor unit.

In this method of monitoring respiration rate, two sets of devices are used. The first device is the Fibre Grating and the other is the Charge - Coupled Device (CCD). The Fibre Grating facilitates an array of invisible infra-red light spots (wavelength of 810 nm). The CCD camera with an optical band-pass filter is utilised to capture the scene of bright spots that are projected on the subject by the infrared light. The technique is to capture, extract, and analyse the moving distances of the bright spots in each image as this would lead to identifying respiration (Al-Khalidi, Saatchi, Burke et al., 2011).

Both contact and non-contact methods have their own advantages and disadvantages. Direct measurements tend to be more accurate but can interfere with normal respiration and bring discomfort to the patient. Thus, noncontact respiration rate monitoring devices have a distinct advantage over contact methods especially in children, as they cause very least discomfort to the patient.

US based technique, as highlighted in the following literature review has many advantages over other noncontact methods of monitoring respiration rates, especially with infants. US beams can be focused on the point of interest and produce good results without harming neither the patient nor the person handling the system.

2.2 RESPIRATION PRINCIPLES

2.2.1 INTRODUCTION

The respiratory region consists of the trachea, lungs, bronchi, bronchioles, and alveoli as shown in Figure 2. The alveoli act both as the functional unit of the lungs and the site of cellular respiration. From trachea, the airways divide gradually where each branch of airways leading away from the trachea becomes smaller, but in turn the total area of cross-sectional airways actually increases. Accordingly, the airflow resistance decreases as air moves from the large airways to the smaller bronchioles (NHANES, 2008).
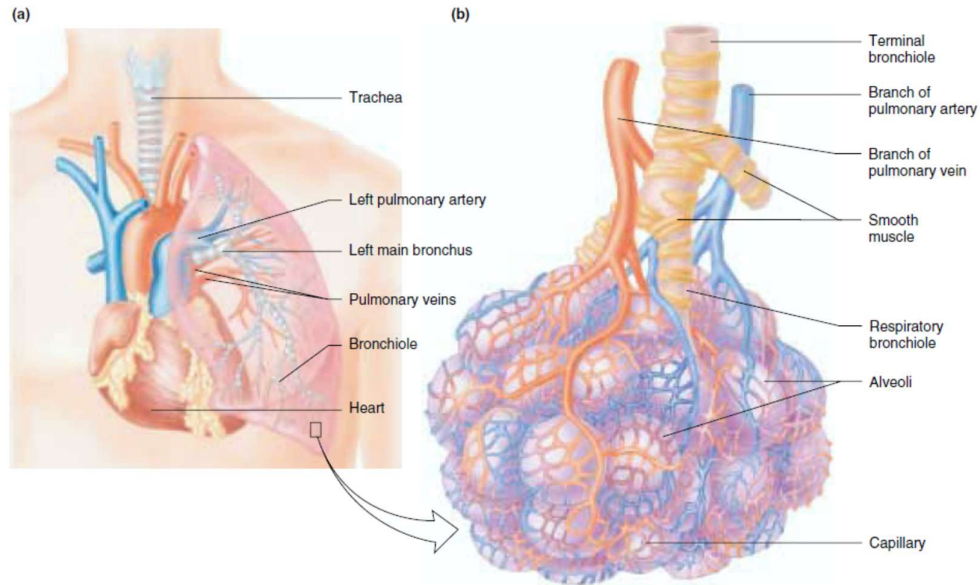
Figure 2: Respiratory Tract (The Mcgraw-Hill Companies, 2001)

Figure 2 exhibits the relationships between blood vessels and airways (The Mcgraw-Hill Companies, 2001).

2.2.2 VENTILATION

Ventilation is the movement of air in and out of the lungs, which depicts the inspiration (inhalation) and expiration (exhalation) phenomena. Inhalation is an active process that uses the muscles in the chest, primarily the diaphragm. Exhalation process is the opposite of inhalation where air leaves the lungs. This is a passive course of action that requires only modest effort of muscular activity (NHANES, 2008).

The method of inhaling oxygen from the open air and exhaling carbon dioxide from venous blood (deoxygenated bloody) denotes the fundamental process of respiration (NHANES, 2008). The alveoli are the sites of gas exchange with the blood. They are tiny air-sacs in the lungs. Lungs are mainly composed of alveoli, numbering to 300 million in adults (The McGraw-Hill Companies, 2001).

Internal Respiration
At systemic capillaries, HbO_2 inside red blood cells becomes Hb and O_2. Hb now combines with H^+ to form HHb. O_2 leaves red blood cells and capillaries.

External Respiration
At pulmonary capillaries, HCO_3^- is converted inside red blood cells to H_2O and CO_2. CO_2 leaves red blood cells and capillaries.

External Respiration
At pulmonary capillaries, O_2 enters red blood cells where it combines with Hb to form HbO_2.

Internal Respiration
At systemic capillaries, CO_2 enters red blood cells. Some combines with Hb to form $HbCO_2$. Most is converted to HCO_3^-, which is carried in the plasma.

Figure 3: External and Internal Respiration (EQA, 2005)

Figure 3 illustrates the internal and external respiration in the lungs. CO_2 leaves the blood and O_2 enters the blood during the external respiration in the lungs. During the internal respiration in the tissues, O_2 departs and CO_2 enters the blood (EQA, 2005).

External respiration occurs in lungs when carbon dioxide leaves the blood through alveoli and oxygen enters blood from the alveoli. This process of diffusion accounts for passage of molecules in different paths. There is more CO_2 in pulmonary blood when it enters the lungs and there is more oxygen in alveoli than in pulmonary blood when it enters the lungs. Furthermore, due to the presence of carbon dioxide in blood as a bicarbonate ion (HCO_{3-}), carbonic acid forms and is broken down into carbon dioxide

10

and water. Subsequently, carbon dioxide diffuses out of the blood. Oxygen is transported to the tissues in combination with haemoglobin as oxyhaemoglobin (HbO_2) (EQA, 2005).

2.3 SLEEP APNOEA

2.3.1 INTRODUCTION

Obstructive Sleep Apnoea (OSA) is a sleep-related breathing disorder that involves a decrease or complete halt of airflow to the lungs. Obstructive sleep Apnoea (OSA) occurs when the muscles relax during sleep, causing soft tissue in the back of the throat to collapse and block the upper airway. This leads to partial reductions (hypopneas) and pauses (apnoea) in breathing that can last several seconds. This can lead to abrupt reductions in blood oxygen saturation, with oxygen levels falling as much as 40 percent or more in severe cases (AASM, 2008).

The brain responds to the lack of oxygen by alerting the body, causing a brief arousal from sleep that restores normal breathing. This pattern can occur several times in a night. The result is a fragmented quality of sleep that often produces an excessive level of daytime sleepiness (AASM, 2008).

Most people with OSA snore loudly and frequently with intermittent periods of silence, when airflow is reduced or blocked. They then make choking, snorting, or gasping sounds when their airway reopens (AASM, 2008).

2.3.2 WAYS OF DETECTING APNOEA

OSA is typically treated by surgical intervention or nasal continuous positive airway pressure (CPAP) treatment. Given the occurrence of OSA and the availability of treatment options, it is important that individuals suffering from the disease are identified. The definitive diagnosis is based on standardised polysomnography (PSG) techniques with overnight recordings of sleep stage (assessed from two channels of EEG and EOG), respiratory effort, oronasal airflow, ECG analysis and oxyhaemoglobin saturation parameters in an attended laboratory setting. This process is labour intensive, requires considerable instrumentation, and is expensive to conduct (Man and Kang, 1995). The raw data from the overnight recordings are screened by clinicians to look

for events in the recorded signals that indicate apnoea or other sleep-related breathing disorders as shown in Figure 4. More recently efforts have been made at designing portable apnoea monitors. Rather than recording the whole set of signals associated with conventional PSG, only oronasal airflow, thorax and abdominal movement, oximetry, ECG and body position were recorded, omitting the EEG. However, although the system gave very high sensitivity and specificity compared with a full PSG, it still required experts to analyse the raw data retrospectively, as with conventional PSG analysis (Mason, 2002).

OSA is associated with arousals in sleep. The recognised way to detect an arousal is from the EEG, but this is difficult and time consuming (Drinnan et al., 2000). The need for less labour intensive measures of sleep fragmentation in OSA patients led to analysis of a number of non-invasive autonomic markers (Pitson and Stradling, 1998). An automated rule-based method was used to search for transient rises (above certain threshold values) in blood pressure and heart rate. It was found that blood pressure rises were better correlated with the more conventional indices (i.e., EEG micro-arousals and oxygen saturation dips) of sleep fragmentation than heart rate rises. It was concluded that automatic detection of blood pressure rises may provide a useful alternative to manual scoring of EEG micro-arousals (the accepted standard) according to the American Sleep Disorders Association (ASDA) criteria (Mason, 2002).

Figure 4 shows frequency spectra where Apnoea detection is demonstrated. The red and blue spectra show Apnoea and non-Apnoea respectively (mason, 2002).
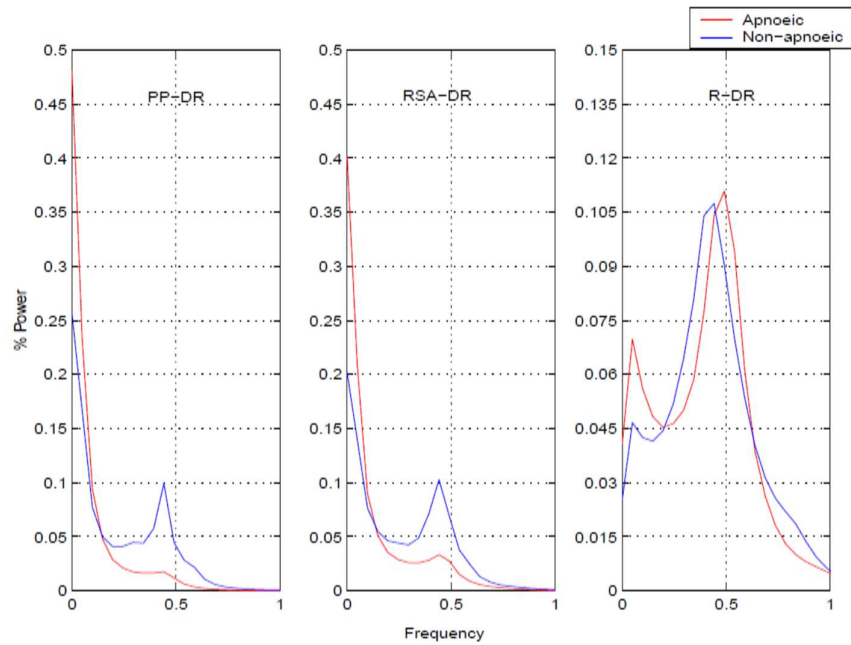
Figure 4: Apnoea Detection. Red Trace showing Apnoea and Blue Trace showing Non-Apnoea (Mason, 2002)

2.3.3 APNOEA DETECTION IN INFANTS USING ULTRASOUND SENSORS

US sensors may be used to record the number of breaths per minute of a premature baby in an incubator. This may enable identifying possible problems in infants' respiration pattern, distinguish sequences or cycles of breathing, determine breathing rate, determine movement of chest wall during breathing cycle as well as finding the effect of different states of infant's breathing pattern. Upon succession, the detection of Apnoea can be done at later stage (Parkes, 2011).

US sensor is used to continuously trigger pulses, send and receive continuous pulses, and detect the distance between a baby manikin's chest in an incubator and the sensor (Arlotto, 2014). The output voltage corresponding to distance of baby's chest is converted back to its corresponding distance value. The distance values captured for a period of time and transferred with the aid of an Arduino board to a PC through USB connection, for recording purpose. Factors like noise, dust, dirt, and high humidity (Ihara, 2008).

2.4 ULTRASOUND PHYSICS

2.4.1 WHAT IS ULTRASOUND?

US is a mechanical disturbance that moves as a pressure wave through a medium (William and Russell, 2002). The sound classification as per frequency is tabulated in Table 1.

The audible sound range for humans is 20 Hz to 20 KHz. US waves have a frequency > 20 KHz. Sound waves are propagated through a medium by the vibration of molecules (longitudinal waves). Within the wave, regular pressure variations occur with alternating areas of compression, which correspond to areas of high pressure and high amplitude, and with areas of rarefaction (which is the reduction of an item's density and is opposite to compression) or with low pressure zones where widening of particles occur (George and Lai, 2006).

Table 1: Ultrasound Classification (William and Russell, 2002)

Frequency (Hz)	Classification
20-20,000	Audible Sound
20,000–1,000,000	Ultrasound
1,000,000–30,000,000	Diagnostic medical ultrasound

2.4.2 ULTRASOUND CHARACTERISTIC WAVE AND PROPERTIES

An US characteristic wave is shown in Figure 5.
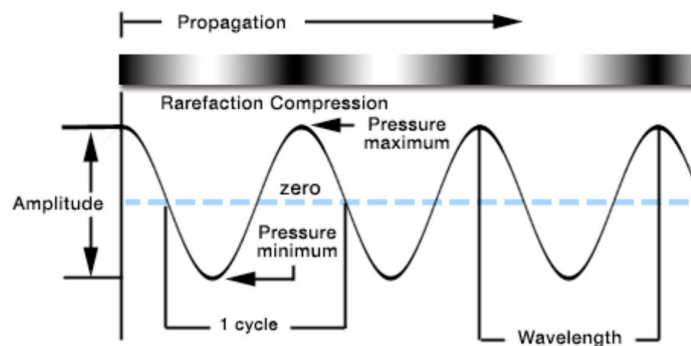
Figure 5: Illustration of Ultrasound Characteristic Wave and Properties
(George & Lai, 2006)

2.4.2.1 TRANSVERSE

In a transverse wave, the displacement of a particle is perpendicular to the direction of wave propagation. The particles oscillate up and down about their individual equilibrium positions as the wave passes (Daniel, 1998).

2.4.2.2 LONGITUDINAL

In a longitudinal wave, the displacement of a particle is parallel to the direction of wave propagation (Daniel, 1998). The particles oscillate back and forth about their individual equilibrium positions. The wave is observed as the motion of compressed region (for example, it is a pressure wave), which moves from left to right.

2.5 ULTRASOUND PROPERTIES - ATTENUATION, REFLECTION, SCATTERING, REFRACTION, AND DIFFRACTION

2.5.1 ATTENUATION

The moment an US beam goes through a medium, it leads to loss of energy by getting converted to heat, along with absorption, scattering and reflection.

George and Lai (2006) state that attenuation is increased (and hence penetration of beam reduced) by:

- Increased distance from the transducer
- Less homogenous medium to traverse due to increased acoustic impedance mismatch.
- Higher frequency (shorter wavelength) transducers. Air forms a virtually impenetrable barrier to ultrasound, while fluid offers the least resistance.
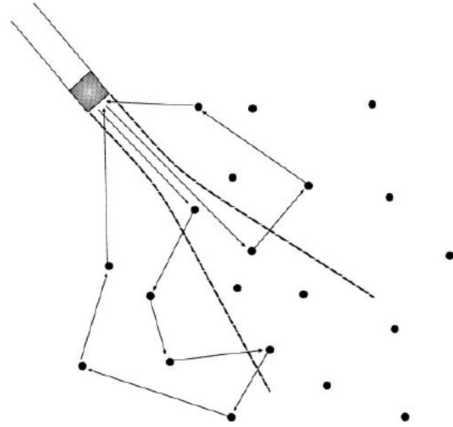
Figure 6: Depiction of Wave Attenuation (William and Russell, 2002)

Figure 6 illustrates the US wave's attenuation, in other terms, constructive and destructive interference effects, that characterise the echoes from non-specular reflections. Here the waves travel in different pathways due to sound being reflected in all directions. They give random interference to the return wave to the transducer, that may either be constructive or destructive. The random interference pattern is known as "speckle" (William and Russell, 2002). Beam energy of an US wave is shown in Figure 7.
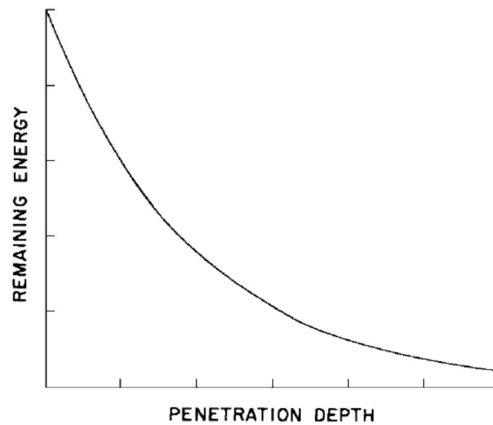
Figure 7: Exemplification of loss of Energy/Remaining Energy in an Ultrasound Beam as it goes through a medium. Remaining Energy over Penetration Depth (William and Russell, 2002)

2.5.2 REFLECTION

When US waves are triggered, they are reflected at tissue boundaries and interfaces. US imagining is created by reflected echoes of the US waves to the transducer. The amount reflected depends on the difference in acoustic impedance between the two tissues traversed by the beam (George and Lai, 2006).

The Acoustic Impedance, Z, is a measure of how ultrasound waves traverse a tissue and depends on (George and Lai, 2006):

- p = Density of the medium
- Z = Acoustic Impedance
- v = Propagation velocity of ultrasound through the medium

such that $Z = p \, v$

A large difference in acoustic impedance is referred to as acoustic impedance mismatch. The greater the acoustic mismatch the greater the percentage of US reflected and lesser the wave transmitted. Examples include soft tissue / bone and soft tissue / air interfaces (George and Lai, 2006).

In terms of gas or air, the acoustic impedance is such that it structures an almost dense barrier to ultrasound. US interactions in a medium are shown in Figure 8.
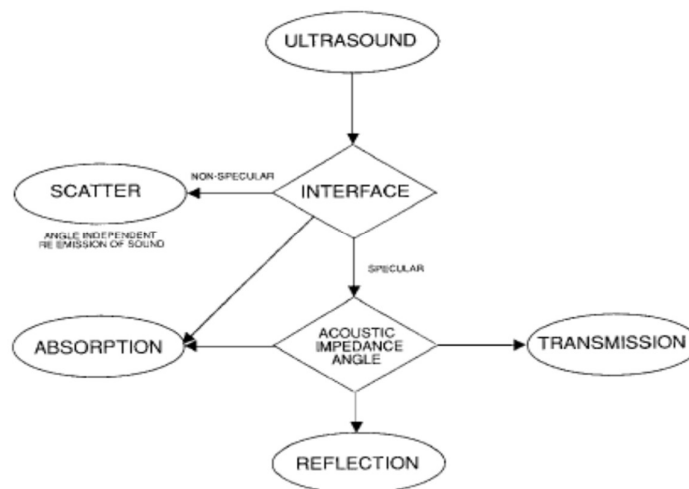
Figure 8: An overview of Ultrasound interactions at boundaries of a medium
(William and Russell, 2002)

2.5.3 REFRACTION

Refraction is the proportion of a beam that is not reflected and is bent, due to the beam encountering media of different velocities. There are many artefacts that this phenomenon is responsible for, one of them being the double image artefact. Furthermore, with the use of acoustic lenses, it can allow better image quality, aided by the method of focusing the ultrasound beam to improve the resolution (George and Lai, 2006).

As per the fundamentals of physics, equation 1 presents the relationship between incident and refraction angles, and equation 2 shows Snell's law (William and Russell, 2002). Figure 9 depicts the refraction of ultrasound wave at an interface.

$$\frac{Sin\,of\,incidence\,angle}{Sin\,of\,refractive\,angle} = \frac{Velocity\,in\,incidence\,medium}{Velocity\,in\,refractive\,medium} \tag{1}$$

EQUATION 1 - THE RELATIONSHIP BETWEEN INCIDENTS AND

REFRACTION ANGLES

$$\frac{\sin\theta i}{\sin\theta r} = \frac{ci}{cr} \tag{2}$$

EQUATION 2 - SNELL'S LAW
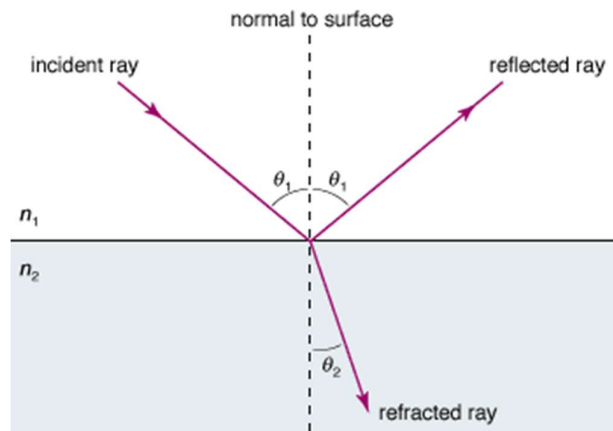
Figure 9: Shows the refraction of ultrasound at an interface. this is where the ratio of the velocities of ultrasound in the two media is related to the sine of the 'angles of incidence' and 'refraction' (William and Russell, 2002)

2.5.4 DIFFRACTION

Diffraction is the effect of attenuation of the intensity of the beam due to the spread of the ultrasound beam with distance from the transducer (George and Lai, 2006).

2.6 ULTRASOUND APPLICATIONS AND FUNDAMENTAL CALCULATION

Ultrasonic intensity is an integral function of the frequency and amplitude of a radiating wave. This creates an impact on many applications. The range of properties for ultrasonic waves are (Dubinsky et al., 2008):

- Dispersion
- Emulsification
- Coagulation
- Chemical effects
- Biological and thermal effects
- Medical applications
- Ultrasonic as a detergent, cleaning, and degreasing agent
- Ultrasonic drilling and soldering
- Ultrasonic delay lines and filters.

All the phenomena and applications of ultrasound depend on its properties like amplitude, velocity, wavelength and frequency. It is possible to calculate the velocity, frequency or wavelength of a wave with equation 3:

$$v = f\lambda \tag{3}$$

EQUATION 3: VELOCITY OF A WAVE

Where:

- The velocity (v) is the speed of the wave. It is measured in m s^{-1}.

- The frequency (f) is the number of times a particle oscillates per second. It is measured in Hz.

- The wavelength (λ) is the distance between two compressions or rarefactions. It is measured in m.

- The amplitude is the distance a particle moves back or forth.

2.7 ULTRASOUND TRANSDUCER PRINCIPLE

2.7.1 ULTRASOUND TRANSDUCERS

- Convert electrical energy into acoustic energy (sound) during transmission.
- Convert acoustic energy to electrical energy during reception.

US transducer (Olympus, 2006) offers a wide range of innovative techniques that set the industry benchmark for ergonomics and extend the diagnostic capabilities of ultrasound like application for real-time imaging (Nimrod, 2005). The patented technologies of advanced transducer design accommodate the broadest range of examinations and applications, offering unparalleled clinical and other industrial flexibility and value. Basic sound relationship is shown in Figure 10.
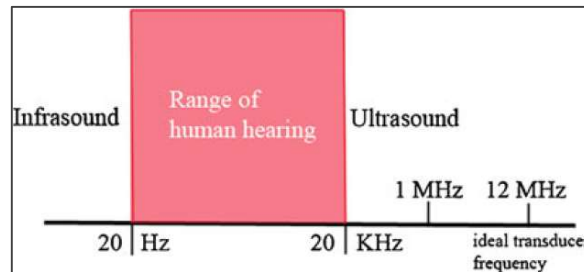
Figure 10: Basic Sound Relationships (Robert, 2011)

Basic US transducer consists of one generator or transmitter that will transmit sound wave, and a receiver to detect the wave that is reflected back. The property of detected sound wave is used to estimate the distance of object (Chan, 2007/2008). The transmitter and receiver can be two separate devices (pitch-catch method), but it is better if both transmitter and receiver reside in the same transducer (pulse echo method) (Pawlak and Wróbel, 2007).

2.7.2 USE OF ULTRASOUND TRANSDUCER TO MEASURE DISTANCE

If both transmitter and receiver are in the same unit, an integrated microprocessor is normally used to measure time for echo pulse to travel back to the receiver. The timer will be started once the transmitter generates a pulse wave and sends it out. When the pulse wave hits an obstacle, large amount of the wave energy will be reflected back.

The receiver detects the reflected pulse echo, and it converts it back into an electrical signal to stop the timer. This elapsed time is proportional to the distance between the transducer and the testing object (Chan, 2007/2008).
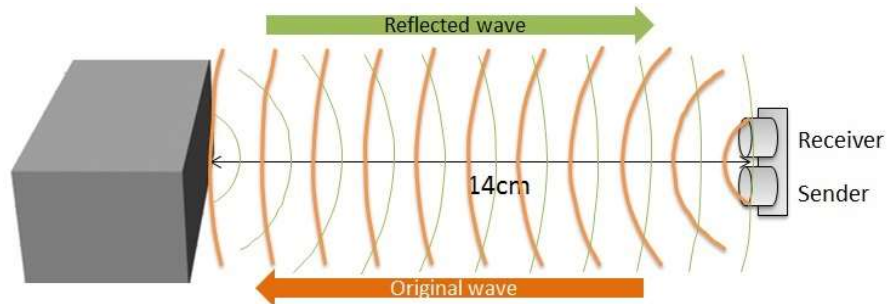
Figure 11: Illustration of distance measurement using an ultrasound transducer (Polytechnic Institute of New York University, 2012)

Figure 11 shows the concept of distance measurement using a US transducer. The distance between object and ultrasound sensor can be calculated using the formula shown in equation 4:

$$L = \frac{1}{2} V. t. \cos(\alpha) \tag{4}$$

EQUATION 4: DISTANCE BETWEEN OBJECT AND ULTRASOUND SENSOR, WHEN TRANSMITTER AND RECEIVER ARE DIFFERENT

Where L is the distance of the object, V is the speed of wave transmitted, t is the time elapsed between the emission and the reception of the ultrasound pulse, and α is the signal angle to object.

If the same transmitter also acts as receiver, the following formula in equation 5 will be used:

$$L = \frac{1}{2} V. t \tag{5}$$

EQUATION 5: DISTANCE BETWEEN OBJECT AND ULTRASOUND SENSOR, WHEN TRANSMITTER AND RECEIVER ARE SAME

When separate transmitter and receiver are used, α is ignored when it is negligibly small. Losses due to harsh environment, attenuation and noise are usually compensated by the integrated circuitry and microprocessor processing of signal.

If the entire object is at a greater angle, the signal is then reflected away from the sensor and no echo is detected. Sound reflection by US under various methods is shown in Figure 12.
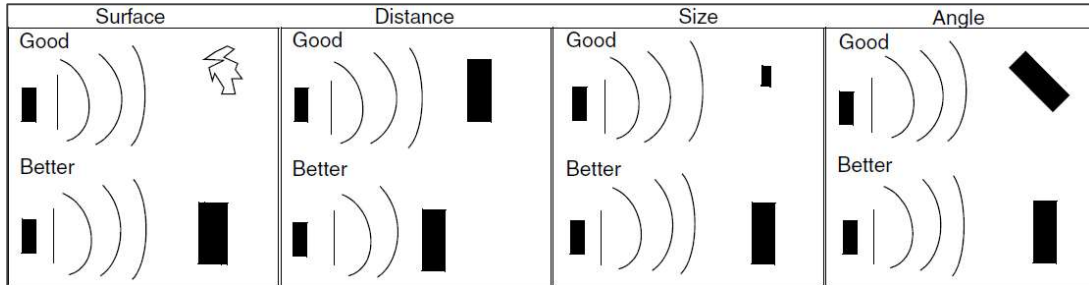
Figure 12: Shows sound reflection under many methods (Palma and Americas, 2008)

2.8 LIMITATIONS OF THE ULTRASONIC WAVES AND SENSORS PHENOMENA

- The speed of sound in the air, environmental effects, and temperature dependence of ultrasonic sensors can affect any kind of experiment (Ihara, 2008).

- Two US sensors cannot be used side by side. If they use the same frequency, it is not possible to distinguish which one has emitted a wave. This is referred to as cross-talk (Ultrasonic sonar sensors, 2008).

- The sensors are positioned in such a way that maximum amount of the emitted sound energy reaches the receiving sensor. For pulse echo types of sensors in object and background mode, the transmitted beam of the sensor should be perpendicular to the object or background target. (Ultrasonic sonar sensors, 2008).

- An intense acoustic noise generated near the sensor may interfere with the sensor's operation. Common sources of this type of acoustical interference may be air nozzles, machine vibration, and sliding friction.

- Ability for penetration is limited thus potentially resulting in incomplete evaluation in many cases (Elmer G., MD, Randy E., et al., 2009).

2.9 ULTRASOUND BEAM FOCUSING

2.9.1 GENERAL SHAPE OF ULTRASOUND BEAM
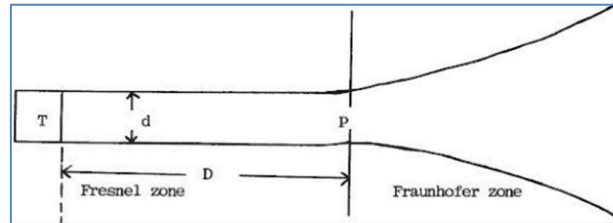
Figure 13: Ultrasound Beam Standard Profile (Zanelli et al., 1993)

The general shape of an ultrasound beam is shown in Figure 13.

The narrow beam associated with near field is required for high quality spatial resolution. The length of this part of the beam determines the approximate tissue depth which can be found using the beam.

2.10 THREE FACTORS INFLUENCING BEAM SHAPE

2.10.1 EFFECTS OF SOURCE SIZE

For a transducer in which no focusing is applied, the length *D*, or the Fresnel zone is determined by the diameter of the transducer and the wavelength of the ultrasound beam as shown in equation 6. The corresponding representation can be seen in Figure 14.

$$D = \frac{r^2}{\lambda} = \frac{d^2}{4\lambda} \tag{6}$$

EQUATION 6: FRESNEL ZONE

Where
 r = radius of the transducer,
λ = wavelength of the ultrasound beam, and
$d = 2r$ is the diameter of the transducer.
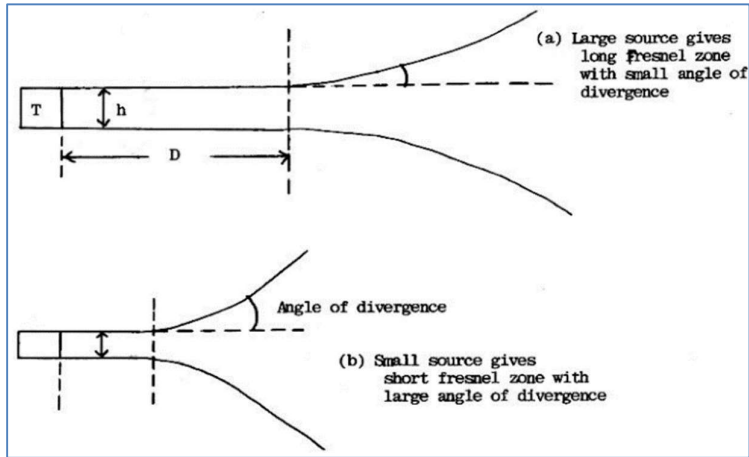
Figure 14: Variation of length of Fresnel Zone and Angle of divergence with source diameter (Zanelli et al., 1993)

2.10.2 ULTRASOUND BEAM FOCUS

US beam focus is shown in Figure 15.
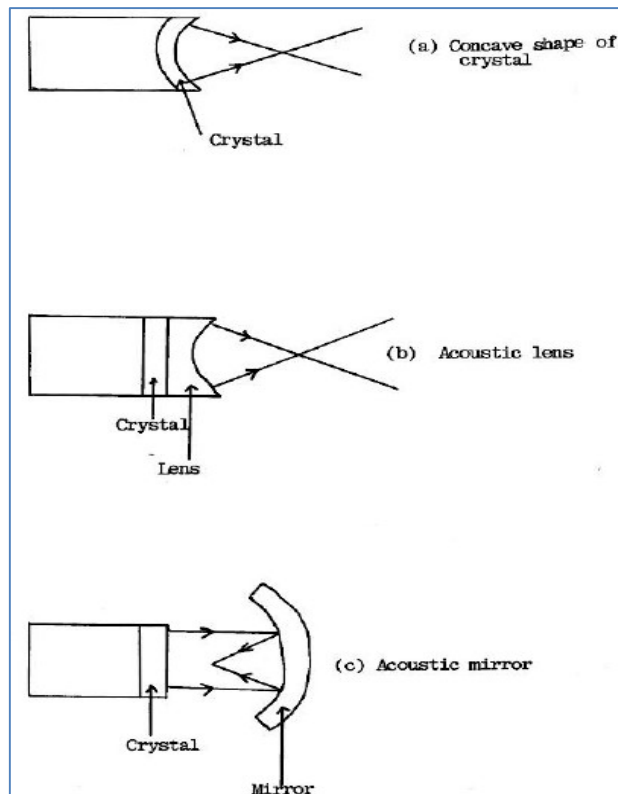
Figure 15: Ultrasound beam focusing method (Zanelli et al., 1993)

2.11 BREATHING PATTERN ANALYSIS IN INFANTS

The aim of this work is to derive robust and accurate respiration rates from the information available from US sensors. In order to adhere to the aims and objectives of this research, knowledge of infant breathing pattern/sequences, movement of chest wall while breathing, and the breathing rate count method is critical. The understanding of such vital and key source of information would be beneficial while designing the device and setting the parameters.

As this study is about the measurement of average respiration rate of infants and children with a non-invasive approach, understanding of past research carried out by other bodies of research institutes is important. Study of measuring and recording average respiration rate of infants in times of normal, sleep, active, and sick health conditions, gives a healthy start to the design and laboratory testing purposes of this device.

2.12 BREATHING PATTERN ANALYSIS IN INFANTS

2.12.1 BREATHING PATTERN IN INFANTS AND CHILDREN

There are numerous studies on respiratory analysis of infants. However, most of these studies only monitor breathing in sleeping infants or infants with illness. There are very few studies trying to monitor breathing pattern in healthy and awake infants. It is mainly because healthy and awake infants are very active with movements and it is hard to collect data using the current available respiratory monitoring equipment on them. No matter what type of respiratory equipment was used, each breathing count is obtained through counting the cycle of breathing. Every cycle of breathing consists of one inhaling followed by one exhaling process of breathing. There can be pauses in between each breathing count.

2.12.2 BREATHING SEQUENCES

A study on respiratory rate of 1007 infants less than six-months-old by doctors in Australia (Morley et al., 1990) stated that when awake, the average mean respiratory rate was 61 breaths per minute, with a range of 43 to 79. Sleeping babies had a

significantly lower mean rate than awake babies at 42 breaths per minute. It indicated that when awake, babies tend to move a lot and breathe shallowly and irregularly.

Babies breathe much faster when awake than while asleep. This study used the simple technique of listening through a stethoscope or placing a hand lightly on the chest for three cycles of 15 seconds to obtain the results (Morley et al., 1990)

Figure 16 shows the respiratory rate results obtained from this study.
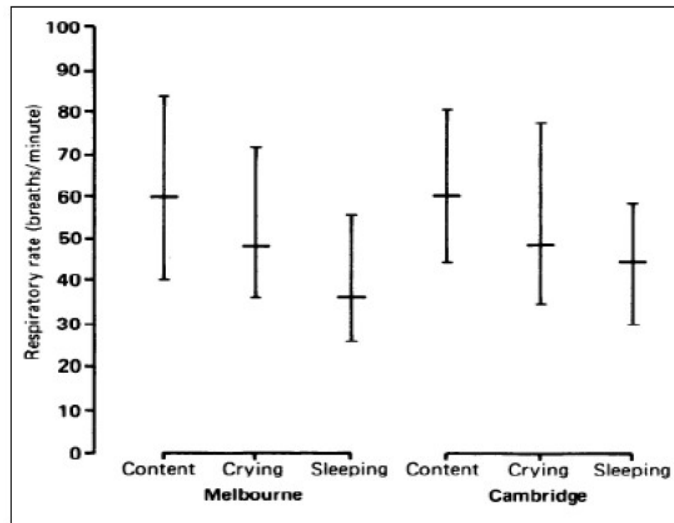
Figure 16: Experiment from Cambridge and Melbourne showing respiratory rate results (Morley et al., 1990)

In another study on morphology of periodic breathing in infants and adults (Weintraub, Cates, Kwiatkowski et al., 2001), it mentions that crescendo-decrescendo is the common breathing pattern for preterm and term infants whereas adult breathing pattern is more decrescendo like.

In other words, breathing pattern of infants start from shallow to deeper to louder and then back to lighter breath before it pauses. While breathing in adults start from deep and loud to a lighter breathing before it pauses.

Figure 17 illustrates the breathing patterns obtained from this study. This study monitors the breathing pattern while the subject is asleep using a flow through system. According to this article, the average breathing rate of infants falls into the range from 40 to 50 breaths per minute, whereas the range is from 10 to 20 breaths per minute for adults.

Many other studies also report monitoring of baby respiratory rate only when they are sleeping (Weintraub et al., 2001).
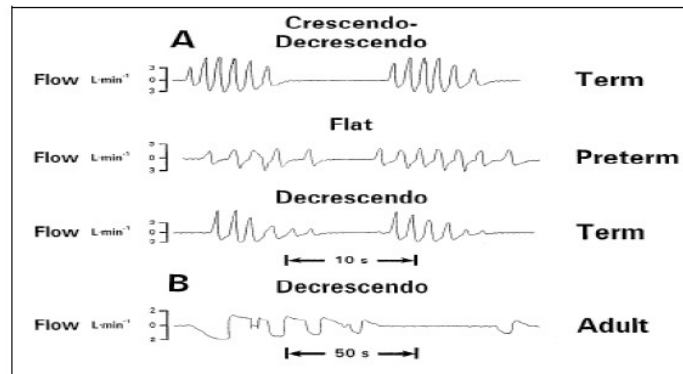
Figure 17: Tracings of periodic breathing in neonates and adult (Weintraub et al., 2001)

In general, the normal breathing pattern for a young baby during sleep is fast and deep at the beginning. They will breathe slower and shallower for a while, then pause or stop for some time before starting breathing at rapid pace again. This pause period can last up to 10 or 15 seconds, especially during sleep.

When awake, babies will breathe shallowly in an irregular pattern. The breathing pattern of babies will change into steadier pace or adult like breathing pattern, as they grow up. A fast breathing period (for one inhaling and exhaling cycle) usually lasts less than 1 second and slow breathing can last up to few seconds.

2.12.3 MOVEMENT OF CHEST WALL DURING BREATHING

Hardly any research has been done on analysis of chest wall displacement during inhaling or exhaling process in terms of distance. This is because researchers are more interested in the pressure (tidal volume) 3-D analysis rather than 2-D displacement of chest wall and lung.

The mechanical movement of breathing is mainly governed by the diaphragm, lungs and ribcages. As Sears (n.d.) stated, our complex nervous system simulates the diaphragm and other important breathing muscles (internal and external intercostal muscles) to act based on an automatic rhythm of breathing. This rhythm of breathing can be either controlled (as during exercise) or uncontrolled/ normal breathing (as

during rest or sleep). At rest, the diaphragm curves up into the thorax area. During inhaling, the external intercostal muscles between the ribs will contract and the diaphragm will flatten. The contraction of these muscles causes the ribcage to raise and expand.

In addition, the diameter of the chest or lungs also increases. This increase in volume inside the lungs causes the internal pressure to go lower than atmospheric pressure. Hence, air is drawn into it due to the difference of pressure. This type of inspiration action is named an active muscular process (Sears, n.d.).

Exhalation, on the other hand is passive, where it relies on the elasticity of the lung and chest to return all structures to their original position. This includes relaxation of muscles, return of diaphragm to normal curves-up position, lowering of ribcage, and inflated lungs (Sears, n.d.). Following the routine, air is exhaled.
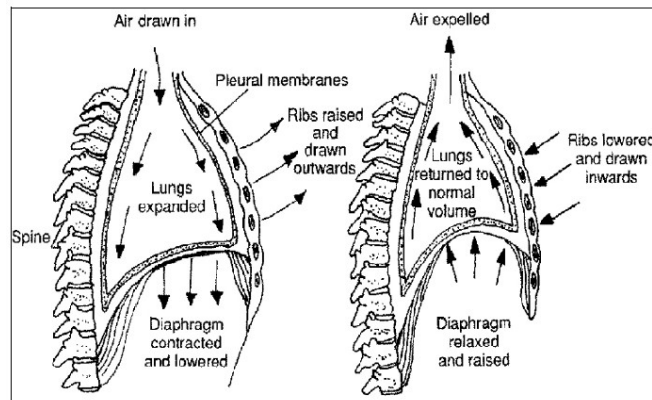
Figure 18: Mechanism of the respiration process: Inspiration and Expiration (Sears, n.d.)

Figure 18 shows the mechanism of breathing process. As mentioned by Sears, in almost all research papers studied, baby breathing is monitored through pressure of air flow. These studies analyse the pressure and volume parameters and hardly mention the chest wall diameter expansion rate during breathing. Neither did it mention the monitored outer chest wall diameter displacement during breathing. It was estimated that during fast and deep breathing, it will be easier to measure using the ultrasound sensor. When breathing is slow and shallow, it will be harder to detect or may not detect the displacement at all. Hence, it is likely to cause miscount of breath (Sears, n.d.).

2.12.4 BREATHING RATE COUNT METHODS

Breathing rate of infants or children can be determined using a number of methods. Each method has its own effectiveness and limitations. Figure 19 shows the general method used to determine one breath count (Sears, n.d.).

For example, one can monitor the time for one full cycle of breathing and calculate the per minute frequency out of the period obtained. However, this calculation is based on the assumption that the breathing pattern is consistent all the way. Unfortunately, this is not true for infants (Sears, n.d.).

On the other hand, babies tend to move actively when awake and this makes measuring of breathing cycle very difficult. Hence, the possibility of this method getting a usable breathing count is higher. This approach might cause more errors, but it is easy and faster to obtain result. If the percentage of error is within the acceptable range, it could be the choice to use (Sears, n.d.).

Another approach is to monitor the breathing count for longer duration, which should be more than 15 seconds since it is the minimum interval for determining respiration rate. The breathing rate is obtained from calculation of this observation. The percentage of error for this method is lower than previous one but the possibility of getting more unusable data will increase. Within these 15 seconds measurement to monitor the breathing count for longer duration, part of the measured period could be interfered with baby's movement. In this case the measured set of data are likely to be unusable. To enhance it further, further data (measurement of every 15 seconds each set) can be obtained and the average or mean count can be calculated. This can increase the possibility of getting more usable measurement for breathing count while reducing the percentage of error in the system (Sears, n.d.).

Lastly, the measurement of breathing rate period can be extended to one minute. Bear in mind that the breathing pattern of infants when awake is irregular where pauses of up to few seconds can appear between breathing. Hence, measurement using this method will be more accurate. However, the possibility of getting unusable data set for breathing rate calculation will also increase at the same time. Despite the measurement period, the state of the baby at the time of measurement should also be considered. The

state of baby can be categorised as asleep, awake and at ease, or awake and crying (Sears, n.d.).
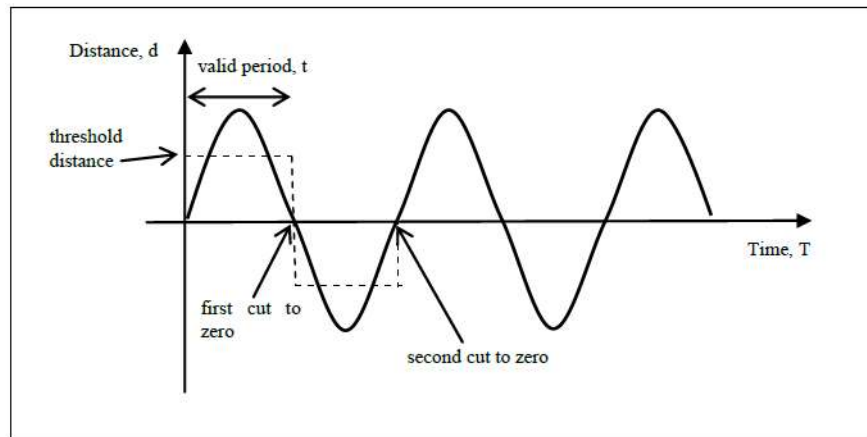
Figure 19: Techniques to count breathing rate (Sears, n.d.)

Chapter 3: Theory - Ultrasound Sensor and IoT Integration

The respiration monitoring system in this study explored different types of US sensors as means of testing purposes to detect infant breathing in the incubator. There are many US sensors available in the market that can measure distance. They are used to find the location and position of the baby in the incubator or respiration rate of a baby monitor by measuring the distance (movement) of the baby's chest/abdomen area from itself. The sensors are placed at different locations and at different distances to gain meaningful information.

Distance is measured using two types of US sensors namely Mini-A and HC-SR04. These US sensors are capable of measuring distances from a minimum of 2 cm to a maximum of 450 cm. Baby monitoring is performed in a controlled temperature and hence temperature will not have any impact on the performance of these sensors. However, for added measures, DHT22 temperature sensor is incorporated into the system to account for any unforeseen temperature changed.

The power supply module to the US system is discussed next. Optimum sensing and positioning of the infant are important for precise sensing of the infant's movements, which is described in the subsequent section.

The infant can be monitored from remote locations through wireless networking system. One such wireless adapter system namely ESP8266 is discussed next. Another remote monitoring system is made possible through IoT (Internet of Things) devices, which is also briefed.

3.1 DISTANCE MEASURING ULTRASONIC SENSORS

Mini-A and HC-SR04 are distance measuring US sensors that were used in this respiration monitoring system. Though they have some differences in their characteristics, their applications in the respiratory monitoring system are similar and hence they can be used interchangeably. MINI-A sensor was used for basic measurements and HC-SR04 was used in laboratory setup inside the incubator with multiple sensors. Features of these 2 sensors, their configuration and setup, and their applications are described in Appendix D.

MINI-A sensor would be a great way to start the investigation of the feasibility of utilising US waves to detect respiration rate. This research requires proximity detection. As the distance of the moving object, i.e. the chest/abdomen in this case varies, the record of the varied distance per peak would give us our respiration count.

The MINI-A sensor is self-contained. The sensor is to be integrated within the incubator and hence this compact design would be ideal for this study. This sensor is also sensitive which is crucial to record the precise chest movement to achieve the correct respiration rate.

MINI-A sensor can work with almost any surface type. The target object or surface will be the premature baby's skin. Instead of absorbing / scattering the US wave, the waves should be received by the US. This US sensor has good resistance to vibration, radiation, background light, noise, dust, dirt or even high humidity and hence fluctuation of US waves are reduced (Senscomp, 2005). This is essential for integration into an incubator.

HC-SR04 sensor can detect objects accurately when the object is directly in front of it. It means the detection is better when the sensor is placed in straight line with the object. In addition, the sensor is still responsive from objects within a 45 degree "window". As per the documentation of the sensor, to fine tune the window, it is recommended to confine the window to 45 degrees to 30 degrees, i.e. 15 degrees on either side, for accuracy in readings purposes (Micropik, n.d.).

In baby monitoring, to measure the distance, these sensors can be placed at different locations in the incubator. However, they will yield good results when they are placed in a straight line.

3.2 DHT22-TEMPERATURE AND HUMIDITY SENSOR

Whilst appreciating the principle of how the environment condition can affect the accuracy of the US wave signals, especially in conditions when the US sensor is placed inside an incubator, the use of a temperature and a humidity sensor is necessary to get improved and accurate US wave signals. DHT22 is a digital sensor used to measure the temperature and humidity of the surrounding air. This is used in baby incubator to monitor its temperature and humidity, so that they can be maintained uniformly. Description of this humidity and temperature sensor is given in Appendix G.

3.3 POWER SUPPLY FOR THE ULTRASOUND SENSOR SYSTEM

3.3.1 INTRODUCTION - PORTABLE POWER SUPPLY DESIGN AND ARCHITECTURE

The objective was to provide a portable power supply from a rechargeable battery to the US sensor. Initially a power pack was considered with a minor alteration to avoid the auto shutoff due to the small amount of power consumed by the board, hence the power pack's false detection and powering off the power back. The Arduino board comes with an onboard power regulator of 3.3V and 5V onboard (Ardunio, 2018). Also, the recommend range is 7V to 12V. The second method being building a power supply with a regulator from 12V to 10V. A battery alarm was to be included to the regulator whilst designing the regulator to indicate when the supply falls below a threshold.

3.3.2 ARDUINO POWER REQUIREMENTS

In respect to the Arduino Uno board, it can be powered via the USB connection or with an external power supply. Further, the board's power source is selected automatically. In addition, as for the external (non-USB) power, this may come either from an AC-to-DC adapter or battery. There are other means of supplying power, this is by utilising the adapter where it can be connected by plugging a 2.1 mm centre-positive plug into the board's power jack. The leads from a battery can be inserted in the ground (Gnd) and analogue input (Vin) pin headers of the POWER connector. In the first means of supplying power to the board using the power pack as shown in Figure 20, there is the need to overcome the auto shutoff issue, whilst bearing in mind that the board can operate on an external supply of 6 to 20 volts (StackExange, 2014). If supplied with less than 7V, the 5V pin may supply less than 5 V and the board may be unstable. Ultimately, if more than 12V is supplied to the Arduino board, the voltage regulator may overheat and damage the board (Ardunio, 2018).

Figure 20: The Use of an External Power Pack (StackExange, 2014)

3.3.3 POWER PINS OF AN ARDUINO BOARD

The recommended range is 7 to 12 volts of power supply to the Arduino board (Ardunio, 2018). The power pins of the Arduino board are given in Appendix E.

3.3.4 PORTABLE POWER SUPPLY CONNECTED TO THE INCUBATOR

Placement of the portable power supply to the incubator is depicted in Figure 21 (Oshpark, 2013).
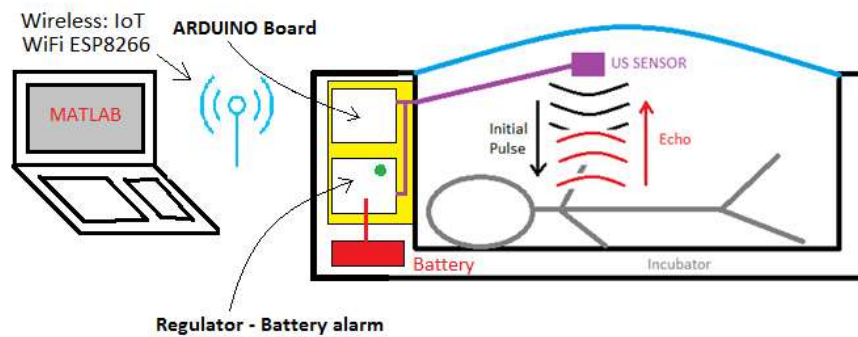
Figure 21: Depiction of Portable Power Supply on the Incubator (Oshpark, 2013)

3.3.5 POWER SUPPLY DESIGN FOR ARDUINO BOARD, ISSUES AND PROOF OF CONCEPT

3.3.5.1 INTRODUCTION

To supply the system with sufficient continuous power that would ideally produce 10V power supply from a 12V battery, a feedback loop regulator is necessary. This is needed to overcome the issue of battery discharge, that can result in the battery switching off. The power supply system ought to remain 10V for Arduino board.

A controlled battery level with a feedback loop would suffice to enable monitoring and preventing the undesirable effect of power cutoff due to battery power deterioration to ensure a continual supply of 10V. Three concepts seem to offer adequate solutions for powering up the US respiration rate monitoring system by providing the required power supply to the Arduino board connected to the US.

3.3.5.2 CONCEPT 1: LM2596 STEP DOWN POWER MODULE DC-DC CONVERTER

The first concept uses a LM2596 Step Down Power Module design based on XL2596 as a main control chip with an attached digital display that displays real-time voltage as a smart function. In addition, a Schottky diode providing protection of reverse connection is used (ICSstation Team, 2014). Blue print of LM2596 is shown in Figure 22. Figure 23 shows the "turn up" and "turn down" functions of LM2596 Converter.
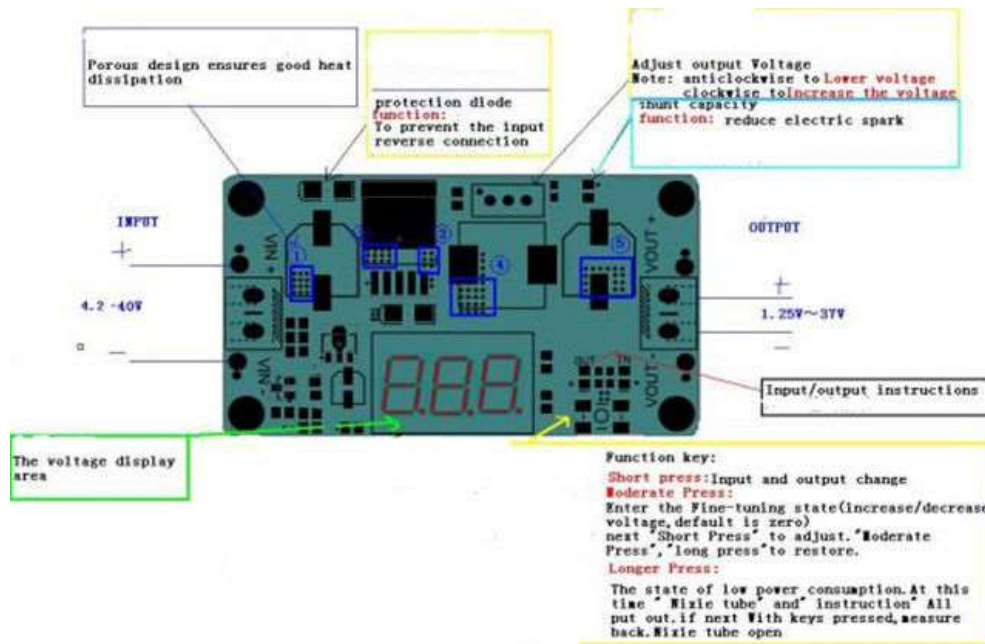
Figure 22: Blueprint of LM2596 Step down DC-DC Converter (IcStation Team, 2014)
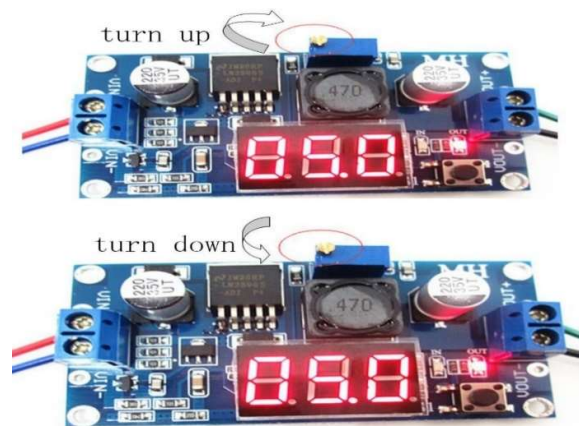
Figure 23: "Turn Up" and "Turn Down" Functions of LM2596 (IcStation Team, 2014)

3.3.5.3 CONCEPT 2. USE OF LM2596 WITH VARIABLE OUTPUT VOLTAGE FEATURE

This concept uses LM2596 from Texas Instruments with a variable output voltage feature as shown in Figure 24. This concept provides simple switching power converter with a step-down voltage regulator (150 kHz 3A) (Garreau, 2015).
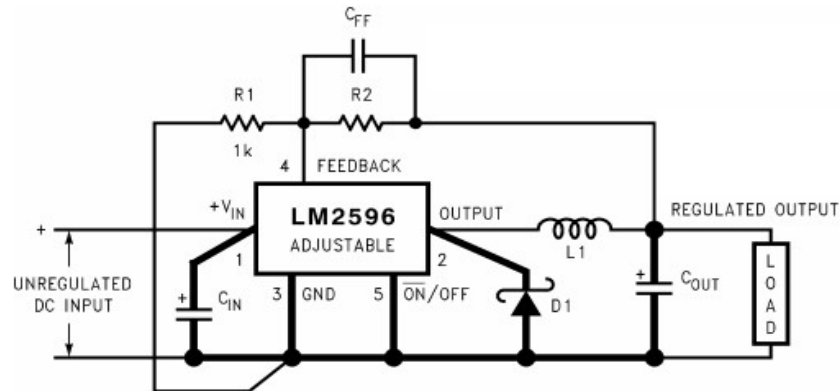
Figure 24: Depiction of a variable output voltage circuit (Garreau, 2015)

The resistor R_1 is fixed at 1 kΩ. The value of the R_2 resistor is used to obtain the output voltage out. Vout is calculated from equation 7 reference in appendix S (Garreau, 2015).

Power supply level indicator system. To prevent from the unexpected switch off of the power supply, a system that would monitor, indicate, and alert is devised. The system ensures that 10V of power is supplied continuously to the Arduino board. If the voltage drops, an alarm is sounded. Both visual (LED) and sound (buzzer) are implemented for the alarm.

The output voltage from the regulator is fed into the alarm system whilst using a potentiometer and a diode. Figure 25 shows a demonstration of the transistors circuit toggling the LEDs and the buzzer. D2 is a Zener Diode with a 3.3V threshold.

Figure 25: Power Supply Level Indicator System (Garreau, 2015)

Monitoring system amalgamation. The joint step-down voltage regulator and the power supply level monitoring system reactions are tabulated and shown in Figure 26. This table outlines the fluctuation of the regulator output voltage.

Input Voltage	Output Voltage	Buzzer	Green LED	Red LED
$V_{BATTERY}$ (V)	$V_{IN,SENSOR}$ (V)	ON / OFF		
13.0	10.24	OFF		
12.5	10.23	OFF		
12.0	10.23	OFF		
11.7	10.24	OFF		
11.5	10.26	OFF		
11.0	10.25	OFF		
10.7	10.16	OFF		
10.5	9.96	OFF		
10.3	9.73	OFF / ON		
10.2	9.64	ON		
10.0	9.47	ON		
9.5	9.06	ON		
9.0	8.67	ON		
8.0	7.75	ON		
7.0	6.77	ON		
6.0	5.81	ON		
5.0	4.84	ON		
4.0	3.88	ON		
3.0	2.92	ON		
2.8	2.72	ON		
2.7	1.80	OFF		
2.6	1.37	OFF		
2.5	0.00	OFF		
2.0	0.00	OFF		
1.0	0.00	OFF		

Figure 26: Power Supply System Analysis (Garreau, 2015)

Figure 27 shows the battery voltage fluctuations while capturing the regulator output voltage, along with observing the buzzer's output state. The tabulated results are then plotted depicting the sensor voltage over battery voltage graph in Figure 51.

Figure 27: Power Supply System Graph (Garreau, 2015)

3.3.5.4 CONCEPT 3. UTILIZATION OF SHORT PULSES IN 2-TRANSISTOR CIRCUIT

Utilisation of short pulses in the 2-transistor circuit that prevents the power pack from switching off whilst keeping it on with very little battery drain time. In this concept of approach, the power pack automatically shuts off, if it does not see a high current usage. Drawing a high current for only a brief amount of time would be sufficient to keep the USB power pack's internal timer active and not shut off (Dorkbotpdx, 2013). Figure 28 shows the 2-transistor oscillator circuit.
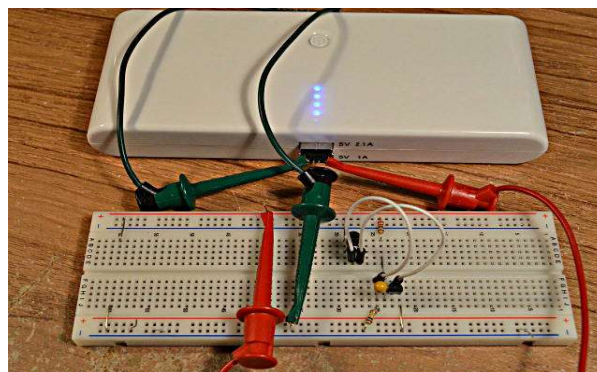
Figure 28: Setup of the 2 Transistors Circuit (Dorkbotpdx, 2013)

3.3.6 SUMMARY

All three concepts seem to provide the required power supply to the Arduino board connected to the US respiration rate monitoring system.

Concept one is out of the shelf system. ICStation Team has tested the system and the results showed that the actual testing of the product was in accordance with the description. Concept two, is a tried and tested system. Lastly, concept three is a system that uses a commonly available power pack. By utilising a USB power pack as a means of supply power to the board, it is established as a source of power for small projects. On the other hand, there was a slight caveat with the USB power packs, it automatically shuts off if the device is drawing a lot of power, as the power packs are meant to be used ideally for charging mobile phones (Dorkbotpdx, 2013).

Out of the three concepts, concept two seems to be a viable solution. Whilst looking at the graph of the power supply system depiction in Figure 41, The regulator ensures a stable 10 V voltage as the input power to the sensor until its own input voltage (battery power) falls under 10 V. During that period, the green LED is turned ON and the buzzer is OFF which indicates the battery level is sufficient. When the battery power falls under 10 V, the regulator could not provide 10 V output any longer. The output voltage decreased following the decline of the battery voltage. At that point, it is observed that the green LED light turned OFF allowing the red LED to turn ON to indicate that the battery needs to be recharged. The buzzer is also turned ON. Under a 3 V input battery voltage, the circuit is not able to provide power supply to the LEDs and the buzzer. Therefore, they turned OFF. Under a 2.5 V input battery voltage, the output voltage fell to 0 V. The functionality is in accordance with the requirements. Hence concept 2 shall be the appropriate solution for this setup of providing power supply to Arduino board connected to US sensor to monitor child respiration rate. However, an important point to consider here is that a 12 Volts rechargeable battery that costs about 20 pounds and that weighs about 200 gm will be needed to realise concept 2. Considering that the purpose is attained, this cost should be borne.

3.4 OPTIMUM SENSING ANGLE AND POSITIONING OF THE INFANT

3.4.1 INTRODUCTION

Incubators are used to provide the required environmental conditions to premature babies in neonatal intensive care units (NICU). The baby is maintained at a constant temperature inside the incubator. The movement of the babies is continuously monitored through sensors installed in the incubator like sensors for monitoring position, temperature, and humidity. US sensors can be installed in incubators to monitor respiration rate of the premature babies. Positioning of babies in incubator for accurate results, single / multiple sensors, angle of placement of sensors in incubator, improving sensor accuracy are some areas discussed in this section. In addition, the means to extract respiration rate and identifying sleep Apnoea from respiration signal are also discussed.

3.4.2 POSITIONING OF OBJECT IN THE INCUBATOR TO GET ACCURATE READINGS

Positioning of the baby in the incubator is a key factor in determining the accuracy of sensor results, while monitoring the respiration rate. The US in the incubator use chest wall movement of baby to measure the respiration rate. Even if premature, the baby is active when awake and may move from side to side, forward and backward, up and down, or turn around. These movements can cause false chest wall movement detection by the sensors or can go out of range of the sensor detection. The babies' hands and leg may sometimes block the chest wall, which causes a major displacement to the breathing curve. Some of the baby movements corresponding to distance measurement are shown in Figure 29 (Chan, 2008).
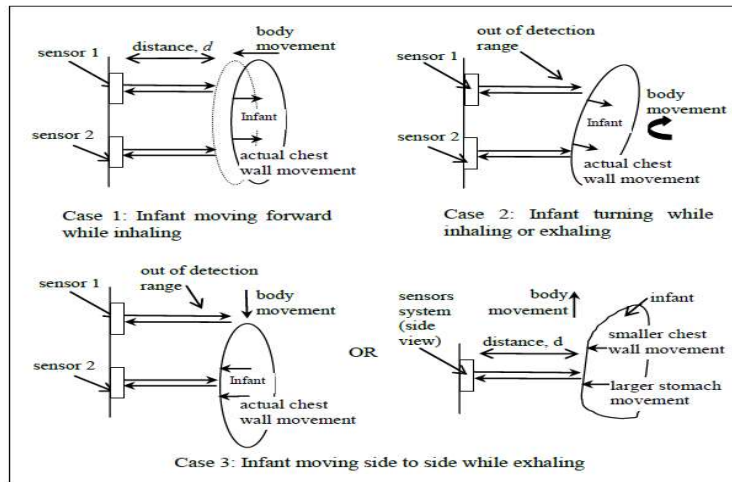
Figure 29: Effects of infant movement on distance measurement (Chan, 2008)

Position displacement of the infants can be a source of noise, and hence interference to measurement by US sensor. The position of the infants like lying down, sitting up (not for premature babies), turn to front are analysed to produce the best measurement. Sample data on real babies helps to find the position where noise interference is less. Methods of mathematical error detection and interpolation help to eliminate noise (Chan, 2008). The optimum position of placing the babies in incubator is determined using these samples which will help to get accurate reading from the sensors for distance measurement (Chan, 2008).

3.4.3 IDENTIFY SLEEP APNOEA OF A PREMATURE BABY IN INCUBATOR WITH EXTRACTED RESPIRATION SIGNAL

Apnoea indicates absence of spontaneous breathing. Sleep Apnoea Syndrome (SAS) is a sleep disorder found widely in the society, including babies. Min et al. (2007) says that if Apnoea of 10 seconds (or shorter than) or longer is experienced by a person for more than 5 times in 1 hour or more than 30 times in 7 hours, then it is considered as SAS. Apnoea of short duration, mostly central Apnoea, are common and frequent during rapid-eye-movement (REM) sleep (Gaultier, 1999). Obstructive Apnoea due to obstruction in windpipes preventing oxygen flow into infants' lungs causes upper airway problems, which eventually leads to sudden infant death.

There are many non-contacting ways of monitoring respiration signal like using microwave antenna, thermal infrared imaging, non-restrictive visual method, and using

US sensors. US attenuation characteristics are used for monitoring respiration signal. The system uses a 40 kHz nominal frequency US sensor. This method uses peak detection technique to count respiration signals after processing and filtering. If peak interval of respiration is less than 10 s, it is normal respiration. If it is more than 5 in 1 hour and 30 in 7 hours, then it is considered as Apnoea (Min et al. ,2007).

The measurement of respiration rate was performed with the sensor placed at 25 cm distance from the infant. This distance yielded satisfactory results. Additional distances could be measured by modifying sensor characteristics or using high frequency sensors (Min et al., 2007).

3.4.4 ANGLE OF SENSING AND OPTIMUM POSITIONING OF ULTRASONIC SENSORS IN THE INCUBATOR

The surrounding environment, ambient temperature, and air humidity of the system can affect the propagation velocity of ultrasound pulse, and hence US sensor accuracy. An incubator can use more than one US sensor. When multiple sensors are used, multiple reflection effect and signal interference from adjacent sensors can occur leading to inaccurate measurement of distance. Hence, sensor placements at angular positions to the baby chest are avoided.

Sensor platform is designed as a straight platform, as shown in Figure 30. Both sensors are parallel and aligned. This way, signals are not reflected back and also signals from sensors do not interfere with one another. Again, this is just one example. There can be many other designs and methods with the ultimate purpose of avoiding reflection and signal interference (Chan, 2008).
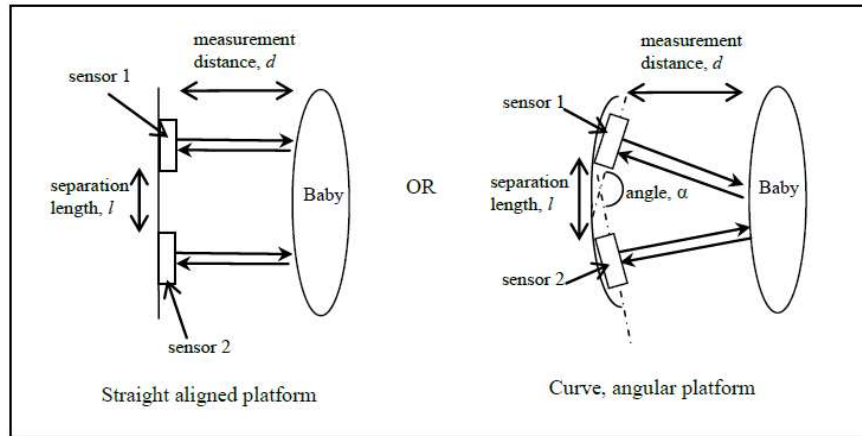
Figure 30: A model of sensor platform shapes (Chan, 2008)

3.4.5 USING MULTIPLE SENSORS TO IMPROVE ACCURACY

US sensor measures its distance to the target by measuring the time of flight of the transmitted acoustic signal. Incubators can use one or more sensors for measuring from multiple locations. Use of two US systems to measure baby's chest movements during inhaling and exhaling improves the accuracy of measured data (Chan, 2008).

Multiple US sensors can be used at same or different frequencies to correctly identify time of arrival (TOA) and to estimate accurately distances and orientations between transmitters and receivers. The orientation error was found to be less than 0.5 degrees when measuring zero, ten, twenty, and thirty-degree angles. Depending upon the angle to be measured, sensors with wider perception angle should be chosen (Hashizume et al., 2005).

When two sensors were used, they were placed in such a way to target chest wall sides of the infant and not in the middle. The separation distance was typically 25 mm for a sampling frequency of 20 Hz. This arrangement helped in getting more accurate results of the respiration rate (Chan, 2008).

3.4.6 OPTIMUM ULTRASONIC SENSOR FOR RESPIRATION SIGNAL

The purpose of US position sensor in incubator is to measure baby's chest wall movements. One or more sensors can be used in an incubator. It should be robust enough to not get interfered by signals from other sensors, noise, temperature, and

humidity. Respiration rate of infants is measured to find if the baby is breathing correctly and alive, to find if any irregular respiratory physiology that indicates cardiac abnormality is present, and to look for presence of Apnoea in infants. The working principle of US sensors used to measure respiration rate of infants is to measure the reflected echo from transmitter to receiver with speed of sound as medium (Min et al., 2010).

The US sensor in a premature infant incubator should have high resolution. For example, UNDK 20U6903 US sensor has 0.3 mm resolution that can detect smallest position change of the baby while MINI-A US sensor has a resolution of 1 mm (Chan, 2008). Sampling frequency of MINI-A is 20 KHz whereas UNDK 20U6903 has a minimum frequency of 40 KHz (Min et al., 2010). This frequency can be varied depending upon the requirements. Similarly, there are many other US position sensors, they many have different characteristics, but the overall characteristics is similar to these US sensors.

3.4.7 MEANS AND METHODS TO EXTRACT RESPIRATION RATE FROM RESPIRATION SIGNAL

US signal is transmitted to the baby's chest wall and the chest movement is reflected back to the receiver of the US sensor. The signal reflected back from the object is used to find the respiration rate of the object / baby under observation. The time taken for the signal to return back is used to compute the distance using the speed of ultrasonic sound waves. US signals travel at 340 m/s in air, same as audible sound. This method of measuring respiration signal using US sensor is a non-contact method of respiration rate measurement.

A model of acquiring and shaping received US signal is shown in Figure 31. Though the figure shows the signals to be transmitted and received towards the nostrils of the subject, the same holds good towards chest area also. In this case, the transmitter is placed at 40 cm distance above the subject's head / chest (soma technology). Receiver placement is a compromise between signal strength and the space needed for the subject to move around without hitting the sensor. The best signal is got when the receiver is close to the subject. The distance could be increased with better receiver sensitivity and

higher transmission level. Respiratory rate of children and new born can be up to 1 Hz (Arlotto et al., 2014).
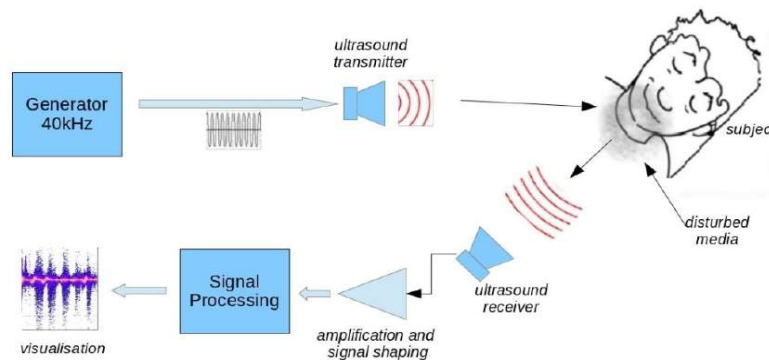
Figure 31: Acquisition and shaping of the received US signal (Arlotto et al., 2014)

The received signal is filtered to remove unwanted high frequency and burst signals using methods like modified envelope detection method and moving average methods. The peak of the signal is detected by zero crossing methods to compute respiration rate. A peak detected signal looks like the one shown in Figure 32. The detected peaks give the respiration rate of the subject (Min et al., 2010).
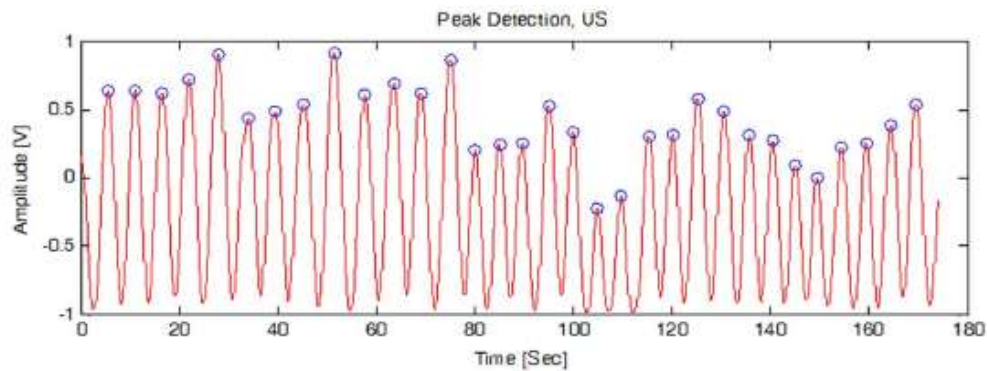
Figure 32: Peak detected signal (Min et al., 2010)

3.4.8 SIGNAL INTERFERENCE WITH MEANS OF MITIGATION

Signals for respiration rate measurement systems have interferences due to hardware limitations, noise caused by working environment, and noise caused by human

behaviour (Chan, 2008). The various interferences and their means of mitigation are discussed underneath:

Hardware Limitations

This depends on the characteristics of the sensor like US sensor range, mismatch of sensor ranges and application requirements like non-allocation of sufficient fading time to sensor, and sampling frequency. Appropriate sensors and ratings have to be chosen based on the application (Chan, 2008).

Limitations due to Signal Interference

When more than one sensor is used in respiration monitoring, multiple reflection and interference from adjacent sensors are factors that need careful consideration in the design and operation of incubator. To minimise these issues, time to capture signal from each sensor or time to trigger each sensor are calculated and planned.

Noise caused by Working Environment

Noise interference is another major issue in respiration rate measurement using sensors in baby incubator. Low-pass filters connected to hardware or software algorithms are used to detect and filter the voltages generated by noises. The ambient temperature and humidity of sensor's working environment can affect the propagation velocity of transmitted pulses. Sensor characteristics must be understood to determine the application of a sensor in a particular environment.

Noise caused by Human behaviour

The movement of the baby's hands and legs can cause false measurement from US sensors. Their rapid body movements and turning around in various directions makes it difficult to measure. The best position of infants is found out to get the correct measurement (Chan, 2008).

3.4.9 SENSOR'S OPTIMUM ANGLE AND SIGNAL PROPOGATION ANGLE

The beam angle of US sensors is typically 10 – 15 degrees and is conical shaped. The response of the sensor to an object depends on the size and orientation of the target, its

angular position, and sensor's sensitivity. It is generally desirable to place the object to be sensed, directly in line with the sensor to get accurate results (Senix Corporation, 2018).

The optimum signal propagation angle is the range up to which the ultrasonic sensor's signals can be transmitted efficiently to get accurate results. The sensors are efficient in sensing objects within 15 degrees. The sensing range is also limited by distance of the object. The sensing range is diagrammatically shown in Figure 33.
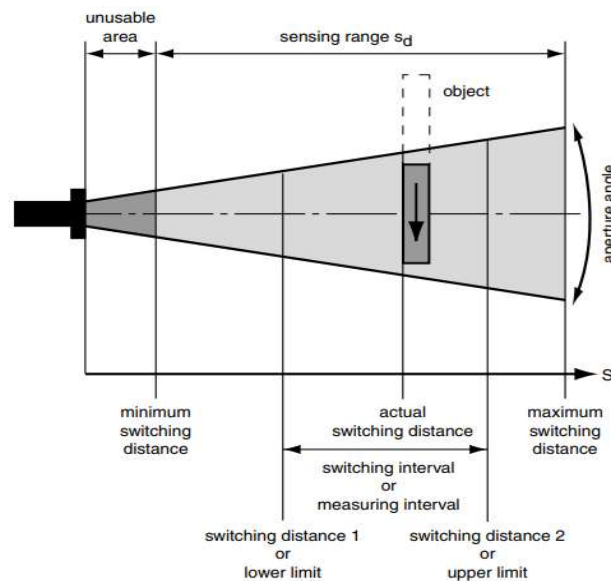
Figure 33: Sensor Range (PEPPERL+FUCKS, 2018)

Figure 33 shows the active area of the US sensor which is called as the sensing range (s_d). It is limited by the shortest and longest operating distance. The US sensor detects objects in its sensing range, irrespective of these objects located axially or laterally (PEPPERL+FUCKS, 2018).

3.4.10 IMPROVING SENSOR ACCURACY

The accuracy of the sensor is affected by the surrounding noise. Advanced signal enhancement techniques are employed to extract useful information from the measured US signals (Lei et al., 2008).

Temperature of air between sensor and the target can affect measurement accuracy since speed of sound varies with temperature. Sensor assumes a constant temperature

when it calculates distance. Temperature compensation is incorporated to improve sensor accuracy in such instances (Senix Corporation, 2018).

3.4.11 SUMMARY

US sensors may be used to monitor respiration rate of premature babies in incubator. The optimum way of utilising US sensors to obtain accurate results like positioning of the baby in the incubator, angle of sensing, mitigating signal interference, optimum angle, and optimum signal propagation angle were discussed in this section. In addition, the means of identifying sleep Apnoea in babies and extracting respiration rate from respiration signal were discussed. Further discussions on using multiple sensors to improve accuracy and ways of improving sensor accuracy are also detailed to make a robust incubator system employing ultrasonic sensor.

3.5 ESP8266 - WIRELESS ACCESS POINT ADAPTER

In order to transfer collected data to the cloud storage, the use of a wireless networking device would be an effective.

A possible device for this purpose is Espressif Smart Connectivity Platform (ESP8266). This is a self-contained Wi-Fi networking solution. There are two ways in which this device can be used. One, it could host the application as it has its own dedicated microcontroller. Second, offload all Wi-Fi networking functions from another application processor. In this study, ESP8266 would be transferring the collected US sensor's data over the cloud whilst using the IoT phenomenon (Espressif systems, 2013). The immediacy of the data collected by IoT devices means faster analysis and distribution of that information whilst having the ability to perform machine learning/big data, predictive and preventative analytics, dash boarding and reporting. The alternative solution would be offline computation, where the system is not connected and not accessible by anyone from anywhere, likewise not being able to leverage the key features as opposed to the incorporation of IoT in times where crucial monitoring is obligatory.

The device will serve as an adapter where wireless internet access is added to any microcontroller-based design with simple connectivity through UART interface or CPU Advanced High-Performance Bus (AHB) bridge interface. Built-in cache memory will

help improve system performance and reduce memory requirements. The device also has powerful on-board processing and storage capabilities that allow it to be integrated easily with the ultrasound sensors through the devices on-board GPIOs. This allows faster development with minimal loading during runtime (Espressif systems, 2013). The hardware connections, applications, and ultra-low power technology of ESP8266 is described in Appendix H.

3.6 INTERNET OF THINGS (IOT)

3.6.1 INTRODUCTION TO IOT

Internet of Things (IoT) has made tremendous progress in the recent past. Today, virtually many human activities are influenced by IoT. IoT is defined as the connection of physical devices such as vehicles, home appliances, and smart communication devices, amongst many others through a network (Osseiran et al., 2017). The devices are normally embedded with electronic actuators, software sensors, and an internet connection which is required for the devices to exchange data and communicate with each other. IoT components are illustrated in Figure 34. However, despite their benefits, IoTs have several security concerns and challenges which calls for the implementation of effective mitigation strategies and the adoption of best security practices.
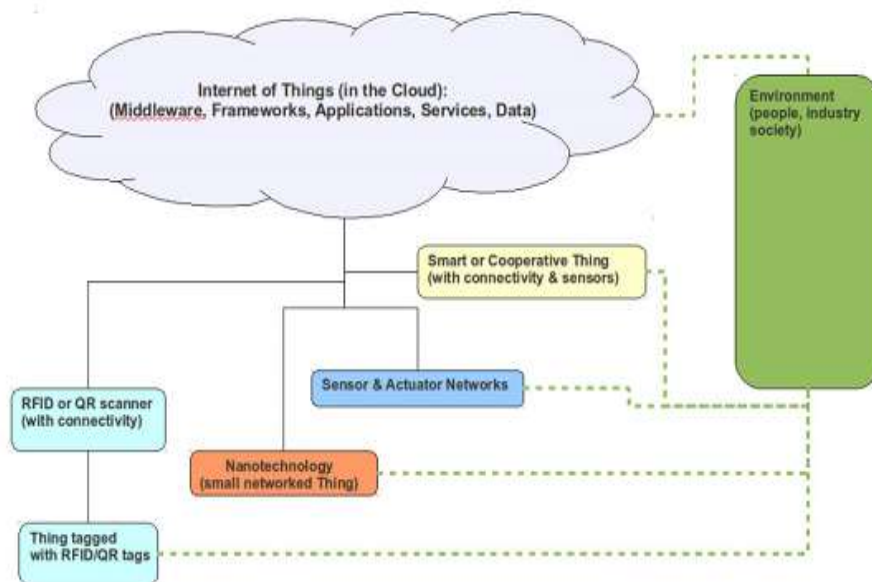
Figure 34: Illustration of IoT Components (Coetzee and Eksteen, 2011)

Neonatal Intensive Care Unit (NICU) is where premature babies are taken care of, typically in incubators. Various sensors like temperature, humidity, heart rate, pulse, and others are placed in incubators to monitor the child's health condition. Sleep Apnoea is a major problem with infants in NICU. Latest technologies like machine learning, predictive and preventive analysis, dashboards, and report generation can be leveraged to predict sleep Apnoea of a premature baby in NICU. With IoT, healthcare industry is moving forward towards monitoring the baby's condition remotely, which includes sensor data and sleep Apnoea condition. These data could be presented over the cloud and make IoT driven monitoring as a self-sustained system by generating alerts to on-duty personnel and physicians when anomalies arise.

3.6.2 NEONATAL INTENSIVE CARE UNIT (NICU)

NICU takes care of premature babies who are unable to survive on their own without the aid of incubators, monitors, and breathing devices. It provides the ideal environmental condition for neonates to prevent them from infection, allergies, and excess noise and light. Incubators monitor baby's temperature, humidity, heart rate (HR), pulse rate (PR), respiratory rate (RR) and other vital signs to know their health condition, to regulate them (Santiago 2018).

3.6.3 IOT AND IOMT

Internet of Things (IoT) is a collection of interconnected devices linked through online computer networks. Internet of Medical Things (IoMT) is a subdivision of IoT that deals with interconnected medical devices and equipment, that constitute healthcare IT. As per statistics, 30.3 % of IoT devices are used in healthcare sector and 60 % of healthcare organisations have already introduced IoT into their healthcare activities. IoMT solutions offered by healthcare organisations fall under categories of clinical efficiency, home monitoring, fitness wearables, infant monitoring, biometric sensors, brain sensors, and sleep monitoring (Internet of Medical Things (IoMT) 2017). An IoT or IoMT system is composed of the thing or the device itself, local network to translate proprietary communication to Internet Protocol, the internet, and back-end services as shown in Figure 35. The back-end services may be embedded or stand-alone.
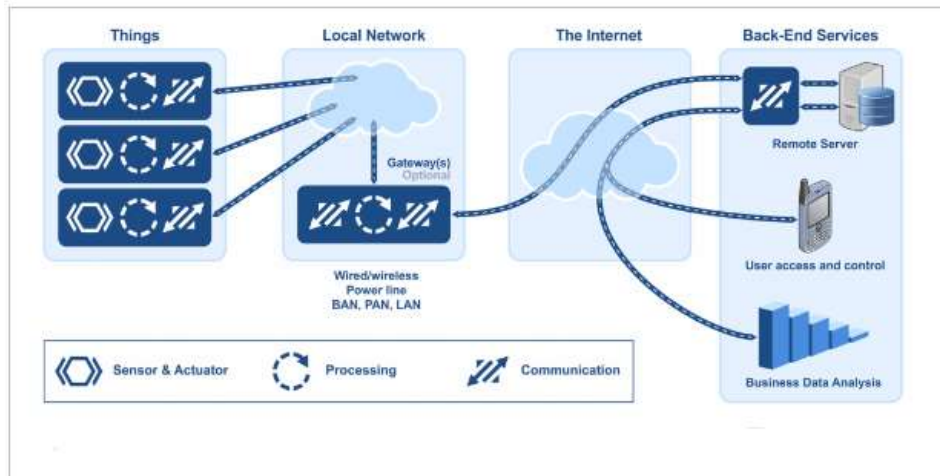
Figure 35: IoT Components (Part 1: IoT Devices and Local Networks, 2017)

3.6.4 APPLICATION OF IOT IN NICU

In a neonatal incubator having IoT, the parameters like temperature, respiration rate, and others are monitored over internet. If the monitored data reaches a threshold limit, it is indicated to the concerned responsible through an SMS or email and an alarm is also raised to indicate the anomaly, thereby providing instant attention to the infants. The electronic devices in NICU are essentially IoT objects which are always connected to internet and then to private or public cloud. These objects are accessible from anywhere and can interact with each other directly, through the process called Machine-To-Machine Communication or M2M. These IoT objects send data continuously to the web using services like ubidots, that also store data online. They trigger certain events in the cloud based on the data monitored in the incubator. The doctors can thus access real-time health data and monitor patients regularly through automated workflows and treat them at the onset of health problem itself. A working model of IoT embedded NICU transmitting data over cloud from sensors is shown in Figure 36 (Shakunthala et al. 2018).
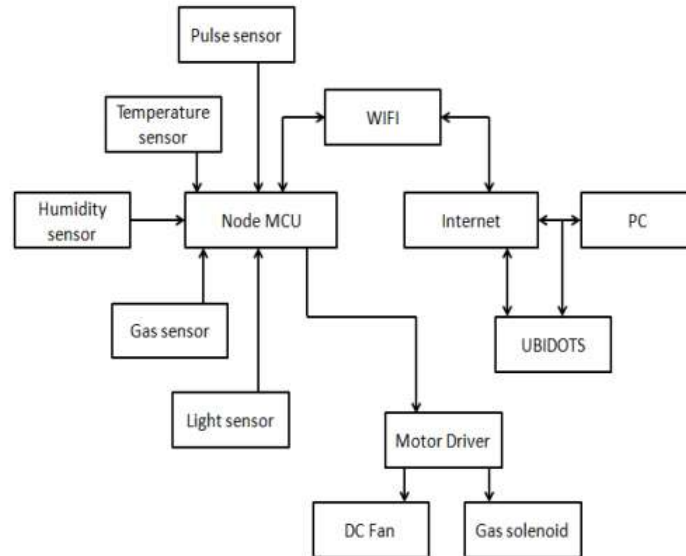
Figure 36: Data Transmission from Sensors of IoT Embedded NICU
(Shakunthala et al., 2018)

3.6.5 DETECTION OF SLEEP APNOEA OF A PREMATURE BABY IN NICU

Apnoea of prematurity (AOP) is a common problem affecting premature infants. Zhao et al. (2011) state that AOP in infants is the condition of "pause of breathing for more than 15 to 20 seconds which may or may not be accompanied by oxygen desaturation ($SpO_2 \leq 80\%$ for ≥ 4 s) and bradycardia (heart rate $< 2/3$ of baseline for ≥ 4 s), in infants born less than 37 weeks of gestation". Premature infants have lot of REM (Rapid Eye Movement) sleep with more inconsistent breathing, caused by less stable baseline of oxygen saturation. Hence sleep Apnoea of infants is more in REM sleep than in quiet sleep. Body movements precede or occur simultaneously with Apnoea. Hence, arousal from sleep can cause Apnoea rather than terminating it. Hence sensors that measure body motion, respiration rate, oxygen saturation, and heart rate can be used to detect sleep Apnoea in premature infants.

Sleep Apnoea in infants is detected by either invasive or non-invasive methods and devices. For example, pulse oximetry is a small clip-like device that can be connected to the infants' toes to measure oxygen saturation level. Temperature and humidity inside a neonatal incubator are measured by non-invasive sensors like DTH11. Photosensitive light sensors are used to measure light (Shakunthala et al. 2018).

3.6.6 LEVERAGING LATEST TECHNOLOGIES TO MEASURE RESPIRATION RATE AND DETECT SLEEP APNOEA

The architecture of Healthcare IoT has four layers namely the medical devices, machine to machine (M2M) connectivity layer, machine to machine integration, and business layer that generate alerts and reports as shown in Figure 37.
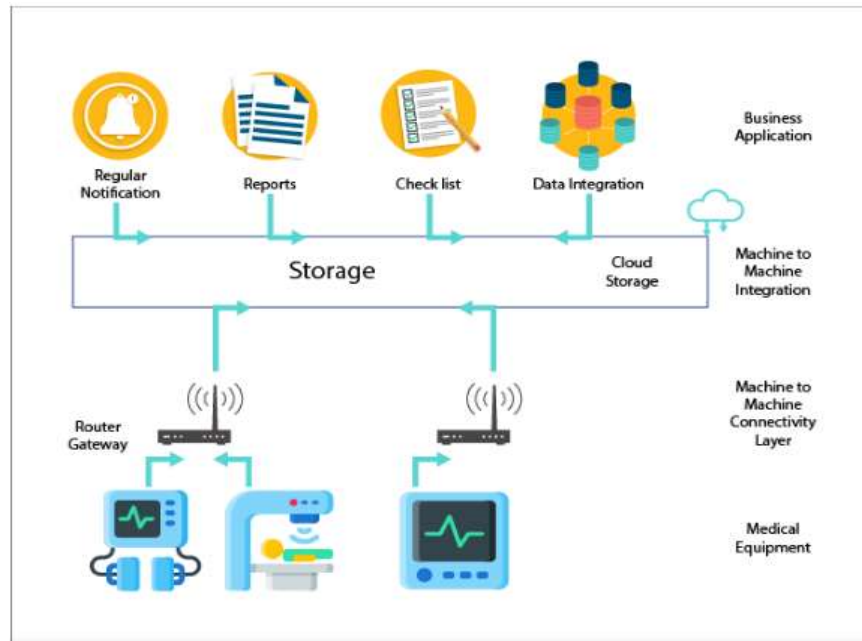
Figure 37: Architecture of IoT in Healthcare (The Role of Internet of Things in the Healthcare Industry, 2018)

The medical devices like incubators and other devices, that are connected to the infant or present in NICU for observation fall under layer1. Layer 2 provides a multi-service gateway to connect to IoT applications with remote management capability. This layer helps in data collection, processing, and transfer for M2M solutions to the cloud or otherwise. Through M2M technology, infant is monitored and emergent care like providing oxygen or regulating temperature can be done until health professionals arrive on the scene. M2M integration layer uses the data collected in the cloud to send alerts, notifications, and reminders.

In a NICU, the M2M integration layer gets data from the sensors and compares them against threshold limits. When there is an anomaly, they trigger alerts to attenders, doctors, and nurses. M2M solutions try to regulate the infant's condition by measures like delivering oxygen, regulating temperature, and others. The integration layer also

displays data in dashboards for easy understanding and management. It also offers analytics features to interpret and deduce reasoning from the data.

3.6.7 PREDICTION OF NEONATAL APNOEA USING MEASURE LEARNING TECHNIQUES

The data collected by IoT sensors in layer 2 is analysed by methods like machine learning and predictive analysis to predict infant Apnoea in NICU. It is predicted by developing a classification model. Machine learning techniques like Support Vector Machines, decision trees, neural networks, Gaussian models, hidden Markov models, and many other methods can be used to process data, classify data, and recognise patterns and anomalies. The methodology of using machine learning algorithms to predict sleep Apnoea in NICU infants is shown in Figure 38 (Shirwaikar et al. 2016).
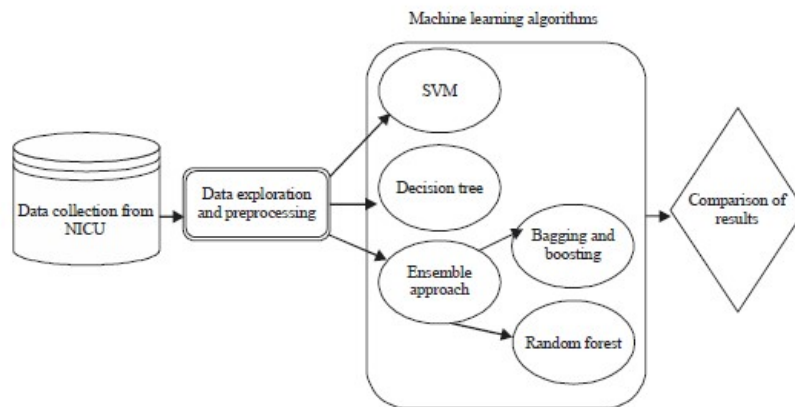
Figure 38: Use of Machine Learning Algorithm in Sleep Apnoea Prediction (Shirwaikar et al., 2016)

Algorithms for machine learning methods are developed to analyse, sample, eliminate unwanted data, pre-process data, and compare data. Statistical computing programming language the likes of Python are used for this process. Classification models are built using models like SVM to train data. The trained data is then compared with collected data to make predictions. Alerts are raised based in predictions and output.

3.6.8 DASHBOARDS

Figure 39: Real-time Example of Dashboard View of a NICU Infant (Singh et al., 2017)

IoT dashboard is the human-computer interface (HCI) between users and the medical devices in NICU. Users use dashboards to remotely monitor processes, provide medications, and control treatments from any location. A real-time dashboard view of a neonatal baby is shown in Figure 39. Such views help to assess the condition clearly as it gives all required parameters cumulatively.

3.6.9 REPORTING AND ANALYTICS USING IOT

Data collected from IoT sensors can be used for decision making, make accurate findings, and optimisation through real-time analytics. IoT data is a continuous one and employing machine algorithm is a great way to process and find hidden information in this data. In a natal ICU, the IoT data is used to make predictions, generate reports and alarms, and send messages and emails. Reports can also be generated for management.

3.6.10 TECHNOLOGIES FOR IOMT DEVICES IN NICU

IoT implementation in NICU requires a wireless connection to IoT devices with 3G or more, WiFi mesh, or WiMax. For data transmission, solutions with universal computing are available like RFID, Bluetooth, ZigBee, and WSN. Many US hospitals use WLAN wireless technology. WPAN or ZigBee is personal area network. WLAN and WPAN are the most affordable wireless network solutions for neonatal monitoring. The

mobility feature of WPAN helps to track other devices and provides room for non-obstructive neonatal monitoring (Gadekar & Vaze 2017).

3.6.11 MAKING A SELF-SUSTAINED SYSTEM

IoT objects interact with one another and regulate themselves based on feedback provided by the sensors. They play an important role in automating applications. NICU is also one area where IoTs play a chief role in collecting data from sensors in the incubator, process them, transmit them, check them again thresholds, provide alert messages, and regulate anomalies like temperature that does not require physician intervention. Thus it becomes a complete self-sustained system by itself, starting from acquiring input, producing output, and acting upon feedback from the output.

3.6.12 OVERCOMING SIGNAL INTERFERENCE

Lots of electronic devices used at one place can lead to signal interference with each other. The frequency and range of devices must be carefully chosen so that their operations do not overlap with one another. Some measures for interference mitigation are fast sleep/wake switching of devices, adaptive radio biasing, spur elimination, and radio co-existence characteristics for common Bluetooth, cellular, and LVDS signals. Assigning non-overlapping channels for Wi-Fi access points helps to reduce interference and packet-collision among channels (Shakunthala et al. 2018).

The manufacturers of IoT medical devices and hospitals must follow standards laid out for medical devices. Standards from HIPAA, HITECH, and FDA MDDS are some regulations that must be followed (Garg 2018).

3.6.13 SECURITY THREATS IN IOMT DEVICES AND THEIR MITIGATION

3.6.13.1 SECURITY THREATS
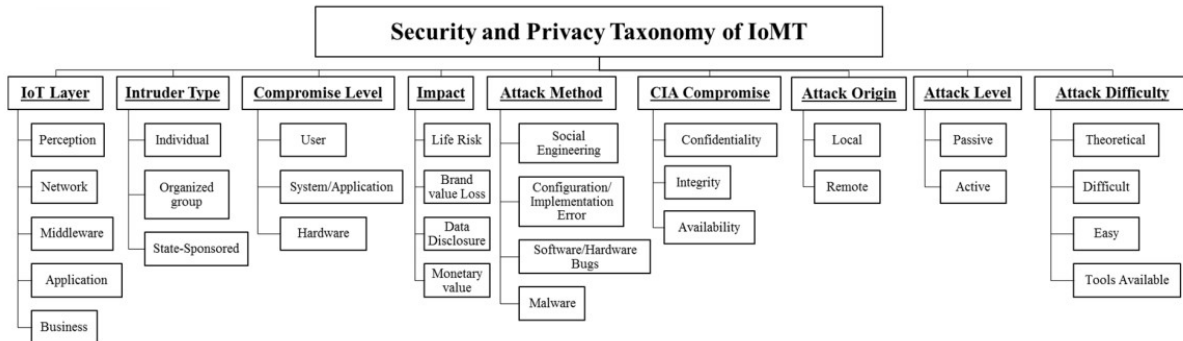
Figure 40: Security and Privacy Issues in IOMT (Alsubaei et al., 2017)

IoT devices are also prone to hardware and software attacks similar to any other technological device. Since the devices in NICU carry sensitive and patient specific information, security and privacy of IoT data have to be safeguarded. The privacy and security issues in IoMT devices are shown in Figure 40. The attacks can be from many dimensions like IoT layers, method, attack origin, level, difficulty, and many others, as shown in the figure (Alsubaei et al. 2017).

3.6.13.2 MITIGATION OF SECURITY THREATS

Some security mitigation measures in IoMT devices are (Panwar and Kumar 2015):

- Implementing a tamper resistant security mechanism
- Strong Authentication mechanisms
- Securing cloud services through methods like implementing access control and encryption
- Implementing security life-cycle management

Chapter 4: Ultrasound Based Respiration Monitoring System – Experiment 1 - Flat Surface (Cardboard)

A non-contact ultrasonic respiration rate monitoring system was developed for use in incubators. Its performance was evaluated on a manikin or on a computer controlled moving surface simulating the chest. The system was tested initially with one US sensor and the chest movement is simulated using a sine wave generator. This is done to check if the US sensor could capture signals and present them as graphs, so that this model could be used as a respiration monitoring system. Based on this basic setup, another laboratory setup with one to 4 US sensors was developed to be used in an incubator. This system also contained the DHT22 temperature and humidity sensor and an LCD to display the simulated respiration and pauses. Both MINI-A and HC-SR04 distance measuring US sensors are suitable for this monitoring system. A subwoofer was used to depict chest movements which was linked with the signal generator to allow the frequency and magnitude of movement to be adjusted.

The distance of the US transceiver to the surface was 50 cm. This is due to the measured distance of the US transceiver to the surface within the incubator would be roughly around 50 cm hence this distance was sufficient for this experiment. The sample rate used in the data recording was 20 samples per second. This was after investigating the best suited for sample rate for this experiment, 20 samples per second gave a smoother wave while witnessing the result. The sampling rate used was directly related to the range of frequencies that can be sampled. In addition, the separating distance for each of the four US sensors was 13.4 cm based on the measurement. This was due to the working angle of the US that was extracted from the datasheet of 15 degree. The distance was then calculated by using the trigonometry theory resulting in 13.4 cm being the distance from which two or many US can be placed next to each other with a 13.4 cm parting/space distance one another to prevent signal interference as demonstrated in Chapter 6.1.

The first part of this section explains the basic setup of the respiration rate monitoring system which contains a single US sensor and a sinewave generator linked to the subwoofer to simulate chest movement. Three different tests were performed with this basic setup, to find the suitability of using an US sensor to measure respiration rate of

an infant. The tests were conducted on 2 different surfaces namely flat surface and fabric cloth and these experiments are explained in chapters 4 and 5. Another experiment was conducted with the same setup to measure the respiration rate at 15 degrees' angle which is explained in chapter 6. All these 3 tests used MINI-A US sensor. Respiration rate monitoring system experimented using 4 sensors for higher precision is explained in chapter 7. This setup used HC-SR04 sensors.

Chapters 4, 5, and 6 depicted that US sensor could be used to measure respiration rate of an infant in an incubator. Chapter 7 which is an extended system of this setup, depicts a real-time system that could be used within an incubator. All these experiments consist of one to four distance measuring US sensors, a temperature and humidity measuring sensor (DHT22), display setup to project results, and the respiration signal simulation setup. Respiration signals and pauses were extracted from US sensor detected data. The practical results were compared against theoretical results obtained from Proteus software tool. The experimental sensor data obtained were analysed using MATLAB© and the results are depicted graphically.

Neonates in incubators do not move around significantly, therefore once the US transceiver is focused on the chest, the neonate's chest remains within the US beam. If the infants move outside the range of the US beam, a repositioning of the US transmitter and its associated receiver would be needed. This repositioning should be automatic through a feedback mechanism, however in this study this feature has not been utilised. Furthermore, in some infants, respiration causes abdomen movement and may be a better body location to track. Again, this feature has not been incorporated in this study. For clinical deployments, these features should be incorporated.

The US source transmits a high frequency sound wave to the surface being tracked. A proportion of its energy is reflected back to the US receiver. This distance between the US source and the surface (L) can be calculated by equation:

$$L = 0.5 \, Vt \, cos(\alpha) \tag{8}$$

EQUATION 7: DISTANCE BETWEEN US SOURCE AND SURFACE

where t is the time taken for the wave to propagate to the surface and reflect back to the US receiver, V is the speed of the US wave in air, and α is the signal angle between the transmitted and received waves. The factor 0.5 included as t represents the time taken for the signal to propagate to the surface and to return from it, i.e. covered distance of $2L$. When the US transmitter and receiver are close to each other, α could be considered as zero, hence $L = 0.5\ Vt$.

The face-to-face meeting restrictions imposed due to Covid-19 at the time of this study prevented a clinical trial involving testing the method on patients to be carried out. Instead, a setup was devised to test the effectiveness of the method. This setup simulated chest movements related to respiration. It consisted of a sinewave generator connected to a subwoofer. The surface of the subwoofer's cone was covered with a flat cardboard. Using this set up, the magnitude and frequency of the movements of the cardboard could be accurately controlled by adjusting the amplitude and frequency of the signal produced by the signal generator. This setup is shown in Figure 41. The distance of the US transceiver to the surface was 50 cm. The sample rate used in the data recording was 20 samples per second.

4.1 BASIC SETUP TO MEASURE RESPIRATION RATE

The platform devised to simulate chest movements is shown in Figure 41. A single MINI-A sensor is used in this setup. This ultrasound transceiver will be appropriately incorporated into an incubator. Captured US signal is processed and respiration rate information is derived from it.

A computer controlled system that simulates chest movements was developed to allow testing under different operating conditions. Utilising a mechanically automated subwoofer to model the breathing process will help carrying out respiration related tests in the laboratory, i.e. changing frequency and amplitude of movement.

<div align="center">

(a)   (b)

</div>
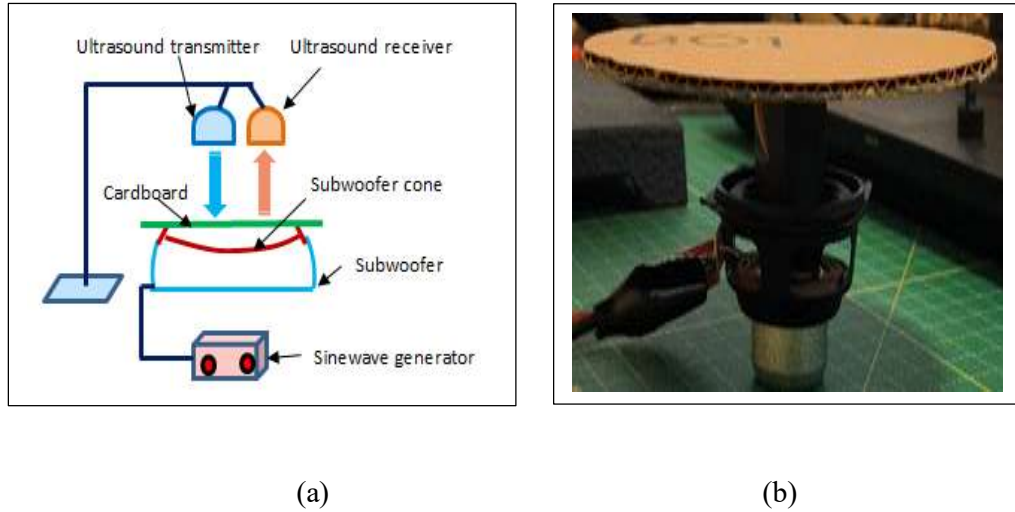
Figure 41: (A) Platform devised to Simulate Chest Movement - Schematic Diagram; (B) Modified Subwoofer Used to Simulate Chest Movement.

4.1.1 US WAVEFORM

Typical US waveform illustration would be as per Figure 42. The figure shows US pulse, echo signal and time measurement allocated.
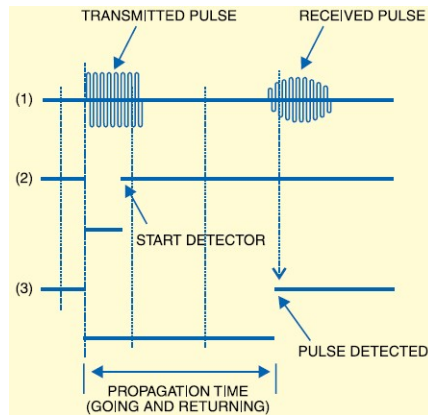
Figure 42: The Ultrasonic Pulse, Echo Signal and Time Measurement (Padmanabhan, 2008)

4.1.2 JUSTIFICATION FOR SELECTING ULTRASOUND TECHNOLOGY

US sensor is suitable for use in incubator for reasons that include:

- Feasibility studies indicated its suitability for this purpose.

- It is non-invasive
- Its operation is harmless
- It is cost effective
- Current US transceivers can measure distances to less than 0.5 mm, thus they tend to be accurate.
- They can be positioned at sufficient distance from the infant (0.5 meters away)
- They can be miniaturised to a small unit.
- They are efficient regarding power supply consumption.
- They can be integrated into an incubator.

4.1.3 NEED TO INTEGRATE ULTRASOUND RESPIRATION IN INCUBATORS

An infant in an incubator requires special care and monitoring. As part of this, his/her physiological signals need to be carefully monitored. A vital sign of health is respiration rate. Respiration rate is difficult to measure and devices that are currently available require contact with the infant's body directly. This causes discomfort and stress to the baby (that in turn affects respiration rate value), and they can also get dislodged. Therefore, there is a need for noncontact respiration rate monitor that can be rightly integrated into incubators.

4.1.4 EXPECTED CONTRIBUTIONS OF THE STUDY

Requirement specification:

- Accurately measure respiration rate (to at least 1 cycle per second) over long intervals.
- Ability to deal with possible unexpected infant movements during recordings.
- Deal with situations where chest movement switches to abdomen movement during respiration.
- Transmit the recorded signal wirelessly to a remote sever for continuous monitoring
- Suitably extract the statistics of respiration rate from respiration signal.
- Accurately study respiration patterns of infants in different scenarios
- Pass all safety tests.

The work is done with the collaboration of Sheffield Children Hospital.

4.1.5 BASIC BLOCK DIAGRAM OF THE SYSTEM

The block diagram of the ultrasound system to measure respiration rate is shown in Figure 43.

- The US sensor which acts as the signal transmitting and receiving device and the core of the project.
- Arduino Board for data capture
- Serial Communication Deployment tool to capture and transfer data to the Computer via a USB Cable

MATLAB$^©$. It is a numerical computing environment and fourth-generation programming language which is utilised for many engineering purposes. It shall be used for graphical depiction in this project.
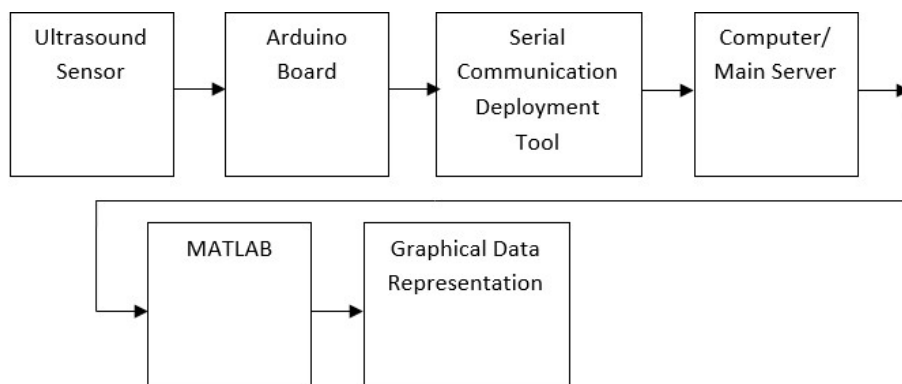
Figure 43: System Process Flow for the experiment performed whilst acquiring and evaluating collected data manually

The focus of this project is to utilise an US sensor to record the number of breaths per minute of a premature baby in an incubator. This would enable identifying any serious deviation in infants' respiration patterns, distinguish sequences or cycles of breathing, breathing rate count, movement of chest wall during breathing cycle, and the effect of different state of infant on breathing patterns. The practical setup of incubator to measure infants' respiration is shown in Appendix A.

The analysis is focused on providing basic understanding of infant's breathing cycles and deviations. It does not discuss about the air volume of breathing in infant as well as the effects of environment, on the breathing rate of infants. It is used in software

design stage especially in detection of errors of measurement and breathing count technique.

The data recorded in the initial stage of this project shall be transferred to MATLAB$^©$ to enable graphical illustration. The graphs are to be utilised for testing and analysis purposes. The MATLAB$^©$ code to graphically depict infant's respiration rate is given in Appendix B.

The US range sensor, is used to continuously trigger signals, send continuous pulses of transmit and receive, detect the distance between a baby manikin's chest, for laboratory testing purposes. The output voltage corresponding to distance of baby's chest is to be converted back to its corresponding distance value. The distance values shall be captured for a period of time and transferred with an aid of an Arduino board to the PC through USB connection. The data capture and transfer are performed offline by an application called "Serial Communication Deployment Version 1". The data are then processed using MATLAB$^©$ with a script built to filter the signal and plot technical/medical depiction graph to demonstrate infant's respiration rate. The use of IoT gives the ability to collect the raw data real-time.

The project would involve prototype exhibition of the whole setup in the laboratory, software design and execution with the aid of the Ultrasound sensor. The use of ThingSpeak server with MATLAB$^©$ built-in feature, will be used for processing the signal and graphically illustrate data to achieve the aim and objectives of this project.

4.2 EXPERIMENT WITH FLAT CARDBOARD PLATE SURFACE

4.2.1 INTRODUCTION

Respiration signals were tested with an aid of a moving surface that was used to simulate chest movement. A subwoofer was used to depict a moving chest which was linked with the signal generator to allow the frequency and magnitude of movement to be adjusted. Continuous ultrasonic pulses were generated and received by the US sensor in conjunction with the Arduino Board as a medium of data capture and transfer through a USB cable that is connected directly to a computer.

In this test, a flat cardboard plate-like surface is placed on top of the subwoofer. In the next test, the same technique is used, but a fabric cloth was placed on top of the cardboard plate.

The largest peak in the magnitude frequency spectrum of the signal recorded from the platform corresponded with signal's frequency thus indicating that respiration rate could be determined from the magnitude spectrum. This frequency was multiplied by 60 to convert cycles per second (Hz) to cycles per minute (unit of respiration rate). The investigations carried out indicated that the approach gave an accurate measure of the platform's movements and thus may have potential for measuring infant's respiration rate.

The recording time period of two minutes was adhered throughout the investigation. The use of Serial Communication Deployment software was in place to capture the data received from the Arduino board. With the aid of MATLAB$^©$ and the script built, the captured data were then saved into a file where it is used to convert numeric data into graphical representation.

The same experimental setup and computational logic is employed in the next experiment also.

4.2.2 RESULTS AND DISCUSSION

4.2.2.1 ILLUSTRATION OF 24 CYCLES/MIN

Output obtained when signals were sent by the US sensor at a frequency of 24 cycles/minute manually selected for a controlled test are shown in Figure 44. In addition, practical calculation and results demonstrated in Appendix T.

Theoretical Frequency Calculation:

Frequency set on the signal generator: 0.4 Hz

Frequency (f) measured from the graph for 24 cycles/min:

      = 24 / 60 sec   = 0.4 Hz
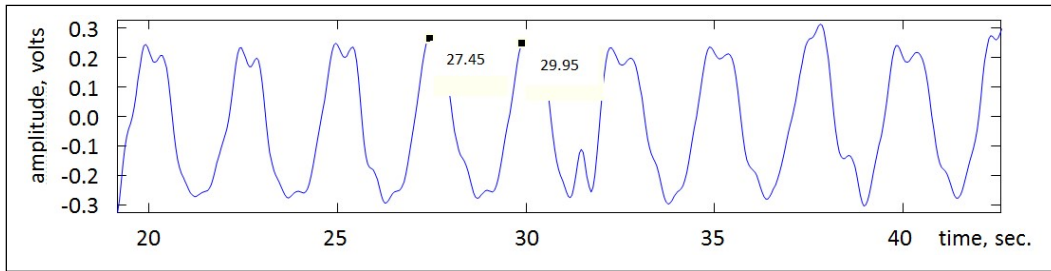
(a)
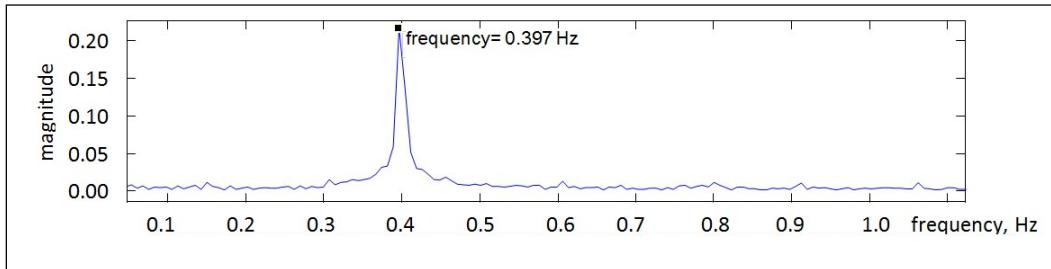
(b)

Figure 44: (A) An example of the recorded US signal. The values shown on the signal represent times associated with two successive peaks and thus their subtraction provides the signal's period. (B) The magnitude spectrum of the US signal

4.2.2.2 ILLUSTRATION OF 40 CYCLES/MIN

Output obtained when signals were sent by the US sensor at a frequency of 40 cycles/min are shown in Figure 45.

Figure 45: Illustration of 40 Cycles/Min

4.2.2.3 ILLUSTRATION OF 66 CYCLES/MIN

Output obtained when signals were sent by the US sensor at a frequency of 60 cycles/min are shown in Figure 46.
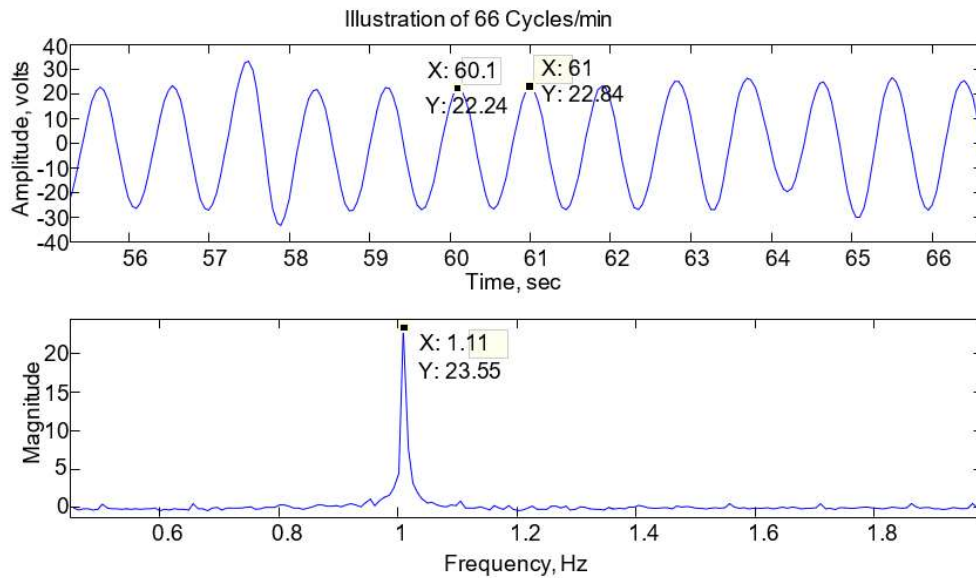
Figure 46: Illustration of 66 Cycles/Min

4.2.2.4 TABLE OF RESULTS

Table 1 provides the measured US signal, determined by identifying the frequency

corresponding to the peak in its magnitude frequency spectrum, as signal generator

67

frequency is increased from 0.1 Hz to 1.1 Hz. Figure 47 shows the plot of ultrasound

signal frequency against signal generator frequency.

Table 2. Measured Frequencies and Their Differences

Signal Generator Frequency, Hz, (F)		Ultrasound Signal Frequency, Hz, (US)	F- US (Hz)
	0.1	0.100	0.000
	0.2	0.201	0.001
	0.3	0.311	0.011
	0.4	0.397	-0.003
	0.5	0.500	0.000
	0.6	0.666	0.066
	0.7	0.699	-0.001
	0.8	0.801	0.001
	0.9	0.901	0.001
	1.1	1.11	0.010
Mean	0.56	0.57	0.0086

Figure 47: Plot of Ultrasound Signal Frequency against Signal Generator
Frequency

4.2.2.5 DISCUSSION

The theory and practical results tally up quite significantly as per Experiment 1, as far
as the flat board test goes.

The frequency range corresponds to a breathing range $0.1 \times 60 = 6$ bpm to $1.0 \times 60 = 60$
bpm. The mean and standard deviation of the frequencies associated with signal
generator were 0.56 Hz and 0.303 Hz. The mean and standard deviation of the
frequencies associated with the US signal were 0.57Hz and 0.300 Hz. The percentage
difference between the stated means is -14.6%. The frequency of the US signal is

68

plotted against that of the signal generator in Figure 47 and a close relationship is observed (gradient 0.93).

The theory and practical results are 0.3Hz and 0.311Hz respectively, where the frequency difference is about 0.011Hz. Relating this signal to respiration rate, 0.3 Hz corresponds $0.3×60=18$ bpm, whereas the results demonstrate $0.311×60=18.66$ bpm. Difference of 0.66 bpm.

The signal generator's frequency was set to 0.4 Hz. The frequency of the recorded US signal determined from its magnitude frequency spectrum is 0.39 Hz. Relating this signal to respiration rate, 0.4 Hz corresponds $0.4×60=24$ bpm, whereas the results demonstrate $0.39x60=23.4$ bpm. Difference of 0.6 bpm.

Furthermore, the signal generator's frequency was set to 1.1 Hz. The frequency of the recorded US signal determined from its magnitude frequency spectrum is 1.11 Hz. Relating this signal to respiration rate, 1.1 Hz corresponds $1.1×60=66$ bpm, whereas the results demonstrate $1.11×60=66.6$ bpm. Difference of 0.6 bpm.

The amplitude of the recorded signal appears to be distorted even after processing the signal. The amplitude of the signal is not constant. In theory, it should be same as the depth of the speaker throughout. On the other hand, the signal fluctuates quite frequently. The higher the frequency the smoother the amplitude and lesser signal distortion.

Looking at the overall practical investigation for all the cycles for this test, the accuracy in findings was observed every time there is an increase in the frequency. It is also evident that practical results are dependent on how controlled the experiment was performed. There was no major fluctuation in the collected signal.

The inaccuracy between the signal generator's frequencies and the US signal's frequency are partly related to:

- Accuracy of the frequency setting on the signal generator.
- Accuracy of reading the frequency associated with the peak in the magnitude frequency spectrum.

By using a more advanced US transceiver, the measurement could also be further improved.

Chapter 5: Ultrasound Based Respiration Monitoring System – Experiment 2 - Fabric Surface

5.1 INTRODUCTION

Respiration signals were tested with an aid of a moving surface that was used to simulate chest movement. A subwoofer was used to depict a moving chest which was linked with the signal generator to allow the frequency and magnitude of movement to be adjusted. Continuous ultrasonic pulses were generated from the signal generator and received by the US sensor. Arduino Board is used as the medium of data capture and data is transferred to a computer directly through a USB cable.

The previous test employed a flat cardboard plate-like surface on top of the subwoofer. In this test, a fabric cloth was placed on top of the cardboard plate.

5.2 RESULTS AND DISCUSSION

The experiment was conducted where ultrasound signals at various frequencies were sent to a surface covered with a cloth.

5.2.1 TABLE OF RESULTS

Table 3 provides the measured US signals obtained by place the ultrasound system setup from the previous setup and placing a fabric cloth on top of the cardboard plate. The data was captured and determined by identifying the frequency corresponding to the peak in its magnitude frequency spectrum, as signal generator frequency is increased from 0.1 Hz to 1.1 Hz. Table 3 shows the plot of US signal frequency against signal generator frequency.

Table 3. Measured Frequencies and Their Differences

Signal Generator Frequency, Hz, (F)	Ultrasound Signal Frequency, Hz, (US)	F-US (Hz)
0.1		
0.2		
0.3		
0.4	9.683	-0.003
0.5		
0.6	9.688	0.022
0.7		
0.8		
0.9		
1.0	9.669	0.11

5.2.2 DISCUSSION

The investigation of this test performed, done on a flat surface covered with a cloth was not a successful test and as it was as expected, because of the properties of the material/surface being used. The US pulses were mainly absorbed and scattered, resulting in partial reading of the receiving echo signal. This is because the US waves were not bouncing off the cloth surface into the US sensor and in result of that, the plot of US signal frequency against signal generator frequency was not provided due to its inaccuracy.

Chapter 6: Ultrasound Based Respiration Monitoring System – Experiment 3 – Setup to Measure Respiration Rate Within The 15 Degree Angle: 7 cm away from the US Centre Point

6.1 INTRODUCTION

The basic setup remains the same as in chapters 4 and 5. The difference in method comes in measuring the signal response from an object that was placed 7 cm away from the centre point of the US. This distance was mathematically calculated based on the trigonometry theory, where, Tan θ = Opposite / Adjacent, where Opposite was 13.4 cm as shown below. The subwoofer was used to depict a moving chest which was linked with the signal generator to allow the frequency and magnitude of movement to be adjusted, the experiment proves that moving object, as long as it is within the 15 degrees angle as per the US datasheet (SENSCOMP, 2016). Sections 3.4.9 and 3.4.10 indicate that sensors are efficient in sensing distances within 15 degrees. Figure 52 shows the angular distances used to carry out this experiment.

Angle A, which was the working angle of the US sensor as per the datasheet, is 15 degrees (SENSCOMP, 2016).

Side b (adjacent), which was the side/height from the base/object to the fixated US, is 50 cm height.

Using the trigonometry theory, side a (opposite), which was the working distance, in addition to the distance from which another sensor was placed to prevent interference that would result in inaccuracy,

Equation 13 is used to work out the working distance to aid the multiple sensors placement experiment.

$$\text{Tan } \theta = \text{Opposite / Adjacent} \tag{13}$$

EQUATION 8: COMPUTE TAN Θ

Here, Tan θ = 15 degrees

b = 50cm

a =?

a = Tan θ * b

angle A
15°

side b
50 cm

side a
13.397 cm

A

c

b

C = 90°

B

a
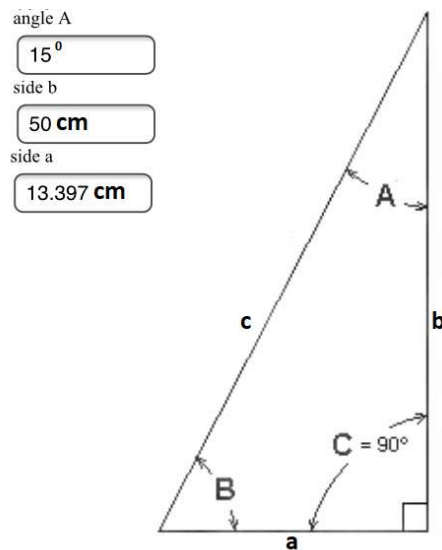
Figure 48: US Working Angle

6.2 RESULTS AND DISCUSSION

The experiment was conducted where US signals at various frequencies were sent to a surface at 15-degree angle. The resultant graphs are shown in Figures 53 to 55.

6.2.1 ILLUSTRATION OF 24 CYCLES/MIN

Output obtained when signals were sent by the US sensor at a frequency of 24 cycles/minute manually selected for a controlled test are shown in Figure 53.

Illustration of 24 Cycles/min
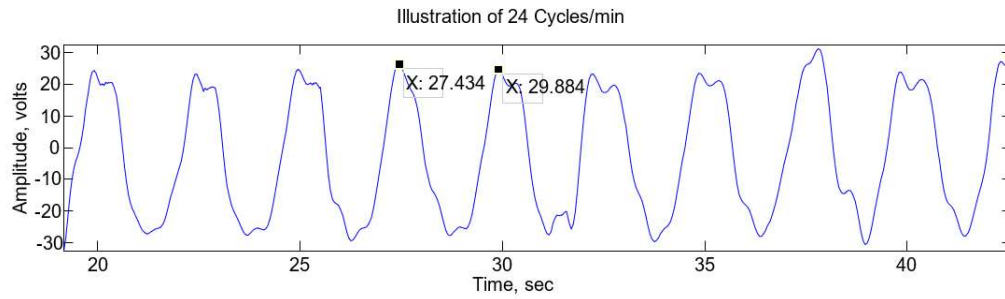
(a)
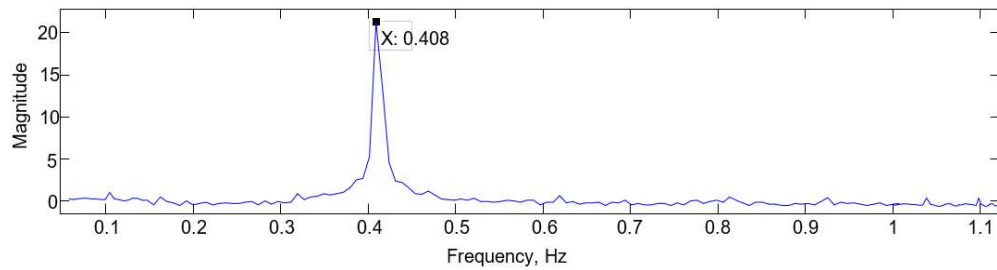
(b)

Figure 49: (A) An example of the recorded US signal. The values shown on the signal represent times associated with two successive peaks and thus their subtraction provides the signal's period. (b) The magnitude spectrum of the US signal

6.2.2 ILLUSTRATION OF 40 CYCLES/MIN

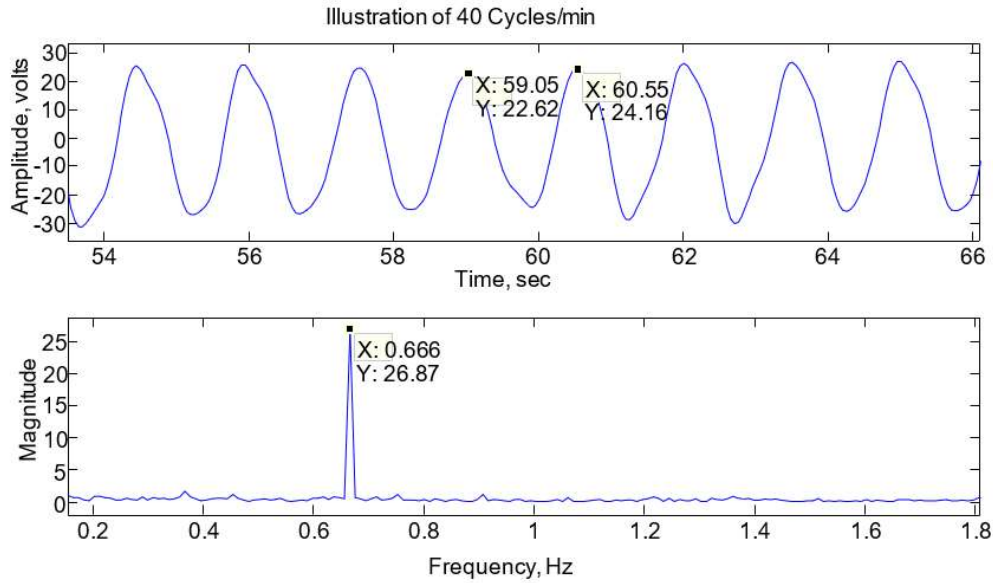Output obtained when signals were sent by the US sensor at a frequency of 40 cycles/min are shown in Figure 54.
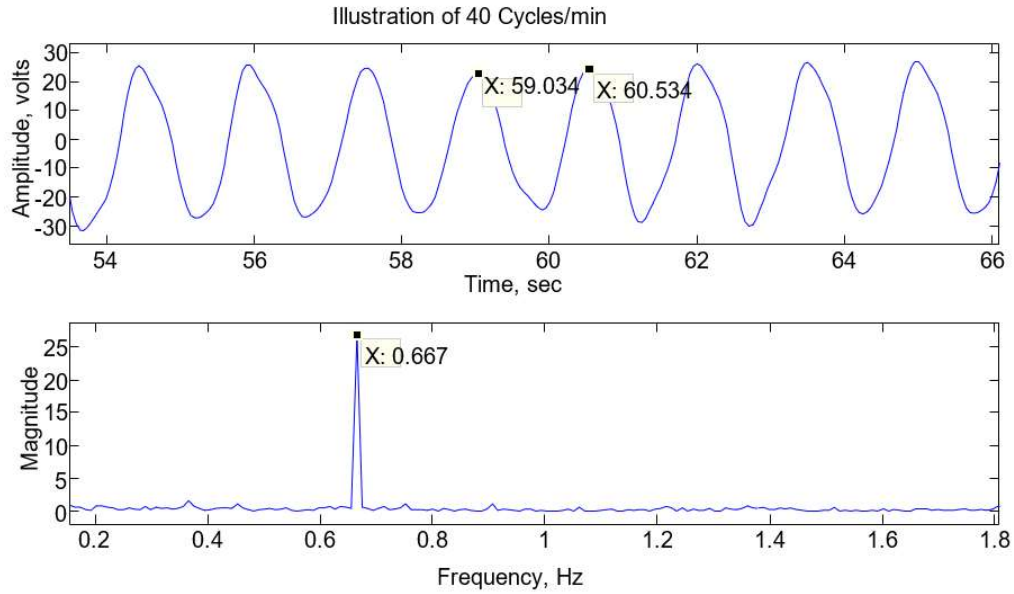
Figure 50: Illustration of 40 Cycles/Min

6.2.3 ILLUSTRATION OF 66 CYCLES/MIN

Output obtained when signals were sent by the US sensor at a frequency of 66 cycles/min are shown in Figure 55.
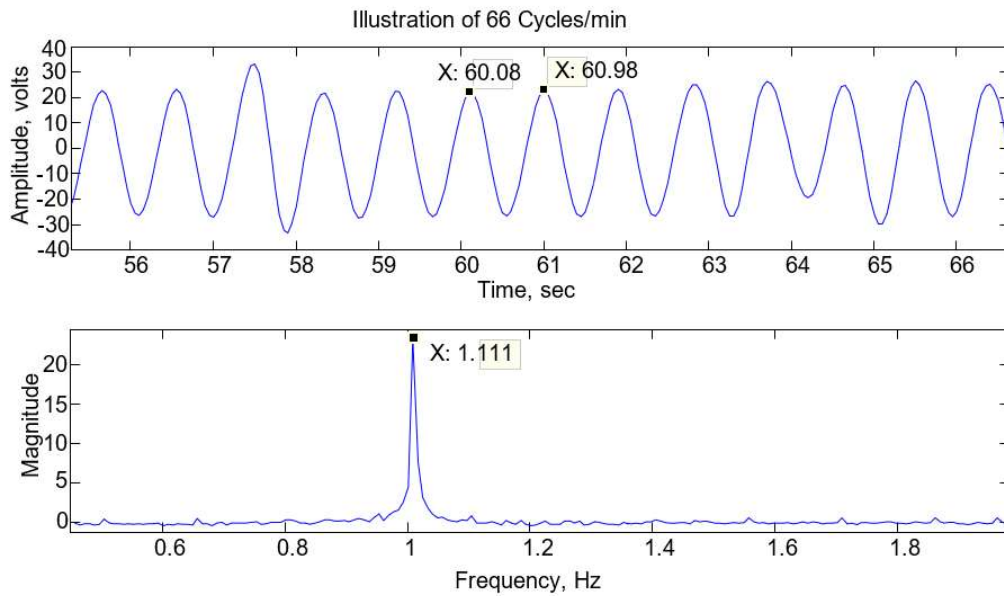
Figure 51: Illustration of 66 Cycles/Min

6.2.4 TABLE OF RESULTS

Table 4 provides the measured US signal, determined by identifying the frequency corresponding to the peak in its magnitude frequency spectrum, as signal generator frequency is increased from 0.1 Hz to 1.1 Hz. Figure 56 shows the plot of ultrasound signal frequency against signal generator frequency.

Table 4: Measured Frequencies and Their Differences

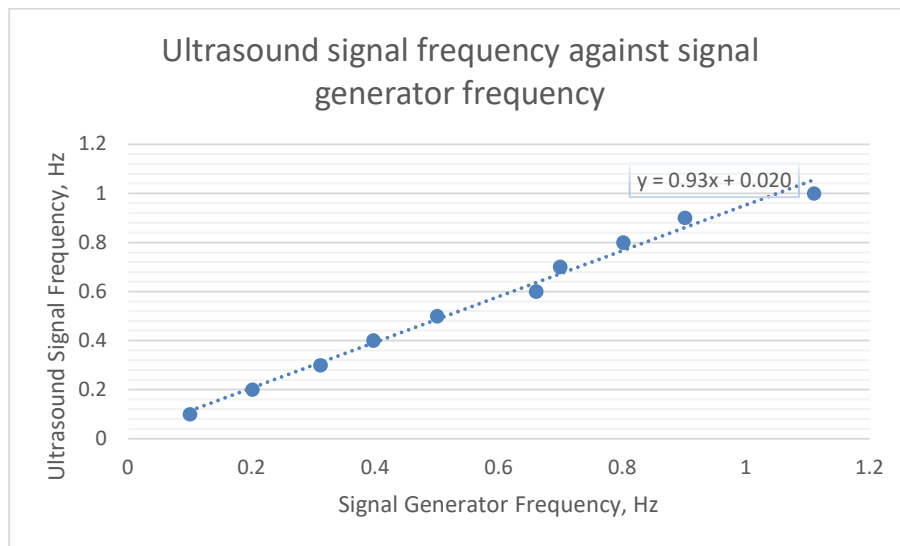| Signal Generator Frequency, Hz, (F)		Ultrasound Signal Frequency, Hz, (US)	F-US (Hz)
	0.1	0.084	-0.084
	0.2	0.193	-0.007
	0.3	0.327	0.027
	0.4	0.408	0.008
	0.5	0.489	-0.011
	0.6	0.667	0.067
	0.7	0.657	-0.043
	0.8	0.769	-0.031
	0.9	0.896	-0.004
	1.1	1.111	0.011
Mean	0.56	0.5601	0.007
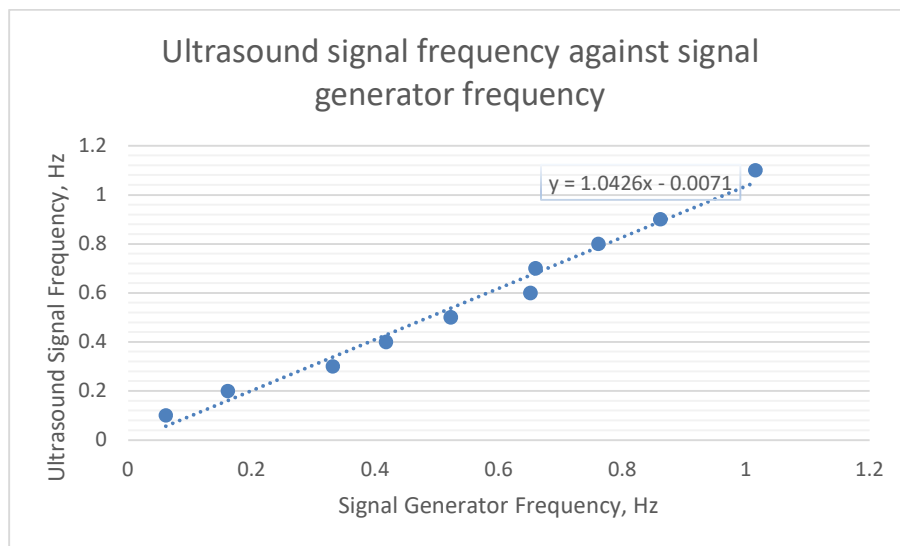
Figure 52: Plot of Ultrasound Signal Frequency against Signal Generator Frequency

6.2.5 DISCUSSION

The theory and practical results tally up quite significantly as per the experiment. The table of results shows near enough accurate result with the occasional signal interference and distortion. It too demonstrates that by moving the object 7 cm away from the centre point of the US, since it is still within the US working range of 15 degrees, based on the datasheet, looking at the results, it does affect the signals negatively, but to an extent where it still adheres to the datasheet (SENSCOMP, 2016). In addition, on some occasions, it was witnessed that the result was more to the positive hence this shows that the use of this US will give us good results but not the best from the accuracy perspectives and for that further tests and or the use of a medical grade ultrasonic sensor would be a viable means of testing signal accuracy.

The frequency range corresponds to a breathing range of 0.1×60=6 bpm to 1.1×60=66 bpm. The mean of the signal generator was 0.56 Hz. The mean of the US signal was 0.5601 Hz. The percentage difference between the stated means is -1.196%. The frequency of the US signal is plotted against that of the signal generator in Figure 56 and a close relationship is observed (gradient 1.0426).

The theory and practical results are 0.3Hz and 0.327Hz respectively, where the frequency difference is about -0.027Hz. Relating this signal to respiration rate, 0.3Hz corresponds to 0.3×60=18 bpm, whereas the results demonstrate as 0.327x60=19.62 bpm. Difference is -1.62 bpm.

The signal generator's frequency was set to 0.4 Hz. The frequency of the recorded US signal determined from its magnitude frequency spectrum is 0.408 Hz. Relating this signal to respiration rate, 0.4 Hz corresponds 0.408×60=24.48 bpm.

Furthermore, the signal generator's frequency was set to 1.1 Hz. The frequency of the recorded US signal determined from its magnitude frequency spectrum is 1.11 Hz. Relating this signal to respiration rate, 1.111 Hz corresponds 1.1×60=66 bpm, whereas the results demonstrate 1.111x60=66.66 bpm. Difference of 0.66 bpm.

The amplitude of the recorded signal appears to be distorted even after processing the signal. The amplitude of the signal is not constant. In theory, it should be same as the depth of the speaker throughout. On the other hand, the signal fluctuates quite

frequently. The higher the frequency, the smoother the amplitude and lesser the signal distortion that is when compared with Figure 54 and Figure 53

Looking at the overall practical investigation for all the cycles, the accuracy in findings was observed every time there is an increase and decrease in the frequency. It is also evident that practical results are dependent on how controlled the experiment was performed. Basing it on the collected result, the test adheres to the datasheet from the angle of the US stand point hence it has been reflected in the result where a mix of positive and negative result was captured resulting in no major fluctuation in the collected signal.

The inaccuracy between the signal generator's frequencies and the US signal's frequency are partly related to:

- Accuracy of the frequency setting on the signal generator.

- Accuracy of reading the frequency associated with the peak in the magnitude frequency spectrum.

By using a more advanced US transceiver, the measurement could also be further improved.

Chapter 7: Ultrasound Based Respiration Monitoring System – Experiment 4: Setup to Measure Respiration Rate Using 4 Ultrasonic Sensors

7.1 INTRODUCTION

In this section, two methods of experiments were adapted to test the placement of the sensors to detect object movement, along with getting accurate results and avoiding signal interference. One of the methods was a statistical approach using the Boolean logic while leveraging other peripherals. The other method was non-statistical approach. The non-statistical method was synchronised where all four sensors collect data at the same time and are later analysed. The aim of signal detection of US sensors was to find primarily the respiration rate at various time intervals. The distance from each of the placed sensor was 13.4 cm apart to avoid signal interference, based on the previous experiment in chapter 6.

The system was implemented using peripherals such as a temperature and humidity sensor and a controller. US signal was recorded using Arduino board and the processing was based on MATLAB$^©$ data analysis tool. A liquid crystal display (LCD) was used to display results. The variation between the previous 3 experiments and this experiment is that this test uses 4 sensors and hence will measure the respiration rate more accurately. It also uses temperature sensor, LCD and alarm system to show the results and the test performed 13.4 cm away from US Centre Points. In addition, a software, namely Proteus, was used to illustrate the setup and functionality with results when the whole system is integrated with the peripherals.

Chest movement was simulated using a sinewave generator controlled moving platform. The results also indicated that US technology for measuring and monitoring respiration rate in infants may be a valid technique, provided that there are multiple US sensors for detection of optimum positioning and that the infant is not covered by clothes. A quick test was performed on human skin just by placing it under the US and seeing the results while calculating the number of movements per minute, trying to depict the movement of the chest roughly near as possible and seeing the result if there were any absorption/distortion/interference in signal. The results were favourable and according

to the initially expected providing the means of continuation with the experiment and investigation.

Lastly, the results are captured in a table and charted to showcase findings.

7.2 MATERIALS AND METHODS

Though many ways are available to solve a problem, a specific and suitable method is chosen to work on that problem and implement a solution. Methodology is defined as the process through which a technique can be used for both simulating in software and implementation in hardware. In this chapter, a technique is described which is used to achieve the objectives of this study.

7.2.1 MATERIALS AND THEIR PURPOSE

The signal used to test the US sensor was a moving platform controlled by a sinewave generator. The hardware used in this study were:

1) 4 US sensors: used for detecting signal measurements
2) Temperature and humidity sensors: used for calibrating the ultrasound sensor
3) ATmega micro-controller (in Arduino Uno): used to interface sensors to computer
4) Liquid crystal display (LCD): used to show results
5) A light emitting diode (LED): used as an indicator of the device's operation.
6) A buzzer: used as abnormal indicator
7) Sinewave generator: Test signal

7.3 AN IMPORTANT QUESTION - WHY 4 ULTRASONIC SENSORS ARE USED?

Why 4 sensors are used instead of 2 or 3?

One distance measuring US sensor was used in the basic study discussed in Part A. Though it senses the movement of the subwoofer or the infant placed in its vicinity, when the infant moves or turns around, the sensor may not be able to sense the movement if the object moves out of its range. More than one sensor can be used to measure the movement effectively. The effectiveness of using 2, 3, or 4 sensors is analysed.

Measurement (Count) and detection are possible using 2 or 3 sensors but there is the problem of angular difference. It is the difference in angle between the object and the US sensors. If two sensors are used, then the difference in angle is 180˚. This setup can be used if only straight measurements are done or the object is placed in a straight line with the sensors.

When three sensors are used for measurement, the difference in angle is 120˚.

When four sensors are used, this difference in angle is just 90˚. With this angle difference, precise, accurate and effective measurement of sine wave ripples, and hence the object, is attained.

7.4 DEMO FIGURE

A schematic diagram of the setup with 4 US sensors is shown in Figure 57.
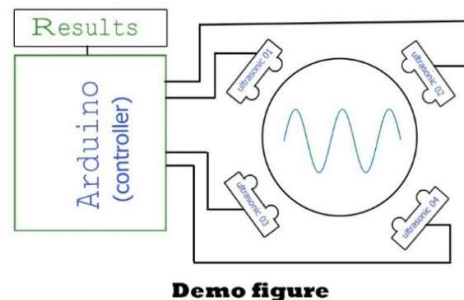
Figure 53: Schematic Diagram of the Setup

7.5 ANALYSIS

Ripple rate (frequency of measured signal) analysis was performed based on some predefined conditions. Abnormal is displayed as "ABNOR" and normal is displayed as "NOR" in the LCD. The conditions are:

➤ If no legitimate ripples were witnessed for ten seconds, then this period was considered as pause and was measured until any legitimate ripples were detected from the breathing perspectives. When this condition happens, the buzzer went ON, along with display of result in LCD. If the pause was less than or equal to 10 seconds, it was considered as normal. The result shown to user are:

Pause: NOR

- ➢ Let the pause be 15 seconds. It is abnormal since it is more than 10 seconds. Displayed: Pause: ABNOR (15)

- ➢ Normally, respiration rate is measured for 1 minute. Hence, Ripple count analysis will be performed after sixty seconds.

- ➢ For infants, the respiration rate is 30 to 60 breaths per minute (Fogoros, 2020). If Ripple rate was less than 30 or greater than 60, then it was considered as abnormal count, (displayed as "ABNOR").

- ➢ On the other hand, if the Ripple count value was between 30 and 60 in a sixty seconds period, then this value was considered as normal count, which was displayed as "NOR" in the LCD. The Ripple signals detected are shown as "Rip" in the LCD. The result for the Ripple count shown to user are:

For normal Ripple:

Rip: NOR (45), where 45 is the ripple (breath) per minute

For abnormal Ripple, the buzzer will also go ON and the status shown to user in LCD will be:

Rip: ABNOR (25), where 25 is the ripple (breath) per minute

7.6 FLOW CHART

The complete working process and analysis of the circuit is given in the flow chart shown in Figure 58.
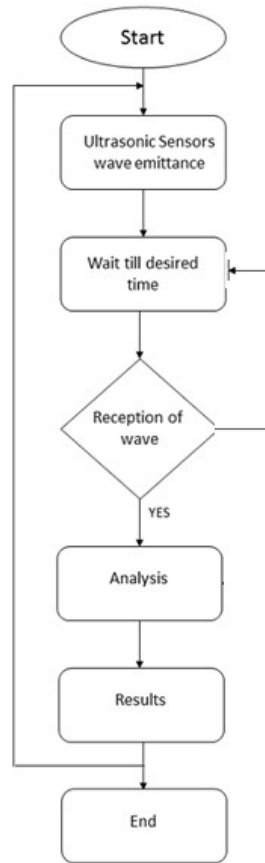
Figure 54: Working and Analysis Procedure

The pause and Ripple analysis of the circuit detected data is extensively described in the flow chart shown in Figure 59.
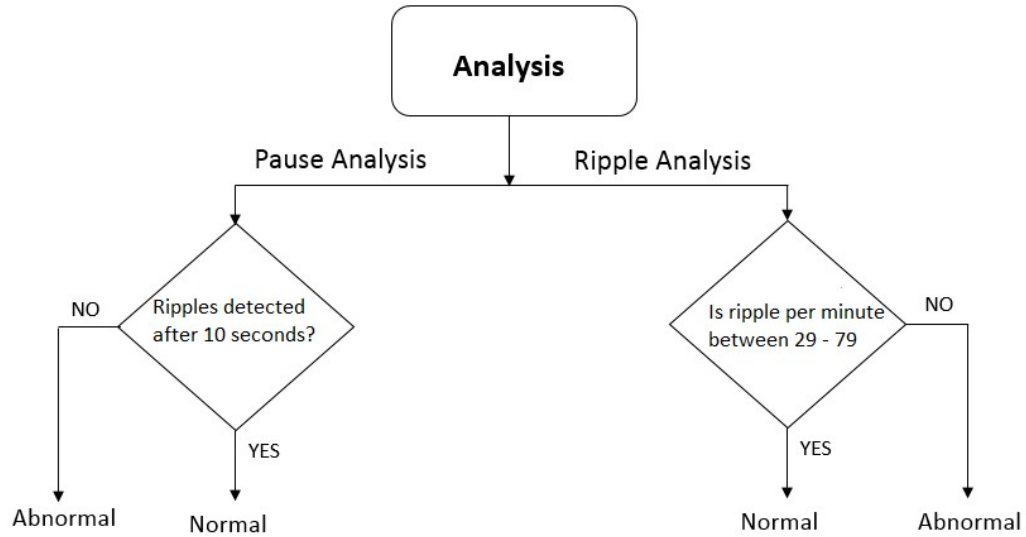
Figure 55: Pause and Ripple Analysis Flow Chart (MORLEY ET AL., 1990)

7.7 CIRCUIT DIAGRAM

The circuit diagram of sinewaves detection and Ripple and pause analysis process is shown in the Figure 60. A basic introduction of hardware components used in the circuit is given in Appendix C. Each sensor was placed at 90 degrees with respect to predecessor and successor.
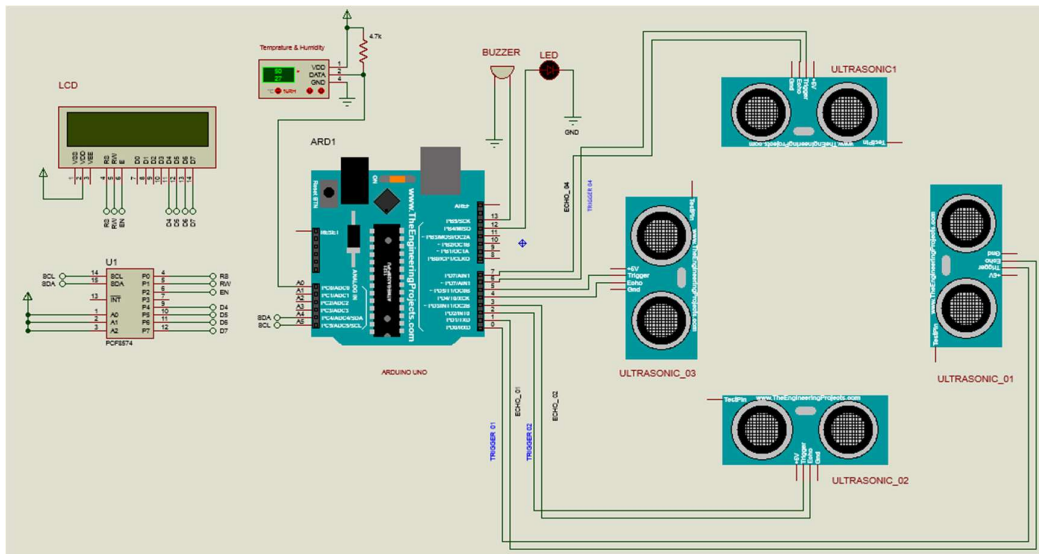
Figure 56: Circuit Diagram of Sine Wave detection and analysis process

7.8 IMPLEMENTATION OF THE CIRCUIT

As shown in Figure 60, the interfacing of the components, US sensors and I2C LCD with Arduino are explained in Appendix C, Appendix E, and Appendix F respectively.

After connectivity is established, the system starts. The following activities takes place.

System statuses are indicated to the user through LED and buzzer.

- Temperature and humidity sensor start working
- The US waves are emitted by all four sensors. To minimise the interference issues, time to capture signal from each sensor or time to trigger each sensor are calculated and planned. The sensors are triggered one by one and not at the same time. When the emitted wave bounces back after reflection then it is counted as ripple count by controller.
- When there are no reflection elapses 10 seconds, then this is considered as 'pause' by the circuit.
- If a pause is detected by the system, then buzzer is powered ON until there is no pause detected there it then becomes as normal.
- When Ripple is detected by the system, the LED blinks. Otherwise, it remains off.
- The buzzer also is on an "ON" state for Ripple abnormality detected over a span of 60 sec.
- The Ripple is abnormal when the count is below 29 or greater than 79.

7.9 KEY LOGIC IN CIRCUIT

The requirements of this project are detection and measurement of movement parameters using four ultrasonic (US) sensors. Therefore, the foremost and important step in the project is integration of these 4 US sensors. There are several methods that can be used for this integration, each having its own advantages and disadvantages.

Some of the methods are discussed below:

1) Simple Method:
- if one of the four sensors detected pulse and range within the predefined parameters, then device showed normal breathing

- if none of the four sensors detected pulse, then device indicated abnormal breathing, resulting in sounding of a buzzer

2) Statistical Method:

Let us consider all states of these four US sensors. Then all possible states from these four US sensors are computed using statistical techniques, which are explained in Appendix I. The notations S1, S2, S3, and S4 are used for US sensors 1, 2, 3, and 4 respectively. The status "1" means ripple was detected by the sensor and status "0" means no ripple was detected by the sensor.

All possible states for the four ultrasonic sensors are described:

   i.   S1 = 0, S2 = 0, S3 = 0, S4 =0 (no detection by any sensor)
  ii.   S1 = 1, S2 = 0, S3 = 0, S4 =0 (detection by only sensor 1)
 iii.   S1 = 0, S2 = 1, S3 = 0, S4 =0 (detection by only sensor 2)
 iv.   S1 = 0, S2 = 0, S3 = 1, S4 =0 (detection by only sensor 3)
  v.   S1 = 0, S2 = 0, S3 = 0, S4 =1 (detection by only sensor 4)
 vi.   S1 = 1, S2 = 1, S3 = 0, S4 =0 (detection by only sensors 1 & 2)
 vii.   S1 = 1, S2 = 0, S3 = 1, S4 =0 (detection by only sensors 1 & 3)
viii.   S1 = 1, S2 = 0, S3 = 1, S4 =1 (detection by only sensors 1 & 4)
 ix.   S1 = 0, S2 = 1, S3 = 1, S4 =0 (detection by only sensors 2 & 3)
  x.   S1 = 0, S2 = 1, S3 = 0, S4 =1 (detection by only sensors 2 & 4)
 xi.   S1 = 0, S2 = 0, S3 = 1, S4 =1 (detection by only sensors 3 & 4)
 xii.   S1 = 1, S2 = 1, S3 = 1, S4 =0 (detection by sensors 1,2 & 3)
xiii.   S1 = 1, S2 = 1, S3 = 0, S4 =1 (detection by sensors 1,2 & 4)
xiv.   S1 = 1, S2 = 0, S3 = 1, S4 =1 (detection by sensors 1,3 & 4)
 xv.   S1 = 0, S2 = 1, S3 = 1, S4 =1 (detection by sensors 2,3 & 4)
xvi.   S1 = 1, S2 = 1, S3 = 1, S4 =1 (detection by all sensors)

For this study, the statistical method was employed to detect ripples from the sensor and hence movement of the infant.

The Arduino code used for Ripple measurement and analysis is explained in Appendix J.

7.10.1 RESPIRATION AND PAUSES AT VARIOUS TIME INTERVALS – THEORETICAL RESULTS (PROTEUS SIMULATION RESULTS)

The simulation of the signal detection circuit was done using Proteus Software tool.

The simulation results are:

1) Setup 1 – Let the ripple be generated for a period (time) of less than 60 seconds. The following cases can occur:

   (7) When no ripple exists, then after 10 seconds, the buzzer goes ON. This effect is shown in Figure 61.
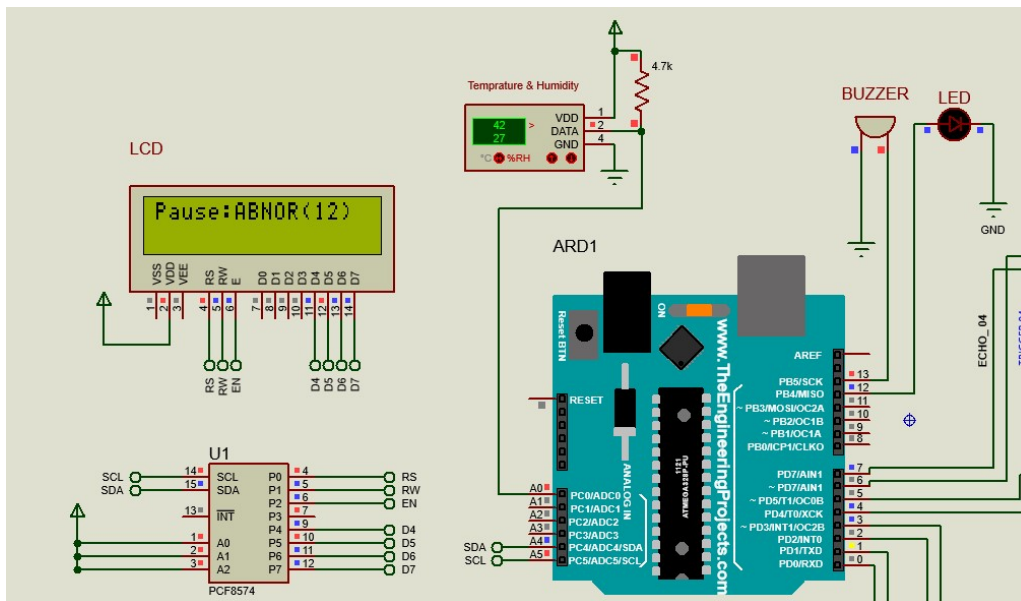
Figure 57: No Ripple Occurs

(ii) The effect in the circuit when pause is normal is shown in Figure 62.
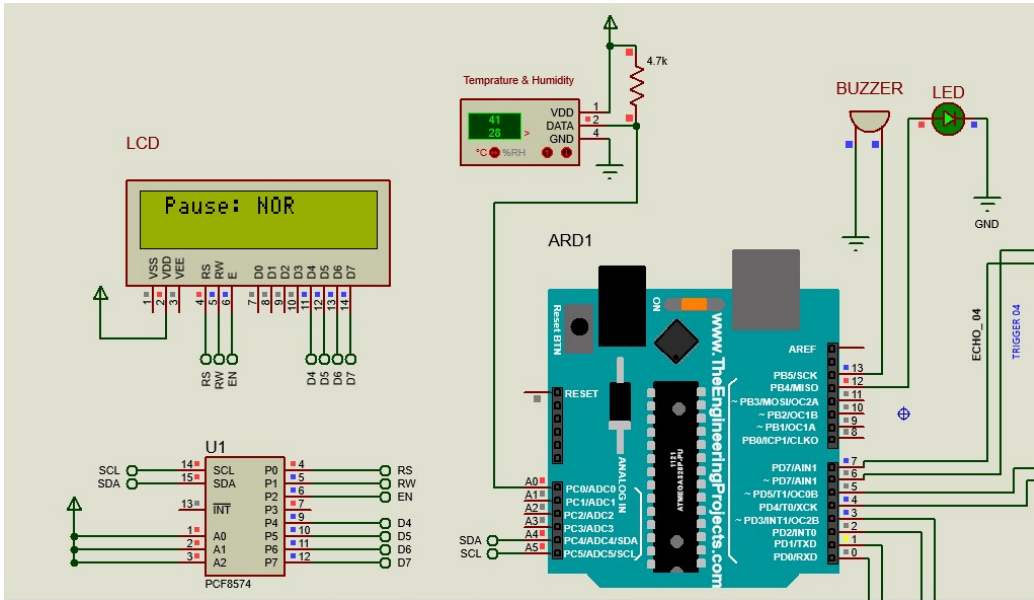
Figure 58*:* When Pause is normal and Ripple are detected

(iii) When pause is normal but there is no detection of ripple, the LED should be OFF and buzzer will not be ON. This effect is shown in Figure 63.
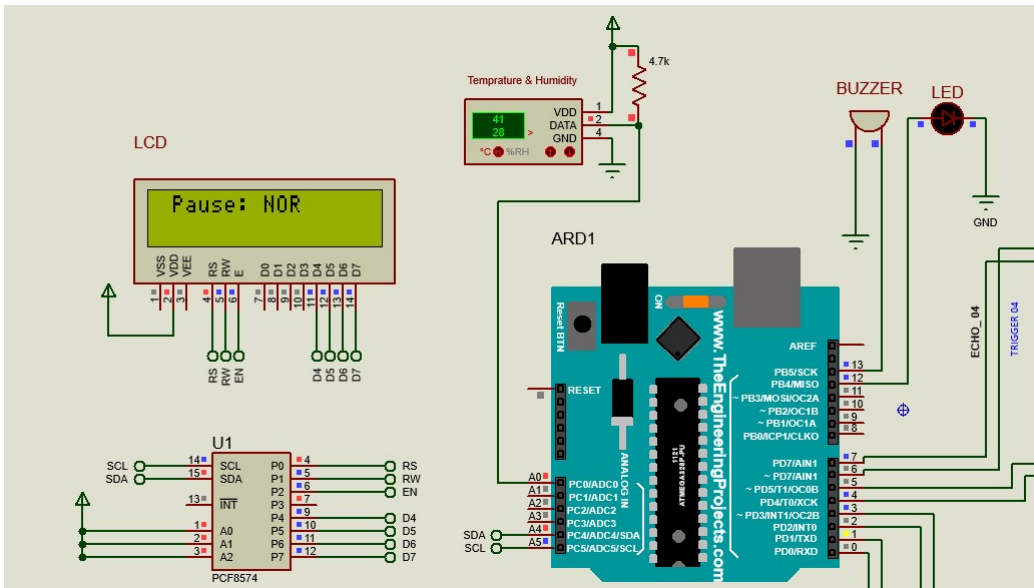
Figure 59: Pause is normal but no detection of ripple

2) Setup 2 – Let ripple generation time be 60 seconds. After 60 seconds, ripple counting results shows. The following cases occurs:

(7) In first iteration, the ripple count was abnormal (less than 29 ripples per minute). Due to this abnormality of ripple count (22 ripples per minute) in sixty seconds, the buzzer went ON. This effect is shown in Figure 64. The LED blinked indicating that ripples were detected by the US sensors.
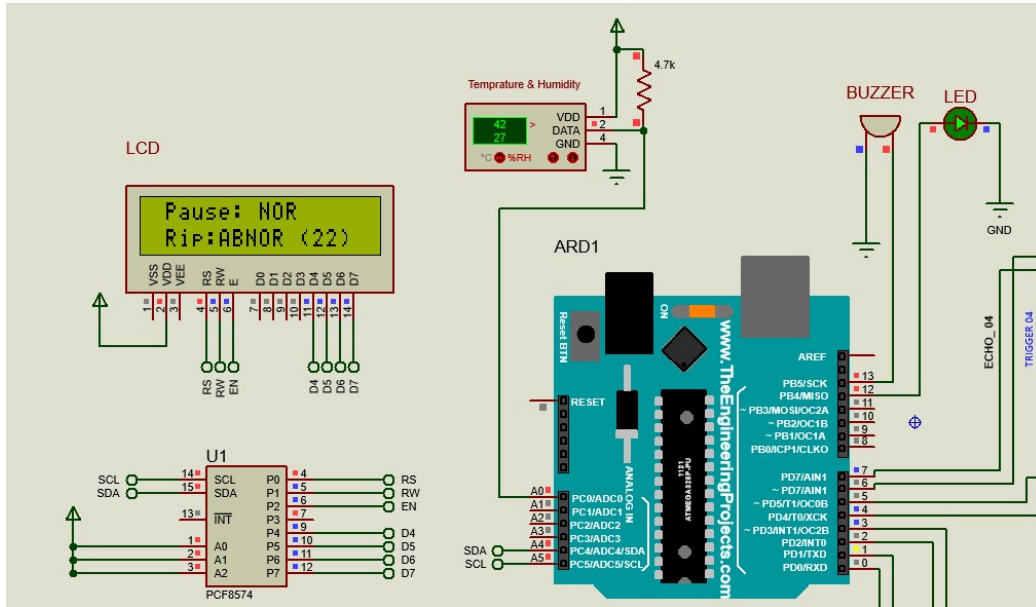
Figure 60: Abnormality in Ripple Count

(ii) In second iteration, the ripple count was normal. Due to normal ripple count (45 ripples per minute being within the range of greater than 29 and less than 79), the buzzer remained OFF. Since ripple were detected by US sensors, LED blinked. This effect is shown in Figure 65.
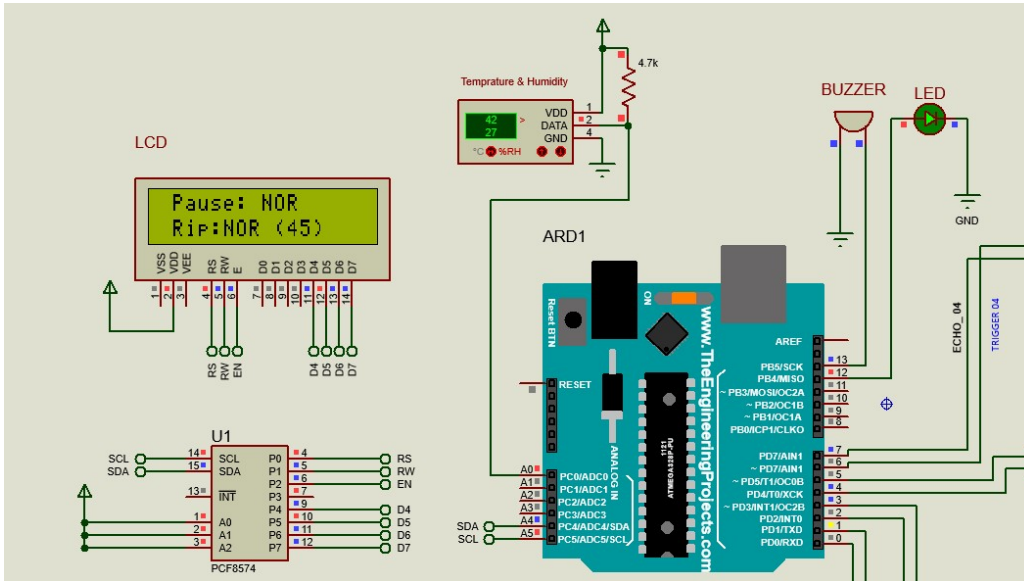
Figure 61*:* Normal Ripple Count

7.10.2 RESPIRATION AND PAUSES AT VARIOUS TIME INTERVALS – PRACTICAL RESULTS

Practical results were obtained by using the Serial Plotter of Arduino and these results were also verified by visualisation of LCD. The cases observed are presented below:

(7) When ripples were detected, the status was observed using a blinking LED. This effect was also observed using the Serial Plotter using Arduino IDE. When ripples were detected, it was indicated with values of ripple as 1 and pause as 0. This effect can be seen in the graphs shown in Figures 66 and 67.

Figure 62: Practical result of pause detection
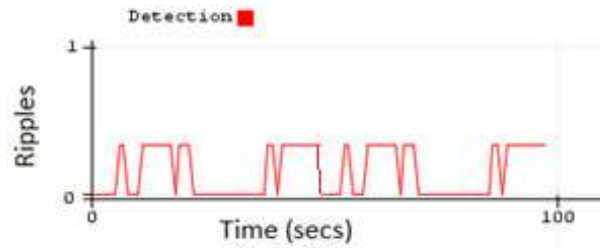
Figure 63: Practical result of ripples detection

The ripples counted as they were detected and their value was shown to user over the 60 seconds period. The detection of ripples and their count is shown in Figure 68. When 60 seconds passed, the counter value again becomes zero and starts ripple count for the next 60 seconds.
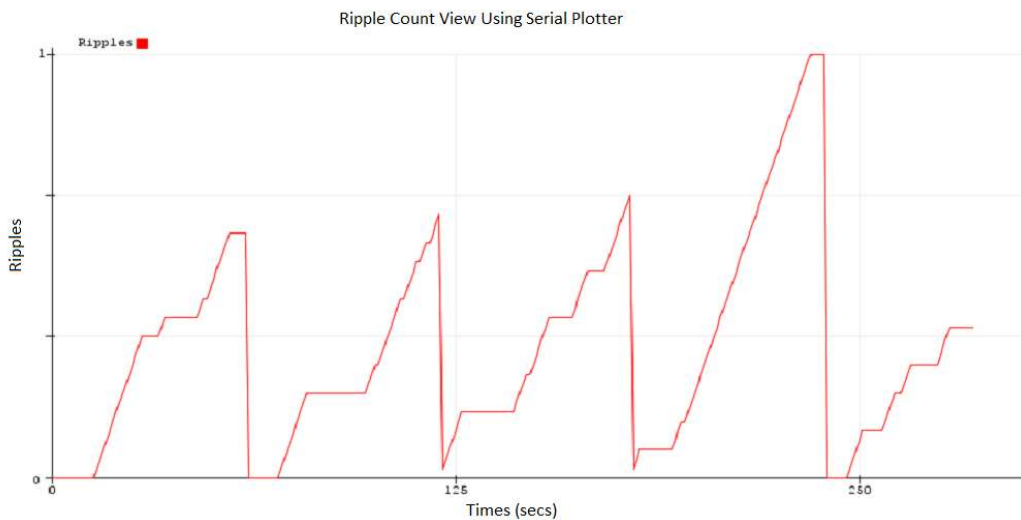
Figure 64: *Practical results of ripple count*

7.10.3 DATA ANALYSIS RESULTS (USING MATLAB)

This section analyses the raw data using MATLAB tool. The complete MATLAB code and its explanation is given in Appendix K.

This raw data was plotted to establish different graphical views which are shown in the following figures. The raw data (duration of 2 minutes) is plotted in two different views namely simple plot and bar plot as shown in Figures 69 and 70 respectively.

92

Each value greater than zero shows the ripple detection where zero value shows that there is no ripple existence.
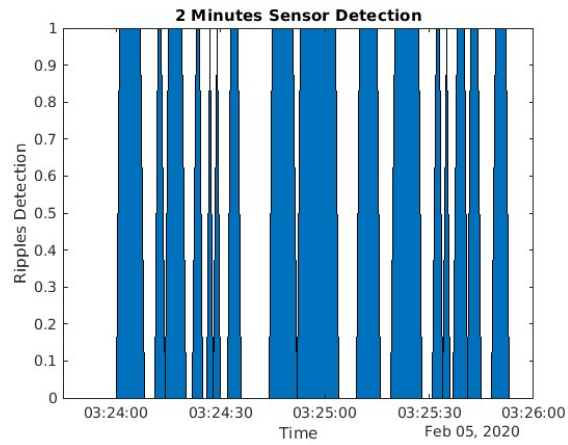
Figure 65: Simple Plot
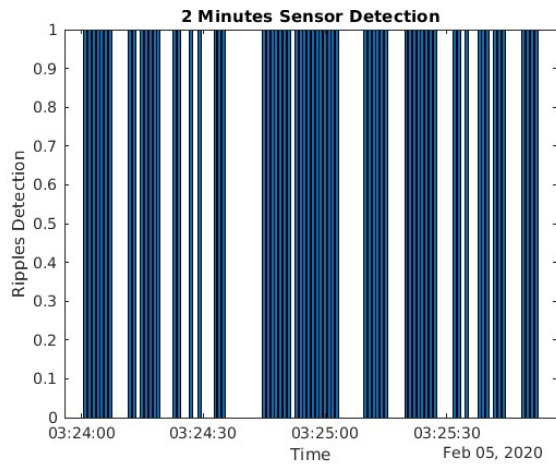
Figure 66: Bar Plot

There is no abnormal pause in the two minutes' data.

Another aspect of analysis was to extract and classify the ripple count for every sixty seconds. The normal and abnormal ripple count analysis of 2-Minutes raw data is shown in Figure 71.
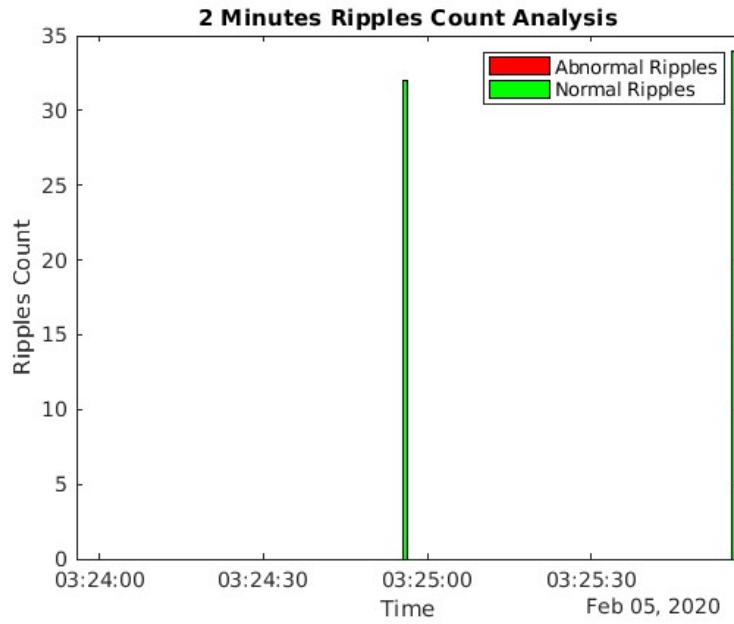
Figure 67: Normal & Abnormal Ripple Status

Similarly, the graphical view of 5 minutes' data is shown in the Figure 72.
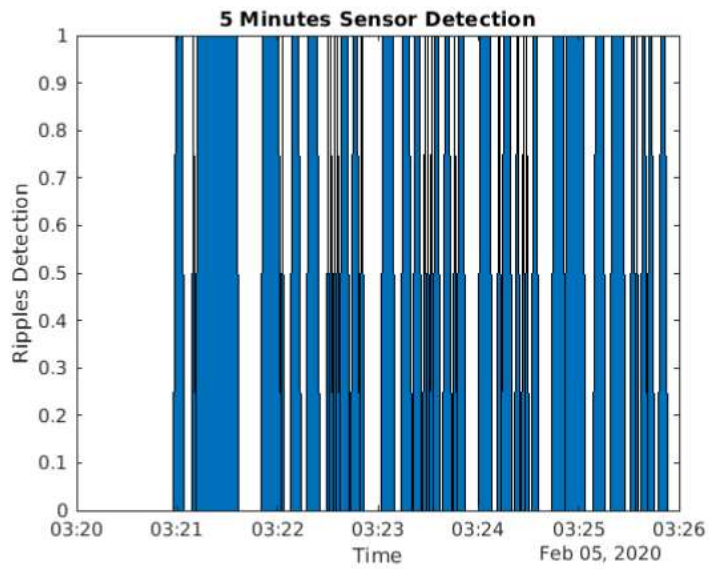
Figure 68: Plot of Five Minutes Detection Data

The abnormal pause in the five -minutes data analysis is shown in Figure 73.
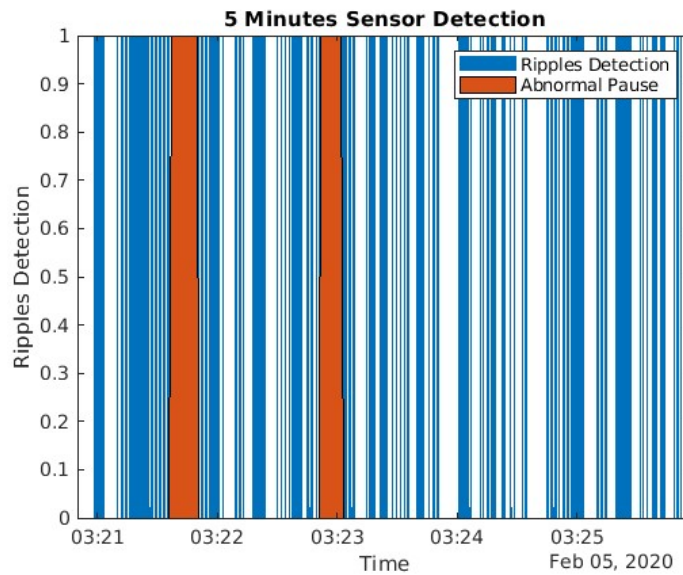
Figure 69: 5-Minutes Data (Abnormal Pause Analysis)

The ripple count analysis of 5 Minutes detected data is shown in Figure 74. Green lines show normal count where the red lines show abnormal ripple count. Normal and abnormal pauses in the 5-minutes detected data analysis is shown in Figure 75.
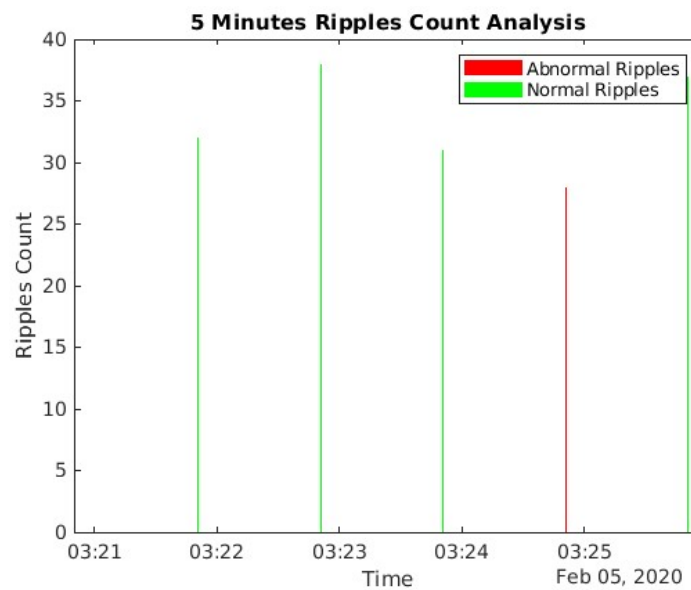
Figure 70: 5-Minute Data (Ripple Count Analysis)
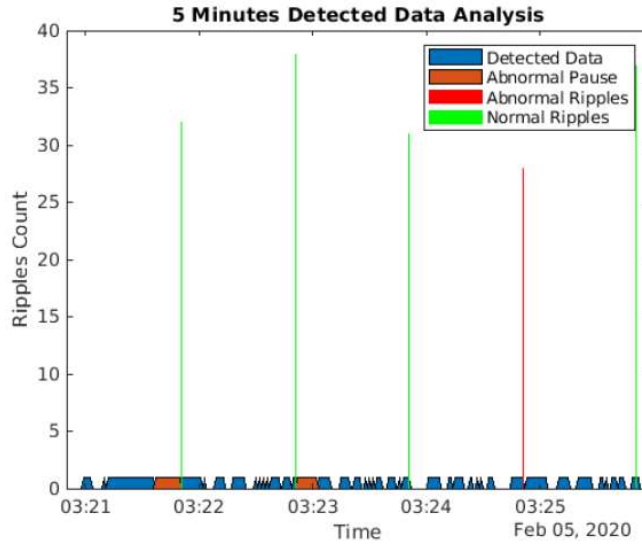
Figure 71:Five minutes Detected Data Analysis

7.10.4 TABLE OF RESULTS

Table 5 provides the measurement of the four independent US signals, determined by identifying the frequency corresponding to the peak in its magnitude frequency spectrum, as signal generator frequency is increased from 0.1 Hz to 1.1 Hz. Figure 76 shows the plot of ultrasound signal frequency against signal generator frequency for four ultrasound sensors.

Table 5: Measured Frequencies

Signal Generator Frequency, Hz, (F)	Ultrasound Signal Frequency, Hz, (US1)	Ultrasound Signal Frequency, Hz, (US2)	Ultrasound Signal Frequency, Hz, (US3)	Ultrasound (1) Signal Frequency, Hz, (US4)
0.1	0.061	0.043	0.09	0.075
0.2	0.161	0.141	0.191	0.196
0.3	0.331	0.371	0.301	0.311
0.4	0.417	0.457	0.437	0.39
0.5	0.522	0.561	0.54	0.498
0.6	0.651	0.719	0.611	0.626
0.7	0.659	0.699	0.719	0.692
0.8	0.761	0.741	0.821	0.812
0.9	0.861	0.841	0.921	0.951
1.0	1.015	0.991	0.975	1.05
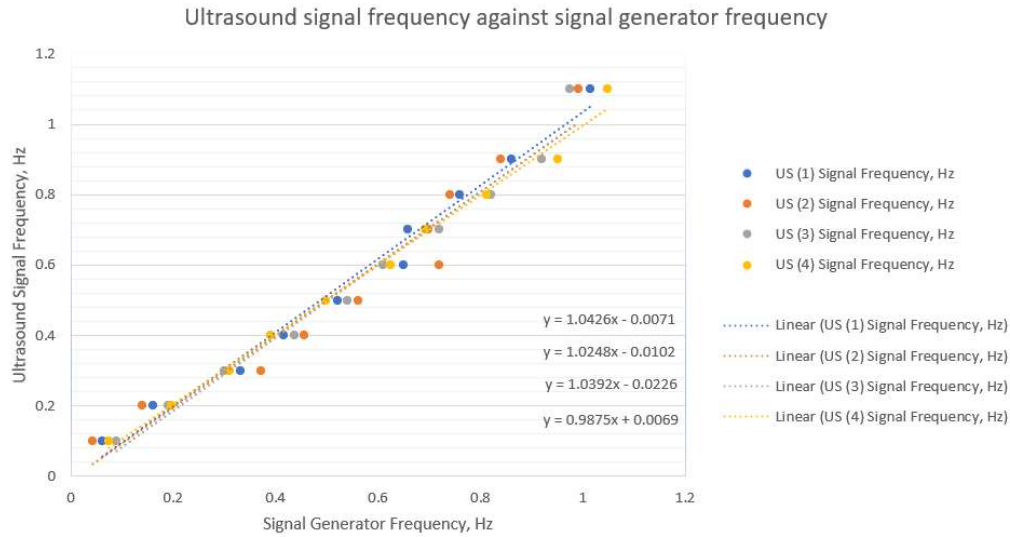
Figure 72: Plot of Ultrasound Signal Frequency against Signal Generator Frequency for four US sensors

7.10.5 DISCUSSION

A set up was developed to simulate respiratory signal effects through a sinewave generator connected to a moving platform. Through this method, controlled pauses were measured and respiration signal were counted under various conditions. Four of the sensors were placed in a fashion where there is little to no signal interference between each of the sensors. This demonstration was primarily for the cause of should the object moves from its initial position, the accompanying sensors should be able to detect the movement and record the received signals.

The experiment performed in the previous chapter aided the experiment of this chapter to be able to successfully place each of the four sensors at a distance that is mathematically presented to avoid signal interference. The results show that this was successfully demonstrated thus can be used for further investigation or even means of future system implementation improvement.

The theory and practical results tally up quite significantly as per the experiment. The table of results showed near enough accurate results with the occasional signal interference and distortion. It too demonstrates that by moving the object 7 cm away from the centre point of the US‚ since it is still within the working range of the US, 15 degrees, based on the datasheet, looking at the results, it does affect the signals

negatively, but to an extent where it still adheres to the datasheet (HC-SR04, n.d.). In addition, on some occasions, it was witnessed that the result was more to the positive hence this shows that the use of this US will give us good results but not the best from the accuracy perspectives and for that further tests and or the use of a medical grade ultrasonic sensor would be a viable means of testing signal accuracy.

The frequency range corresponds to a breathing range 0.160=6 bpm to sensor 1: 0.061×60=3.66 bpm; sensor 2: 0.043×60=2.58 bpm; sensor 3: 0.0×60=5.4 bpm; sensor 4: 0.075×60=4.5 bpm. The frequency of the US signal is plotted against that of the signal generator in Figure 76 and a close relationship is observed (gradient 1.043, 1.025, 1.040 and 0.988 respectively).

It showed that sensor 3 and 4 are picking up the signal and that the object is right under sensor 3 as the bpm equals to 5.4 bpm that is close to the actual bpm of 6 bpm.

The experiment was designed in a way where the object was placed under the four US sensors and seen whether they all receive the signals successfully in addition to the introduction to moving the object that was placed directly under the US to determine if the sensor still manages to record without signal interference hence the results for all sensors being close to the actual set signal generator's signal. We do witness that one of the sensor's signal is close to the set signal and this is because it indicates that the object is right beneath it while being shifted from the rest of the sensors.

The amplitude of the recorded signal appears to be distorted even after processing the signal. The amplitude of the signal is not constant. In theory, it should be same as the depth of the speaker throughout. On the other hand, the signal fluctuates quite frequently. The higher the frequency the smoother the amplitude and lesser signal distortion.

Looking at the overall practical investigation for all the cycles, the accuracy in findings was observed every time there is an increase and decrease in the frequency. It is also evident that practical results are dependent on how controlled the experiment was performed. Basing it on the collected result, the test adheres to the datasheet (HC-SR04, n.d.) from the angle of the US standpoint. Hence it has been reflected in the result where

a mix of positive and negative result was captured resulting in no major fluctuation in the collected signal.

The inaccuracy between the signal generator's frequencies and the US signal's frequency are partly related to:

- Accuracy of the frequency setting on the signal generator.
- Accuracy of reading the frequency associated with the peak in the magnitude frequency spectrum.

By using a more advanced US transceiver, the measurement could also be further improved.

SUMMAY OF CONTRIBUTIONS

The primary contribution of this project is summarised hereunder:

1. The four ultrasonic sensors are integrated to deal with body movement
2. The data sets are recorded under different frequencies of sine wave. They are analysed using MATLAB for desired results according to predefined parameters.
3. By analysis of simulation and practical results, it is concluded that the desired project goal and objectives have been achieved.

LIMITATIONS

A possible limitation was faced during this project execution. If there is only partial detection (partial input) in these four US sensors, then the proposed integration and calculation techniques will not give accurate results.

For example, S1 detects 50 ripples, S2 detects 40 ripples, S3 detects 0 ripples, and S4 detects 5 ripples, where "S" denotes sensor and "rip" denotes ripples. Then the result after calculation will be 24 rip which is not the accurate result. This is the main drawback of this approach hence why each of the sensor is triggered one at a time and monitored separately.

AVENUES FOR FURTHER RESEARCH

Further improvements:

1. Artificial intelligence like Deep learning, Machine learning, or Neural networks algorithms can be used

2. To perform such high-level algorithms like artificial intelligence, the Arduino UNO Controller cannot be used as it does not have necessary and sufficient processing power for Machine learning.

3. To perform these algorithms, Raspberry Pi will be a better alternative.

Chapter 8: Integration of IoMT - Monitoring Respiration Rate from Remote Locations using IoT (Internet of Things)

8.1 INTRODUCTION

This part of the study outlines development of an IoT (Internet of things) system, a methodology that includes detection of the simulated respiratory signal, data transmission, data analysis and data visualisation. This setup can be used to monitor an infant's respiration from a remote location, by accessing the transmitted data from the cloud by IoT devices.

The hardware employed are:

- an open source IoT platform "NodeMcu ESP8266" and
- US sensors.

The ripple detection is done with Ultrasonic sensor and NodeMcu code. The live data detection stream transmits data to ThingSpeak (data transmitted every 15 seconds for free version). A brief analysis is performed using the live data and results are visualised in the cloud. The steps involved were:

 i.   Accessing US signals
 ii.   Live data transmission to ThingSpeak
 iii.   Brief analysis that includes Pause detection and Ripple count
 iv.   Results visualisation

8.2 DESIGN AND IMPLEMENTATION

8.2.1 METHODOLOGY

Methodology selected for this study is a technique that can be used for both simulations in software and implementation in hardware. The techniques employed were:

- US sensor was used for ripple detection. The method of detecting respiration using a single US sensor discussed in earlier sections is adopted here. After detecting the signal, it is transmitted to remote location.
- NodeMcu was used for data accessing and live transmission

- ThingSpeak was used for data analysis and visualisation in cloud
- Data can be analysed and visualised remotely from anywhere in the world via a mobile phone or other

8.2.2 INTEGRATION OF IOT INTO A RESPIRATION RATE MEASUREMENT SYSTEM

This section explains integration of the IoT as part of the respiration rate measurement setup. It outlines the methodology used to record the signal, its transmission, analysis, and display. The setup for remote monitoring of the recorded data from the cloud by IoT devices is explained. The hardware elements employed were: ESP8266 NodeMCU and US sensors. The recorded real-time data were transmitted to ThingSpeak every 15 seconds. Data analysis was performed in real-time and results were displayed in the cloud. The steps involved were:

i.   Accessing the US signal.

ii.   Real-time data transmission to ThingSpeak server.

iii. Aggregation and analysis that included respiration rate calculation through the ThingSpeak server.

iv.   Displaying results through ThingSpeak Server with the aid of integrated Matlab©.

The elements used for the set up are shown in Figure 77.
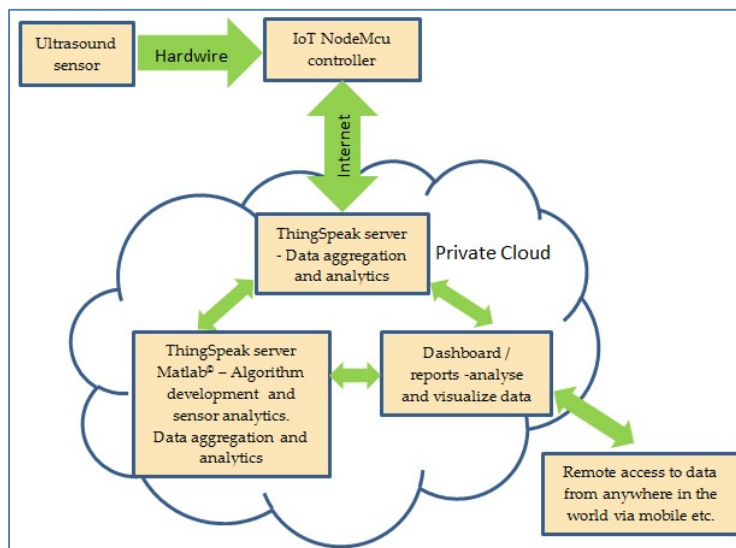
Figure 73: Block Diagram of the IoT Setup

The components used as part of the setup were:

- Ultrasound Sensor - The type of ultrasonic sensor used in this project was a transceiver, which could both transmit and receive ultrasonic waves. The type used was HC-SR04. This is a 4-pin module, whose pin names are supply voltage (VCC), trigger, echo, and ground. It provides 2 cm to 400 cm non-contact distance measurement and its accuracy can reach to 3 mm. The module includes US transmitter, receiver, and control circuit. It uses an input-output trigger for at least 10 μS high level signals. It operates by automatically sending eight 40 kHz for its detection.

- ESP8266 NodeMCU - This is an IoT device that connects to an active wireless network. It was used to capture the US signal and transmit it to the ThingSpeak for processing over the cloud. NodeMCU connects an active wireless network for data transmission to ThingSpeak. It is an open source IoT platform. It has a firmware which runs on ESP8266, an integrated Wi-Fi chip, a power amplifier, power management modules, antenna switches, and filters.

- ThingSpeak - This is an open source web-based IoT analytics platform that allows users to aggregate data, analyse them using web integrated Matlab$^{©,}$ and visualise live data streams in cloud. It allows users to create channels like YouTube or Television channel (THINGSPEAK 2020). The data were analysed and visualised using different ThingSpeak applications based on packages such as Matlab$^{©}$. In this work, for data analysis, Matlab$^{©}$ coding was used. ThingSpeak has designed a well secured system for user data protection. Each ThingSpeak channel has its own unique and secure read and write API keys.

8.2.3 PROJECT HARDWARE

The hardware used are:

- US Sensor
- NodeMcu (ESP-12E module)
- A Wireless Connection
- A light emitting diode (LED)

103

- Connecting Wires
- Sinewave generator

8.2.4 SIMPLE CIRCUIT DIAGRAM

The simple circuit diagram of this project is shown in the Figure 78. This approach is taken to demonstrate the IoMT integration. A brief overview about the hardware components used is given in Appendix C and Appendix L.
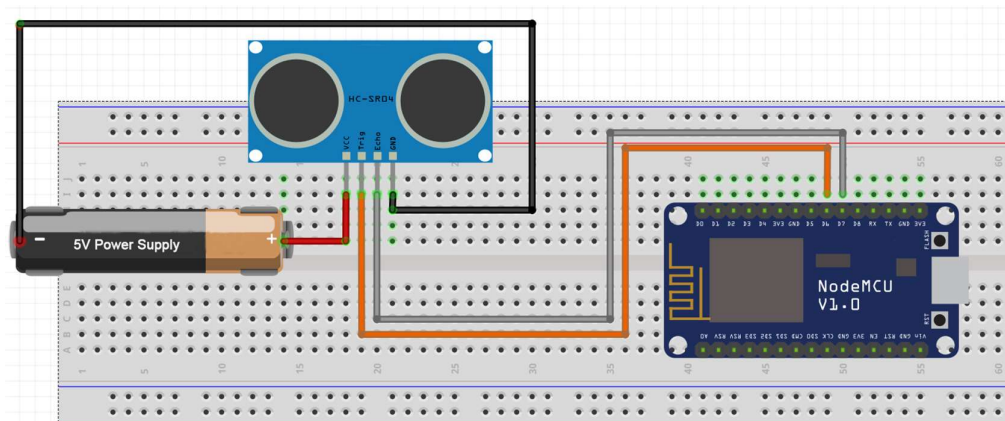
Figure 74: Simple Circuit diagram

8.2.5 IMPLEMENTATION

The interface US sensor was connected to the NodeMcu according to circuit diagram. Interfacing of US sensor with NodeMcu is shown in Appendix M.

The US sensors were used for detection of ripples as ripples have a certain amount of height from the base of the sine wave. More information about ultrasonic sensors is given in Appendix C and Appendix L.

For accurate working, this circuit should be first connected to a wireless network. When IoT device (NodeMcu) is connected to a wireless connection, the hardware circuit starts working. The Arduino code is given in Appendix O.

8.2.6 WORKING PROCEDURE OF CIRCUIT

- The US signal used to this study was a continuous or discontinuous ripple wave. This wave was generated using a signal generator.

When the circuit is ON, then:

- The IoT device connects to wireless connection that is used for data transmission to cloud. Refer code in Appendix O.
- The US waves were emitted by ultrasonic sensor. When a wave was reflected back towards US sensor, the resulting signal was recorded by NodeMcu as a detection.
- When there was no reflection occur up to 15 seconds (for practical purposes only), then this was considered as pause by the circuit.
- After every 15 seconds of circuit start up, the detected live data is transmitted to ThingSpeak channel using IoT device (NodeMcu).
- The transmitted data were analysed using ThingSpeak analysis tools with the aid of MATLAB$^©$ to make sense of the collected IoT data and results are shown to user.

A Graphical view of working procedure is shown in the flow chart in Figure 79.
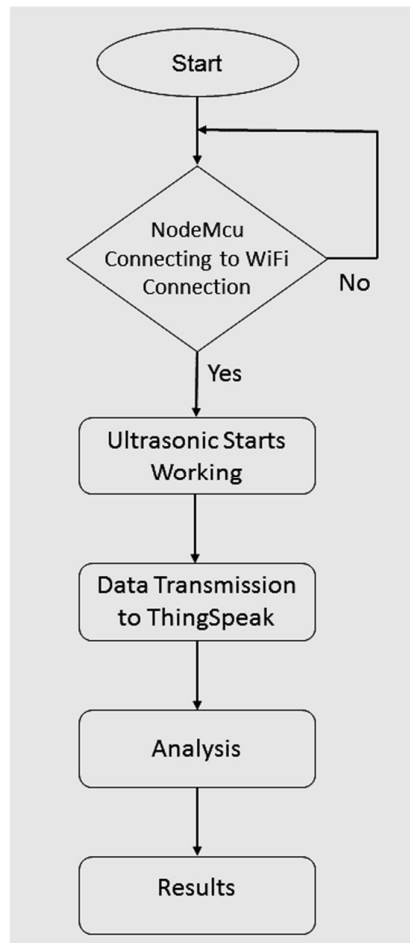
Figure 75: High-level Project working procedure

8.2.7 THINGSPEAK

ThingSpeak is an IoT analytics platform that allows a user to aggregate, analyse and visualise live data streams in the cloud. In ThingSpeak platform, channels containing a number of fields are created. The live data are sent to these fields using Read and Write API Keys. The data are analysed and visualised using different ThingSpeak app functions like MATLAB[c] Analysis, MATLAB Visualisations.

More details about ThingSpeak are given in Appendix N. Things to remember when using ThingSpeak are given in Appendix Q. In addition, the setup is illustrated in Appendix R.

8.2.8 THINGSPEAK ANALYSIS

The ThingSpeak channel named "Ultrasonic Data" was created. The channel consists of one field named "Sensor detection", which contains the data set sent through NodeMcu.

ThingSpeak uses the "Sensor detection" data set to perform several analyses namely Pause Detection, Ripple Count, and Fourier analysis.

Some predefined conditions that should be considered during analysis are:
➢ If no ripple was present till 15 seconds or more, then this time is counted and considered as pause until any ripple was detected.
➢ Ripple count analysis was performed every sixty seconds. If ripple count was less than 29 or greater than 79, then this result was considered as Abnormal Count.

On the other hand, if the ripple count value was between 29 and 79, then this value is considered as Normal Count.

A Graphical view of ThingSpeak analysis was shown in the following Figure 80.
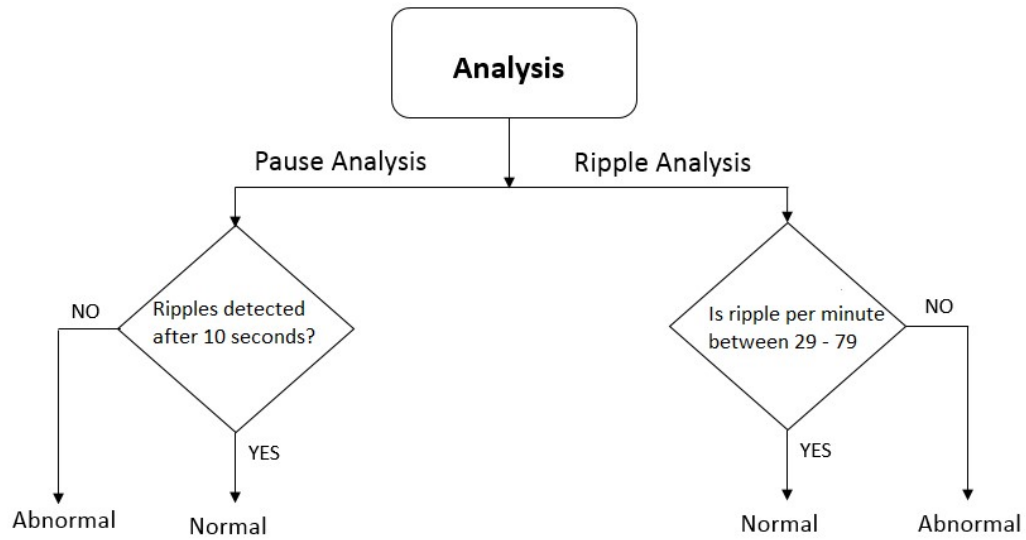
Figure 76: ThingSpeak Analysis Flow Chart

8.3 DATA ANALYSIS RESULTS (USING THINGSPEAK)

8.3.1 PAUSE DETECTION AND RIPPLES COUNT RESULTS

In this section, a brief analysis using ThingSpeak is explained. First the data were imported into analysis and visualisation environment in ThingSpeak Channel. This data contained sensor detection values, time and date. The complete ThingSpeak (MATLAB) Code and its explanation are given in Appendix P.

For analysis, simple approach containing predefined conditions was applied. Figure 81 shows the saved data in ThingSpeak Channel.
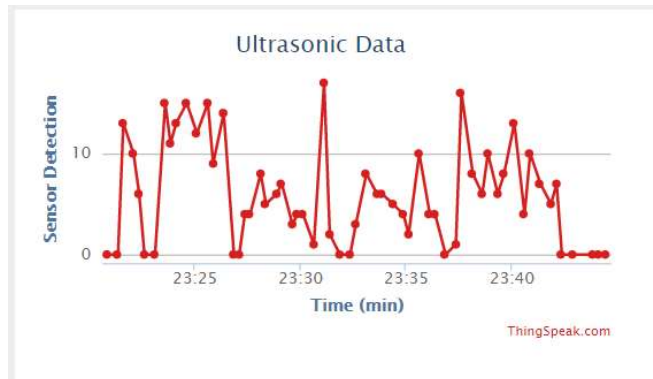
Figure 77: ThingSpeak Ultrasonic Detection Data

Though "Pause" means no ripple detection, for understanding and visualisation to user a decimal value of 0.75 is taken. The pause analysis of ultrasonic data is shown in Figure 82. Each segment shows 15 seconds time duration or interval.
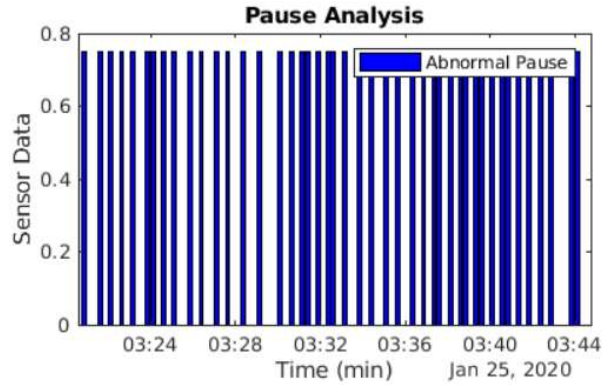
Figure 78: Pause Analysis of Ultrasonic Data

As mentioned in the predefined conditions, when ripple detection is either less than 29 or greater than 79 cycles, the wave should be considered as abnormal ripples count. The Ripple count analysis of Ultrasonic data is given in below in Figure 83. Each line in bar graph shows average ripple count over the past sixty seconds. Green colour shows normal ripple count whereas red colour shows abnormal ripple count.
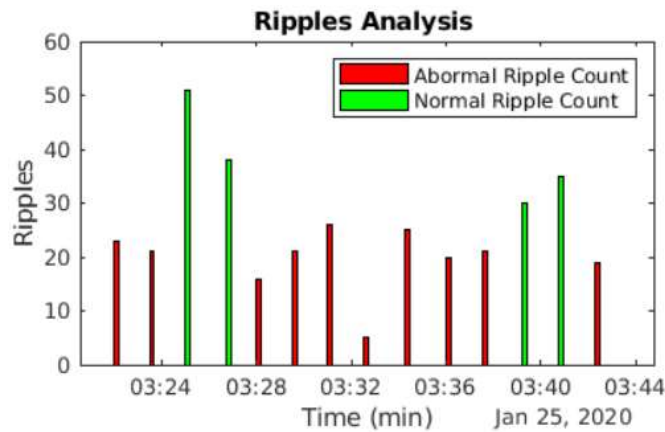
Figure 79: Ripple Analysis of Ultrasonic Data

Pause analysis and ripples count analysis are visualised in a single figure as shown in Figure 84.

Figure 84 contains both Abnormal Pause and Ripple Count analysis.
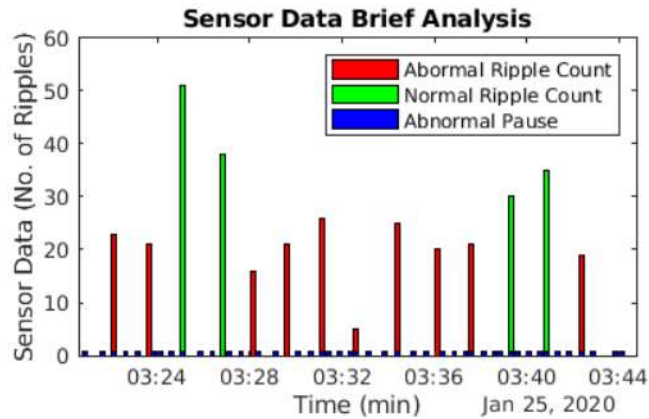
Figure 80: Combined Pause and Ripple Count Analysis

8.3.2 ANALYSIS EXPLANATION

In data analysis, the data were interpreted and visualised by considering different aspects. For these tasks, different analysis and visualisation tools were used.

The conversion of data from one domain to another domain is called transformation and the converted data is called transform (data).

In our daily life, almost all signals are seen (Data visualisation) to be in the time domain. The time domain graph in Figure 85 shows how the signal changes over time. The bar graph plot shows the IoT input signal in time domain. Blue lines show ripple detection values where blank shows that there is no ripple detection.
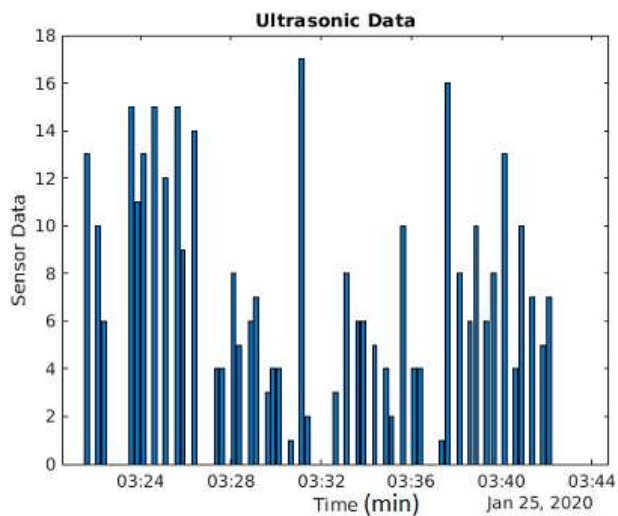
Figure 81: Time Domain Analysis

109

8.4 NETWORK AND SYSTEM SECURITY AND ACCURACY

8.4.1 SYSTEM ACCURACY

The US sensor works on same principle as the radar system. An US system when triggered, converts electrical energy into acoustic waves (signals) and during echo, converts acoustic waves into electrical energy.

The acoustic waves propagate at particular frequency with the speed of sound. When the acoustic waves collide with a solid surface, they are reflected back.

- The objects like fabric and carpet can absorb acoustic signals. If the signal is absorbed, the wave will terminate, no reflection (bounced back) occurs, and object detection will be zero. This is the limitation of ultrasonic sensor. To make a system having ultrasonic sensor more accurate, this limitation should be considered.
- The ultrasonic sensor can also detect false signals coming from the airwaves, to make system more efficient use a closed environment system rather than open environment.

8.4.2 NETWORK SECURITY

Network security is an action to keep data in safe mode for all legitimate users and block unauthorised users. A good network security system boosts up a business by reducing risk of data theft.

In communication system, for secure network, the technical terms SSL and TLS are used. SSL stands for "Secure Sockets Layer" where TLS stands for "Transport Layer Security" (dzone).

SSL and TLS both are cryptographic protocols that authenticate data transmission between servers, systems, applications and users (dzone).

TLS is an advanced form of SSL. Nowadays, SSL has been replaced by TLS.

8.4.3 HOW TO CHECK A NETWORK SECURITY

The TLS protocol encrypts internet traffic of all types where the most common is web traffic. The user can know if its browser is connected via TLS or not. If the URL of user address starts with "https" and there is an indicator with a padlock, it tells the user that the connection is secure (Harris, 2015).

8.4.4 SSL / TLS WORKING PROCEDURE

Encryption is necessary to communicate securely over the internet: If user data is not encrypted, anyone can examine user packets and read confidential information. The safest method of encryption is called asymmetrical cryptography; which requires two cryptographic keys or pieces of information. They are usually very large numbers, one public and one private. Public key is used to encrypt the data where private key is used to decrypt data (Harris, 2015).

ThingSpeak provides both SSL and TLS securities to users.

8.4.5 CHANNEL PUBLIC OR PRIVATE OPTION

ThingSpeak is designed and handled by MathWorks Community. ThingSpeak has both free version and paid version. Each has its own limitations. In free version, only limited number of channels and fields can be created. Regarding security, both are well and sound (Nettikadan & Raj, 2018).

A Channel can be public or private depending upon the user. ThingSpeak facilitates their users by providing graphical view options instead of actual public or private keys. The Figure 86 depicts this information.

Channel Sharing Settings

- ◉ Keep channel view private
- ○ Share channel view with everyone
- ○ Share channel view only with the following users:
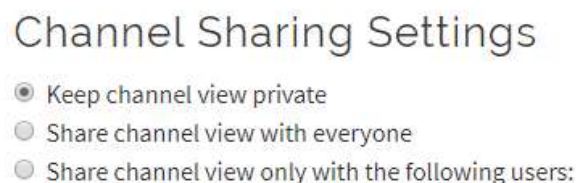
Figure 82:Channel Sharing Settings in ThingSpeak (Thingspeak)

8.4.6 THINGSPEAK DATA SECURITY

ThingSpeak has designed a well secured system for user data protection. Not anyone can access, read, or write in a user channel data. An outsider can read or access data only if ThingSpeak user has created a public channel, but cannot change it, i.e. read-only mode (Nettikadan & Raj, 2018).

Each ThingSpeak channel has its own unique and secure read and write API keys. Using these keys, a user or outsider can change or access actual channel data.

The channel URL address security (https:) is shown in Figure 87.

API Requests

Write a Channel Feed
GET https://api.thingspeak.com/update?api_key=QZJM8SDBB9OFGH3S&field

Read a Channel Feed
GET https://api.thingspeak.com/channels/936270/feeds.json?api_key=P1

Read a Channel Field
GET https://api.thingspeak.com/channels/936270/fields/1.json?api_key

Read Channel Status Updates
GET https://api.thingspeak.com/channels/936270/status.json?api_key=P

Figure 83:Thingspeak Channel Address Security (Thingspeak)

8.4.7 REMOTE ACCESS SETUP THROUGH MOBILE PHONE APPLICATION

➤ Access the ThingSpeak webportal while selecting API Keys tab and navigating to "Read API Keys" and copy and paste the key onto the mobile phone IOS app (download application via Appstore: ThingView) as shown in Figure 88.
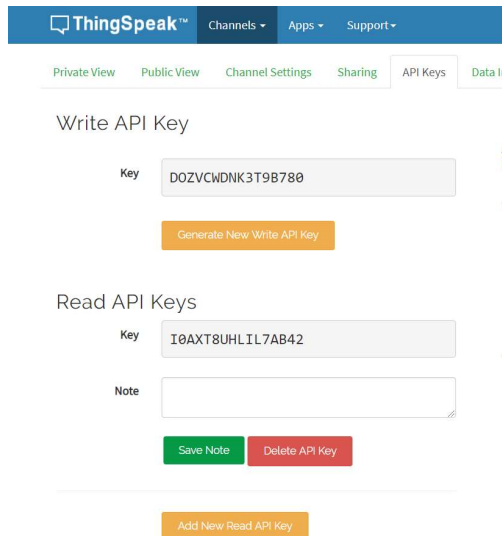
Figure 84:ThingSpeak Web portal

➢ Setup mobile application

While adding a channel, the following are required as shown in Figure 89:

• Channel ID, which is extracted from the ThingSpeak server web portal
• Disabling Public, since it is a private channel
• While navigating to the API Keys and copying pasting the Read API Keys
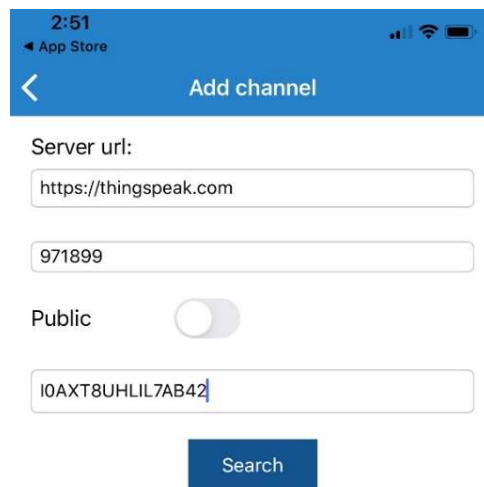
Figure 85: Adding a channel in ThingSpeak

➢ Saving the configuration as shown in Figure 90:
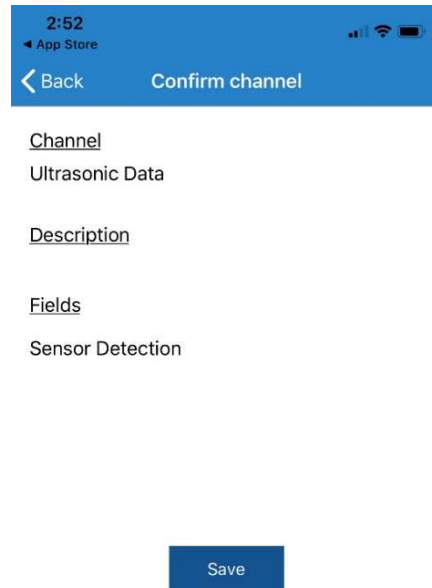
Figure 86: Saving the configuration in ThingSpeak

➢ After successfully establishing the connection with the server, the channel is accessible as shown in Figure 91.

Figure 87: Channel Accessibility in ThingSpeak

➢ Remote access and data visualisation as shown in Figure 92.

The following data can be successfully visualised remotely by any medical personnel as shown below:
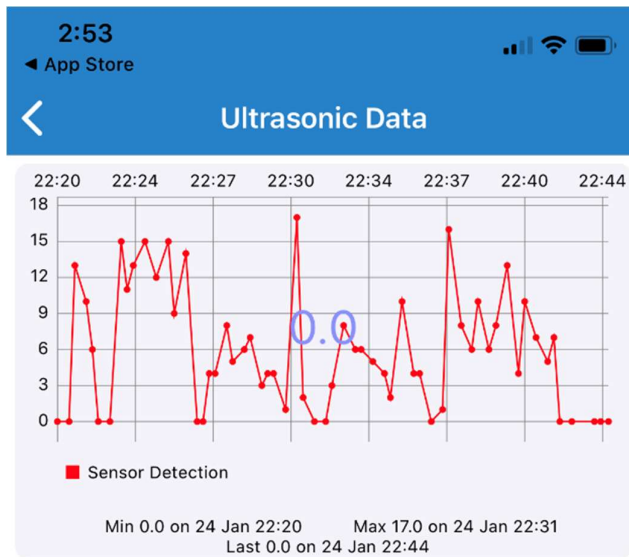
Figure 88: Remote Access in ThingSpeak

➢ Data can be visualised with zoom capabilities and timestamp allocation as shown in Figure 93.
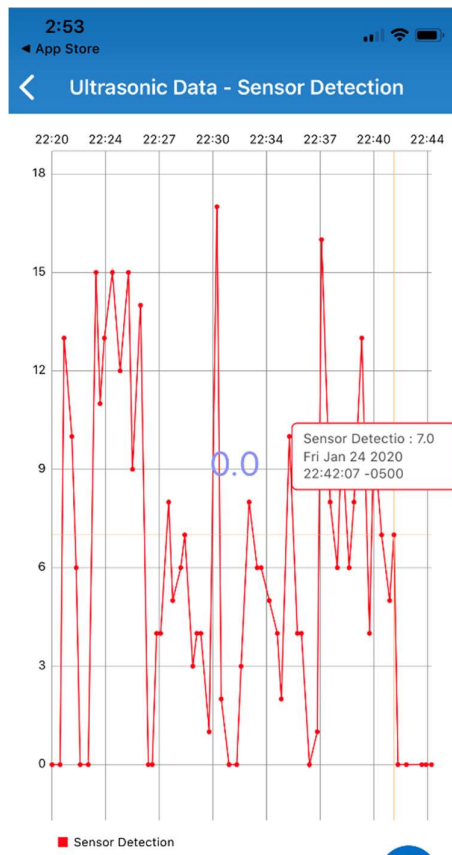
Figure 89: Zoom and Timestamp Capabilities in ThingSpeak

8.5 CONCLUSION

The results indicated successful transmission of data to the ThingSpeak cloud server where data were then analysed using the built-in features of ThingSpeak, MATLAB$^©$ analysis was performed to interpret the pause and signal ripple counts for every sixty seconds. In addition, the system was then further developed by integrating it with a mobile application where in utmost ideal cases would be a viable solution for the doctors / nurses to check up on their patience on-the-go, basically anywhere in the world whilst receiving alerts on the health of the patients. Furthermore, graphs and charts with timestamp is presented in a user-friendly user interface that would allow the healthcare workers to swiftly access the patient data as and when required for future analysis. This would aid the healthcare works to be more efficient and productive as they can manage their patients in a systematic way since they will have access to their patients' data on one single platform, and they can make further analysis and perform decision making.

The investigation and the system integration were successfully implemented where it demonstrates not only the use of IoMT in the medical settings, but also shows how they can be leveraged further with machine learning. This helps to detect early patterns in patients to prevent critical situations from happening. Machine learning, artificial intelligence, predictive and preventative analysis, stream analytics, dash boarding and reporting features are some of the features that were demonstrated in this chapter.

Summary of Contributions

The primary contribution of this project is summarised as follows:

- The US sensor was used for detection of ripples from sinewave.
- The data value of different frequencies is transmitted to ThingSpeak by using NodeMcu.
- By using ThingSpeak cloud analysis, conditions given in predefined parameters are applied and results are visualised.
- A secure SSL / TLS communication Protocol is provided by ThingSpeak

Chapter 9: Conclusions and Future Work

9.1 CONCLUSION

The study's aim was to develop a non-contact, ultrasound (US) based respiration rate and respiratory signal monitor suitable for babies in incubators. Respiration rate indicates average number of breaths per minute and is higher in young children than adults. It is an important indicator of health deterioration in critically ill patients. The current incubators do not have an integrated respiration monitor due to complexities in its adaptation. Monitoring respiratory signal assists in diagnosing respiration rated problems such as central Apnoea that can affect infants. US sensors are suitable for integration into incubators as US is a harmless and cost-effective technology.

A US beam was focused on the chest or abdomen. The chest or abdomen movements, caused by respiration process, result in variations in their distance to the US transceiver located at a distance of about 0.5 m. These variations were recorded by measuring the time of flight from transmitting the signal and its reflection from the monitored surface. Measurement of this delay over a time interval enabled a respiration signal to be produced from which respiration rate and pauses in breathing were determined.

The challenging part was when utilising a single US to focus the beam on one targeted point to measure the movement. Since the object was not stationary, an alternative mean to overcome this hurdle was devised thus the use of four US was seen as a suited approach. The use of four US sensors did provide clarity and accuracy to the entire use case reflected by the results captured. This is due to the precise practical calculation was carried out to ensure that the spacing between each of the placed sensor adheres to the datasheet, i.e. angle of coverage. With that in mind, the results were promising and provide leverage for further investigation on how to ensure 100% system accuracy and reduction in interference is tackled.

A platform with a moving surface was devised to introduce accuracy to measure the movement. The magnitude and frequency of its surface movement were accurately controlled by its signal generator. The US sensor was mounted above this surface at a distance of 50 cm. The US signal was wirelessly transmitted to a microprocessor board to digitise. The recorded signal that simulated a respiratory signal was subsequently

stored and displayed on a computer or an LCD screen. The results showed that US could be used to measure respiration rate accurately. In order to cater for possible movement of the infant in the incubator, four US sensors were adapted. These monitored the movements from different angles. The algorithm to interpret the output from the four US sensors shown to have provided the suitable platform for further evaluation. The developed algorithm interpreted which US sensor detected the chest movements.

Using a single sensor, the percentage difference between actual and US based respiration rate measurement was 1.5%

Using a single sensor with shifting by 7cm to the right form the US centre point, the percentage difference between actual and US based respiration rate measurement was 4%

Using four sensors, US1, US2, US3 and US4, the percentage difference between actual and US based respiration rate measurement was 1.11%, 1.16 %, 1.93 % and 1.84, respectively.

Integration of IoMT to provide remote real time access to data for physicians and keep historical data for future prediction

The developed methods facilitate the built-in features in the cloud to carry out data analysis relevant to respiratory data

The adaptation of the IoT in healthcare can provide flexibility in patient data collection and storage. It has the potential to improve patient experience and reduce cost. This study also outlined a simulated setting, whereby the IoT could be adapted into a neonatal intensive care unit (NICU) to measure respiration rate. Chest movements were simulated through a devised platform built from the previous use case with a controllable moving surface. US was used to accurately measure the platform's surface movement. ESP8266 NodeMCU was used as an IoT device to connect to the active wireless network, capture the US signal and transmit it to the ThingSpeak server residing in the cloud.

Real-time wireless data transmission took place in the ThingSpeak server, where data aggregation and analysis to determine respiration rate were performed using Matlab©. The frequency of the platform surface movement closely matched with the frequency measured by the IoT-integrated US system.

An IoMT system was devised that incorporated NodeMcu to capture signals from the US sensor. The detected data were transmitted to the ThingSpeak channel and processed in real-time by ThingSpeak's add-on Matlab© feature. The data were processed on the cloud and then the results were displayed in real-time on a computer screen. The respiration rate and respiration signal could be observed remotely on portable devices e.g. mobile phones and tablets. These features allow caretakers to have access to the data at any time and be alerted to respiratory complications.

A method to interpret the recorded US signals to determine respiration patterns, e.g. intermittent pauses, were implemented by utilising Matlab© and ThingSpeak Server. The method successfully detected respiratory pauses by identifying lack of chest movements. The approach can be useful in diagnosing central apnoea. In central apnoea, respiratory pauses are accompanied by cessation of chest or abdominal movements. The devised system will require clinical trials and integration into an incubator by conforming to the medical devices directives. The study demonstrated the integration of IoMT-US for measuring respiration rate and respiratory signal. The US produced respiration rate readings compared well with the actual signal generator's settings of the platform that simulated chest movements

The study indicated that ultrasound (US) technology as a mean of measuring and monitoring respiration rate and pauses in breathing in infants can be a valuable technique, yet it also requires further studies to determine its overall use for sleep studies such as central Apnoea detection. This study's aim was to reduce reliance on the use of contact-based methods of measuring and monitoring respiration rate and pauses in breathing. The monitoring system has the ability to be expanded so that an US sensor is mounted on top of an incubator, facing down, recording the premature baby's respiration. The US sensor used is very cost effective and measured distances to an accuracy of 0.5 mm. Being a self-contained sensor is a positive factor when it comes to integrating it within an incubator.

The results were obtained using a devised platform that simulated chest movements of an infant. The US sensor was mounted over the moving platform surface. The frequency and amplitude of movements could accurately be set, thus allowing comparison of the measured and actual readings. The data were recorded for two minutes for a variety of tests. The signals recorded were analysed and it was observed that measured respiration rate closely matched to the set frequency. The observations provided evidence to demonstrate US technology could be valuable to measure an infant's respirations rate and pattern.

In central apnoea, intermittent pauses in breathing during sleep is accompanied by lack of chest movements. Several experiments were devised that demonstrated US could be effective in detecting respiratory pauses in central apnoea

The single sensor US set up was expanded to an array of four US sensors and its was shown the method could further enhance detection of chest and abdominal movements.

The US signals from the infant were transmitted to a remote location by integrating the US sensors with IoT / IoMT devices. A system to detect central Apnoea of an infant in NICU was devised. It transmitted the respiratory information over the cloud using IoMT and through mobile. The results demonstrating the operation of the scheme were presented. A laboratory illustration with NodeMcu IoMT platform integrated with US sensors and ThingSpeak data analysis was also demonstrated. Although the results were satisfactory, further tests and development will be required for accuracy this is due to the movement obstacle that does through an erroneous result occasionally.

Currently, contact methods are being utilised to measure and monitor the respiration rate and pauses in breathing causing discomfort to the infant. This new contactless way of acquiring respiration information would eliminate skin irritation and discomfort issues. The method is also useful in analysing respiration related disorders such as central apnoea.

This study focused on the manner the IoMT can be utilised in healthcare. It demonstrated a prototype IoMT integrated US based respiration monitoring system.

9.2 FUTURE DEVELOPMENT

Further work is needed to integrate the proposed method into an incubator for monitoring infants' and neonates' respiration rate and pauses in breathing. This will require interaction and collaboration with the manufacturers of incubators.

The study's results were obtained using a platform that simulated chest movements. It will be important to have clinical trials that evaluate the method on patients in clinical settings.

Medical devices require CE marking and conformance with regulatory issues. Both hardware and software need conformance with medical devices standards. This will be essential to take the device forward to medical use.

Currently, a basic microprocessor board is used. The microprocessor board could be replaced with a more advanced version that will allow real-time display of respiration signal and computation of respiration rate. This will allow an integrated recording and data processing.

Several challenging issues needed to be resolved. A baby's respiration can cause movement of either the chest or abdomen or both. Therefore, mechanisms to optimally focus the US to the chest or abdomen need to be devised. As baby can move in an incubator, therefore refocusing the US beam to the chest/abdomen is necessary. A possible approach would be to use Kalman filter to track the baby's body and reposition the US sensor adaptively. The Kalman filter has proved very effective in tracking objects in numerous applications. The close loop feedback needed to establish the baby's actual position could be gained through infrared sensors that can operate without background lighting.

The use of an advanced microprocessor will enable extensive algorithmic calculation and interpretation the signals providing irregular respiration rate and central Apnoea detection. In addition to leveraging and incorporating the use of machine learning, predictive and preventative measures, create real-time analytical dashboards and automated reports.

It is possible to add an alarm to the system to alert the carer of possible respiratory difficulties.

All in all, further work and development work will be needed to fully adapt the system as part of NICU and use it in a hospital environment. In addition to ensure security and reliability of data handling before use of the system in medical environments.

References

RUSSELL, A. DANIEL (1998). Acoustics and Vibration Animations. [online]. Last accessed 16 June 2013 at:
http://www.acs.psu.edu/drussell/demos/waves/wavemotion.html

AASM (2008). Obstructive sleep Apnoea. *American academy of sleep medicine,* **1**.
www.aasmnet.org

ALESSANDRO, CARONTI, et al. (2006). Capacitive micromachined ultrasonic transducer (CMUT) arrays for medical imaging. *Microelectronics Journal (MJ)*, **37** (8).

ALKALI, A. H., SAATCHI, R., ELPHICK, H., et al. (2013). Noncontact Respiration Rate Monitoring Based on Sensing Exhaled Air. *Malaysian Journal of Fundamental and Applied Sciences (MJFAS),* **9**, 129.

AL-KHALIDI, F. Q., SAATCHI, R., BURKE, D., et al. (2011). Respiration rate monitoring methods: A review. *State of the Art,* **3**.

ABUHUSSEIN, F, ALSUBAEI, A., & SHIVA, S. (2017). Security and Privacy in the Internet of Medical Things: Taxonomy and Risk Assessment. *In Conference: IEEE International Workshop on Networks of Sensors, Wearable, and Medical Devices, Singapore*. Available from:
https://www.researchgate.net/publication/318452054_Security_and_Privacy_in_the_Internet_of_Medical_Things_Taxonomy_and_Risk_Assessment

ANON (2002). Breathing Tests for Babies. [online]. London, *GOSH Trust.*
http://www.ich.ucl.ac.uk/factsheets/families/F020801/index.html

ARAR, S. (2017). An Introduction to the Fast Fourier Transform. EETech Media, LLC. [Online]. Last accessed 22 Jan. 2019 at:
https://www.allaboutcircuits.com/technical-articles/an-introduction-to-the-fast-fourier-transform/

ARDUINO. 2018. Arduino Uno Rev3. [Online]. Last accessed 27 Jan. 2018 at:
https://store.arduino.cc/usa/arduino-uno-rev3

ARLOTTO, P., GRIMALDI, M., NAECK, R., & GINOUX, J. (2014). *Sensors, 14*, 15371-15386.

ARLOTTO, P., GRIMALDI, M., NAECK, R., et al. (2014). An Ultrasonic Contactless Sensor for Breathing Monitoring. *Sensors Journal*, ISSN 1424-8220.

ASHTON, K. AND ASHTON, K. 2018. *Internet of Things case study: Boston Children's Hospital and smarter healthcare.* IoT Tech News. [online] Last accessed 5 Jul. 2018 at
https://www.iottechnews.com/news/2017/feb/28/internet-things-case-study-boston-childrens-hospital-and-smarter-healthcare/

BAYES DE LUNA, ANTONI, N. BATCHVAROV, Velislav and MALIK, Marek (2005), The Morphology of the Electrocardiogram.1.

BAYRAM, B., et al. (2003). A new regime for operating capacitive micromachined ultrasonic transducers. *IEEE Trans. Ultrason. Ferroelectr. Freq. Control*.

Beijing Ultrasonic. (2012-2013). [online]. Last accessed 30 August 2013 at: http://www.bjultrasonic.com/ultrasonic-technical-info/ultrasonic-transducers-and-ultrasonic-sensors/

BESL, P. And MCKAY, M. (1992). A method for registration of 3-d shapes. *IEEE Transactions on Pattern Analysis and Machine Intelligence.*, **14** (2).

CHAN, LAI SAN (2007/2008). *Development of an ultrasound system to monitor breathing in infants*. Msc. Project, Sheffield.

COETZEE, L. AND EKSTEEN, J., (2011), May. The Internet of Things-promise for the future? An introduction. In *IST-Africa Conference Proceedings, 2011* (pp. 1-9). IEEE.

COOKING-HACKS (2013). E-Health Sensor Platform for Arduino and Raspberry Pi, Biometric / Medical Application. [online]. *Airflow: breathing*,. http://www.cooking-hacks.com/documentation/tutorials/ehealth-biometric-sensor-platform-arduino-raspberry-pi-medical

COX, BEN (2013). *Acoustics for Ultrasound Imaging*, 5-44.

DORKBOTPDX. 2013. Battery Pack Load. [Online]. Last accessed 27 Jan. 2018 at: https://www.dorkbotpdx.org/blog/paul/battery_pack_load

DRINNAN, M J, ALLEN, J, LANGLEY, P, et al. (2000). In Computers in Cardiology Proceedings. *Detection of Sleep Apnoea from Frequency Analysis of Heart Rate Variability*, 259-262.

DRONEBOT WORKSHOP. (2017). Using the HC-SR04 Ultrasonic Distance Sensor with Arduino. [Online]. Last accessed 16 Jan. 18 at: https://dronebotworkshop.com/hc-sr04-ultrasonic-distance-sensor-arduino/

DUANE M., BLACKBURN (2001). Face Recognition The Technology and Its Applications.

ECHOCARDIOGRAPHER (2013). Axial, Lateral and Temporal Resolution. [online].

ELMER G., PINZON, MD, MPH, and RANDY E., MOORE, et al. (2009). A brief overview of diagnostic and therapeutic applications in musculoskeletal medicine. *Musculoskeletal ultrasound*, 34-43.

EQA (2005). 8.1 The Respiratory System. *Respiration System*, Chapter 8, 142-153.

ESP8266 PIN DIAGRAM. 2016. Circuits4you.com [Online]. Last accessed 28 Feb. 19 at: https://circuits4you.com/2016/12/14/esp8266-pin-diagram/

ESPRESSIF SYSTEMS. (2013). Espressif smart connectivity platform: ESP8266. [Online]. Last accessed 28 Feb. 19 at: https://cdn-shop.adafruit.com/datasheets/ESP8266_Specifications_English.pdf

FENSTER, AARON, DOWNEY, DONAL B. AND CARDINAL, H. NEALE (2000). Three-dimensional ultrasound imaging. *Institute of Physics Publishing*, **46** (1), R67–R99.

FERNANDO .L, ARBONA, BABK, KHABIRI, AND JOHN A., NORTON (2011). In: Ultrasound-Guided Regional Anesthesia: A Practical Approach to Pheripheral Nerve Blocks and Perineural Ceatheters. *Chapter 2: Introduction to ultrasound*, 10-23.

GADEKAR, C. & VAZE, V.M. (2017). Context Aware Computing: IOT for Neonatal Health Monitoring. *Advances in Computational Sciences and Technology, 10*(1), 53-62. Available from: https://www.ripublication.com/acst17/acstv10n1_05.pdf

GARG, A. (2018). *The Internet of Things: Impacts on Healthcare Security and Privacy*. Berkeley Research Group. Available from: http://www.litmos.com/wp-content/uploads/2016/06/webinar-IoT.pdf

GARREAU, F. 2015. Non-contact Respiratory Rate Monitoring in Children. [Thesis]. Medical Electronics research group in Materials and Engineering Research Institute (MERI) of Sheffield Hallam University, UK, *12-14*.

GAULTIER, C. (1999). *Sleep Apnoea in Infants*. Sleep Medicine Reviews*, 3*(4), 303–312.

GENE, BALL, AND JACK, BREESE (2000). Relating Personality and Behaviour: Posture and Gestures. 1814, 196-203.

GEORGE, DR LENORE, AND LAI, DR JAMES (2006). Ultrasound Physics. *AACA Pre-conference Workshop perioperative ultrasound*, 1-5.

GHOSH, S. K. (2013). 1. Concept of Images. *In: Digital Signal Processing*. Oxford, Alpha Science International Ltd., 1.1-1.8.

GHOSH, S. K. (2013). 2. The Process of Imaging. *In: Digital Image Processing*. Oxford, Alpha Science International Ltd., 2.1-2.17.

GUILLEMINAULT, C, CONNOLLY, S J, and WINKLE, R A (1984). Cyclical variation of the heart rate in Sleep Apnoea syndrome. *Lancet*, 1:126.131.

HARRIS, I (2015). *Understanding Security in IoT: SSL/TLS*. [Online] Last accessed 24 Mar 2020 at: https://dzone.com/articles/understanding-security-in-iot-ssltls

HASHIZUME, H., KANEKO, A., SUGANO, Y., YATANI, K., & SUGIMOTO, M. (2005). Fast and accurate positioning technique using ultrasonic phase accordance method. *TENCON 2005 – 2005 IEEE Region 10 Conference*,

Melbourne, 1–6.
Http://echocardiographer.org/Echo%20Physics/Axresolution.html

HC-SR04. (n.d.). Ultrasonic ranging Module HC – SR04. ElecFreaks.
https://cdn.sparkfun.com/datasheets/Sensors/Proximity/HCSR04.pdf

ICSTATION TEAM. 2014. The introduction of lm2596 step down power module dc-dc converter. [Online]. Last accessed 1 Feb. 2018 at:
http://www.instructables.com/id/The-Introduction-of-LM2596-Step-Down-Power-Module-/

IEC 60601-1-2:2014. (2018). IEC Webstore. [Online]. Last accessed 09 Jul. 18 at
https://webstore.iec.ch/publication/2590

IHARA, IKUO (2008). *Ultrasonic Sensing: Fundamentals and Its Applications to Nondestructive Evaluation*. Nagaoka University of Technology, *21*, 287-305.

IKNOW SENSORS (2003). Training Note Understanding Beam Pattern. Data Sheet, *Banner Engineering Corp*.

"*Internet of Medical Things (IoMT)*" (2017). UST Global Inc. Available from:
https://www.ust-global.com/sites/default/files/internet_of_medical_things_iomt.pdf

JIANG, BIHAN, VALSTAR, F. MICHEL AND MICHEL, MAJA (2011). Action Unit detection using sparse appearance descriptors in space-time video volumes. *Social Signal Processing Network*, 314-321.

JOSHI, PUSHKAR, et al. (2003). Learning Controls for Blend Shape Based Realistic Facial Animation. *Eurographics/SIGGRAPH Symposium on Computer Animation*.

KALMAN, R E (1960). A New Approach to Linear Filtering and Prediction Problems. *Transactions of the ASME. Journal of Basic Engineering*, 35-45.

LADABAUM, I., et al. (1998). Surface micromachined capacitive ultrasonic transducers. IEEE Trans. Ultrason. Ferroelectr. Freq. Control , **45** (3), 678-679.

LADY ADA. (2012). DHT22 Overview. [Online]. Last accessed 27 Mar. 18 at:
https://learn.adafruit.com/dht

LADY ADA. 2018. DHT22 Overview. [Online]. Last accessed 27 Mar. 18 at:
https://cdn-learn.adafruit.com/downloads/pdf/dht.pdf

LEI, H., LIANG, W., & QUE, P. (2008). Maximum nongaussianity principle for ultrasonic flaw detection. *17th World Conference on Nondestructive Testing*, Shanghai, China.

LEIGHTON, G. T. (2007). What is Ultrasound? *Prog. Biophys. Mol. Biol*., **93**, 3-83.

LUIS, PIZARRO, et al. (1999). Airborne ultrasonic electrostatic transducers with conductive grooved backplates: tailoring their centre frequency, sensitivity and bandwidth. *Ultrasonics*, **37** (7), 493-503.

MAN, G C W, and KANG, B V (1995). Chest. *Validation of a Portable Sleep Apnoea Monitoring Device*, 108:388.93.

MANTHEY, W., KROEMER, N. and MÁGORI, V. (1992). Ultrasonic transducers and transducer arrays for applications in air. *Meas. Sci. Techn*., 249-261.

MASON, L. (2002). Obstructive Sleep Apnoea. *Signal Processing Methods for Non-Invasive Respiration Monitoring*, chap 7, 7.3, 136-139.

MICROPIK. (n.d.). Ultrasonic Ranging Module HC – SR04. [Online]. Last accessed 16 Jan. 18 at: http://www.micropik.com/PDF/HCSR04.pdf

MIN, S.D., KIM, J.K, SHIN, H.S., YUN, Y.H., LEE, C.K., & LEE, M. (2010). Noncontact Respiration Rate Measurement System Using an Ultrasonic Proximity Sensor. *IEEE Sensors Journal,* **10** (11).

MIN, S.D., YOON, D.J., YOON, S.W., YUN, Y.H., & LEE, M. (2007). A study on a non-contacting respiration signal monitoring system using Doppler ultrasound. *Med Bio Eng Comput,* **45**, 1113–1119.

MOEBUS, MARCO AND ZOUBIR, ABDELHAK M. (2007). Three-dimensional ultrasound imaging in air using a 2d array on a fixed platform. II, 961-964.

MORLEY, C.J., THORNTON, A.J., FOWLER, M.A., et al. (1990). Archives of Disease in Childhood. *Respiratory rate and severity of illness in babies under 6 months old*. **65** (8), 834-837.

MYELECTRONICSLAB. (2016). Getting started with esp8266 Arduino Connection – Part 1. [Online]. Last accessed 28 Feb. 19 at: https://myelectronicslab.com/getting-started-with-esp8266-connecting-with-arduino-part-1/

NETTIKADAN, D, RAJ, S. (2018). *Smart Community Monitoring System using Thingspeak IoT Platform.* International Journal of Applied Engineering Research ISSN 0973-4562 Volume 13, Number 17 (2018) pp. 13402-13408 © Research India Publications. http://www.ripublication.com

NEWNHAM, R.E., et al. (1980). Composite piezoelectric transducers. *Materials and Design*, **2** (2), 93-106.

NHANES (2008). Respiration Health Spirometry Procedures Manual: Basic of Respiration. [online]. *National Health and Nutrition Examination Survey*. http://www.cdc.gov/nchs/data/nhanes/nhanes_07_08/spirometry.pdf

NIMROD M., TOLE (2005). Chapter 5 Ultrasound Beam Shape. In: OSTENSEN, Harald (ed.). *Basic Physics of Ultrasonographic Imaging*.

NOBLE, R. A., et al. (2001). Wide bandwidth, micromachined ultrasonic transducers. *IEEE Trans. Ultrason. Ferroelectr. Freq. Control*, **48** (6), 1495-1507.

OLYMPUS, NDT (2006). *Ultrasonic Transducers Technical Notes*. Data Sheet, Panametrics-NDT.

OSHPARK (2013). 2-layer board of 0.56 x 0.61 inches (14.1 x 15.4mm). [Online]. Last accessed 27 Jan. 2018 at: https://oshpark.com/shared_projects/Da8m8oAz

OSSEIRAN, A., ELLOUMI, O., SONG, J. AND MONSERRAT, J.F. (2017). Internet of Things. *IEEE Communications Standards Magazine*, *1*(2), pp.84-84.

PADMANABHAN, K. (2008). Microcontroller-based Ultrasonic Distance Meter. *Electronics For You*, 68.

PALMA, LUIS PUEBLA and AMERICAS, RTAC (2008). Ultrasonic Distance Measurer. *Application Note, Freescale Semiconductor (AN3481)*.

PANWAR, M. & KUMAR, A. (2015). Security for IoT: an effective DTLS with public certificates. In *Computer Engineering and Applications (ICACEA), 2015 International Conference on Advances,* 163-166.

PARKES, RACHEAL (2011). Rate of Respiration: The Forgotten Vital Sign. *Emergency Nurse*, **19** (2), 7.

PART 1: IOT DEVICES AND LOCAL NETWORKS. (2017). Micrium. Available from:
https://www.micrium.com/iot/devices/

PAWLAK, S. And WRÓBEL, G. (2007). A comparison study of the pulse-echo and through-transmission ultrasonics in glass/epoxy composites. *Journal of Achievements in Materials and Manufacturing Engineering*, **22** (2), 51-54.

PEPPERL+FUCKS. (2018). *"Ultrasonic Sensors"*. [Online] Last accessed 26 Jul 2018 at: http://files.pepperl-fuchs.com/online-catalogs/911360/files/assets/common/downloads/page0648.pdf

PEPPERL & FUCHS. (2018). Ultrasonic Sensors Knowledge (Part 4). [Online]. Last accessed 12 Jul. 18 at: https://www.pepperl-fuchs.com/usa/en/25518.htm

PIEZOELECTRIC FILM SENSOR. [Online]. Datasheet 1, last accessed 27 Oct. 13 at: http://www.farnell.com/datasheets/81206.pdf

PITSON, D J and STRADLING, J R (1998). Autonomic Markings of arousal during sleep in patients Undergoing investigation for obstructive sleep apnoea, their relationship to EEG Arousals, respiratory events and subjective sleepiness. *Journal of Sleep Research*, 7:53.59.

POLYTECHNIC INSTITUTE OF NEW YORK UNIVERSITY (2012). Hands-on Activity: Measuring Distance with Sound Waves. [online]. http://www.teachengineering.org/view_activity.php?Url=collection/nyu_/activities/nyu_soundwaves/nyu_soundwaves_activity1.xml

POOLE, IAN (2013). What is SMT Surface mount technology. [online]. Last accessed 18 June 2013 at: http://www.radio-electronics.com/info/data/smt/what-is-surface-mount-technology-tutorial.php

RAFAEL C., GONZALEZ and RICHARD E., Woods (2001). Chapter 2. *In: Digital Signal Processing*, 2nd ed., Pearson Education, 34-74.

RAFIQ, M. And WYKES, C. (1991). The performance of capacitive ultrasonic transducers using v-grooved backplates. *Meas. Sci. Technol*., (2), 168-174.

RANCIDBACON. N.D. 2018. ESP8266 WiFi Module Quick Start Guide. [Online]. Last accessed 28 Feb. 19 at: http://rancidbacon.com/files/kiwicon8/ESP8266_WiFi_Module_Quick_Start_Guide_v_1.0.4.pdf

REIF, F. Section 6.3, 7.8, 10.6, 10.7. In: Fundamentals of Statistical and Thermal Physics. Mcgraw-Hill.

ROBERT A., SOFFERMAN (2011). 2. Physics and Principles of Ultrasound. *In: Ultrasound of the Thyroid and Parathyroid Glands. Springer*, **11**.

SANTIAGO, A.C. (2018). *NICU or Neonatal Intensive Care Unit*. verywellhealth. Available from: https://www.verywellhealth.com/nicu-what-is-a-nicu-neonatal-intensive-care-unit-1736230. [08 Oct. 2018]

SCHINDEL, D. W., et al. (1995). The design and characterization of micromachined air-coupled capacitance transducers. *IEEE Trans. Ultrason. Ferroelectr. Freq. Control*, *42* (1), 42-50.

SEARS, TOM (no date). Breathing. [online]. US, *Answer.com*. http://www.answers.com/topic/breathing?Cat=health

SENIX CORPORATION. 2018. *Frequently asked questions about Ultrasonic Sensors*. [Online] Last accessed 24 Jul 2018 at: https://senix.com/frequently-asked-questions/.

SENSCOMP (2005). MINI-A PB Ultrasonic Transducer and MINI-A Application Note 2005-2. [online]. http://www.senscomp.com

SENSCOMP (2016). SonaSwitch MINI-A Ultrasonic Sensor. [Online]. http://www.senscomp.com/pdfs/Mini-A-Ultrasonic-Sensor-Spec.pdf

SENSCOMP GLOBAL COMPONENTS (2004). MINI-A Ultrasonic Sensor. Data Sheet, *Senscomp*.

SHAKUNTHALA, M., JASMIN BANU, R., DEEPIKA, L., & INDU, L. 2018. Neonatal Healthcare Monitoring in Incubator Using IoT *International Journal of Electrical, Electronics and Data Communication, 6*(6), 59-64. Available from: http://www.iraj.in/journal/journal_file/journal_pdf/1-478-153414320559-64.pdf

SHAUN, CANAVAN, et al. (2011). 3D Face Sketch Modeling and Assessment for Component Based Face Recognition. In: *2011 International Joint Conference on Biometrics (IJCB)*, Washington, DC, 11-13 Oct. 2011. IEEE, 1-6.

SHIRWAIKAR, R.D., DINESH ACHARYA, U., MAKKITHAYA, K., SURULIVELRAJAN, M., & LEWIS, L.E.S. (2016). Machine Learning Techniques for Neonatal Apnoea Prediction. *Journal of Artificial Intelligence, 9*, 33-38. Available from: https://scialert.net/fulltext/?doi=jai.2016.33.38

SINGH, H., YADAV, G., MALLAIAH, R., JOSHI, P., JOSHI, V., KAUR, R., BANSAL, S., BRAHMACHARI, S. 2017. iNICU – Integrated Neonatal Care Unit: Capturing Neonatal Journey in an Intelligent Data Way. *J Med Syst, 41*(132). Available from: https://www.researchgate.net/publication/318709338_iNICU_-_Integrated_Neonatal_Care_Unit_Capturing_Neonatal_Journey_in_an_Intelligent_Data_Way/fulltext/5978eac9aca27203ecc62f8b/318709338_iNICU_-_Integrated_Neonatal_Care_Unit_Capturing_Neonatal_Journey_in_an_Intelligent_Data_Way.pdf?origin=publication_detail

SOMATECHNOLOGY. *Isolette Incubators*. [Online] Last accessed 07 Jul 2019 at: https://www.somatechnology.com/blog/press-releases/isolette-incubators/.

STACKEXANGE. 2014. 2-layer board of 0.56 x 0.61 inches (14.1 x 15.4mm). [Online]. Last accessed 27 Jan. 2018 at: https://arduino.stackexchange.com/questions/9069/powering-an-arduino-mega-with-external-usb-power-bank

SUBBE, C. P., DAVIES, R. G., WILLAMS, E., et al. (2003). Effect of introducing the Modified Early Warning score on clinical outcomes, cardio-pulmonary arrests and intensive care utilisation in acute medical admissions. *Anaesthesia,* **58**, 797-802.

THE MCGRAW-HILL COMPANIES (2001). Respiration. *The Mechanism of Body Function*, 8th ed., Chap 15.

THE ROLE OF INTERNET OF THINGS IN THE HEALTHCARE INDUSTRY (2018). Hackernoon. Available from: https://hackernoon.com/the-role-of-internet-of-things-in-the-healthcare-industry-759b2a1abe5

THEODORE J., DUBINSKY, et al. (2008). High-Intensity Focused Ultrasound: Current Potential and Oncologic Applications. *Ultrasound Imaging. Review*, 191-199
.

THINGSPEAK (2020). Portal [Online] Last accessed 28 Mar 2020 at: https://thingspeak.com/channels/971899/private_show

ULTRASONIC SONAR SENSORS. (2008). [online]. Last accessed 22 June 2013 at: http://www.generationrobots.com/ultrasonic-sonar-sensors-for-robots,us,8,19.cfm

WEINTRAUB, Z., CATES, D., KWIATKOWSKI, et al. (2001). Respiration Physiology. [online]. *The morphology of periodic breathing in infants and adults*, **127** (2-3), 173-184. http://www.sciencedirect.com.lcproxy.shu.ac.uk/science/journal/00345687

WHITE, M.G (no date). The Baby Belly Breath. [online]. USA, *Breathing.com*. http://www.breathing.com/articles/baby-belly-breathing.htm

WILLIAM R., HENDEE, and E. RUSSELL, RITENOUR (2002). In: Medical Imaging Physics. *Chapter 19 Ultrasound Waves*, 4th ed., 304-315.

ZANELLI, c. I., et al. (1993). Beamforming for therapy with high intensity focused ultrasound (hifu). *Ultrasonics symposium*.

ZHAO, J., GONZALEZ, F., & MU, D. (2011). Apnoea of Prematurity: From Cause to Treatment. *European Journal of Pediatrics, 170*(9), 1097–1105. Available from:
https://www.ncbi.nlm.nih.gov/pmc/articles/PMC3158333/

Appendices

Ultrasound based Respiration Rate Monitoring System for Incubators - Practical setup in Figure 94.
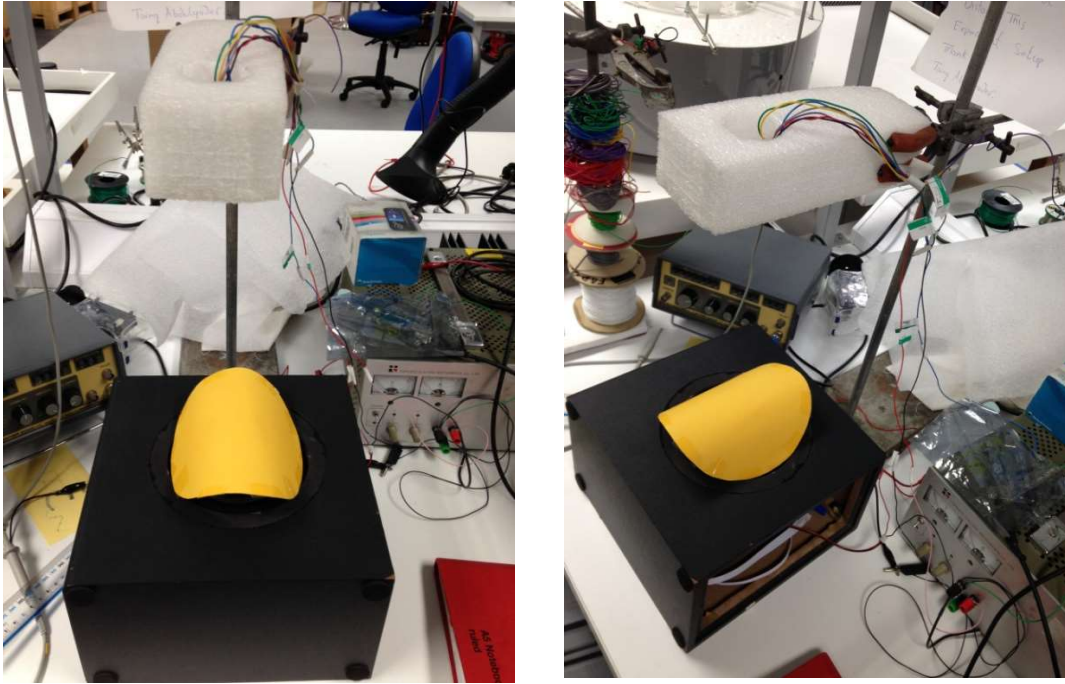
Figure 90: Practical Setup of Incubator

MATLAB Code to graphically depict infant's respiration rate

```matlab
res.m

clc
close all
clear all

load data2herts.dat %load data

data=data2herts;  %common variable
data=data-mean(data);  %removes dc

fs=20;  %defines sample rate
Ts=1/fs;  %sample interval

L=length(data);  %how many samples
k=0:L-1;
t=k*Ts;    %creates time axis

N=8;  %filter order
fc=2; %filter cutoff
wc=fc/(fs/2);  %normalise cutoff
[B,A]= butter(N, wc);  %designs filter
y=filter(B,A, data);  %performs filtering

figure
subplot(211)
plot(t,y)
xlabel('Time, sec')
ylabel('Amplitude, volts')
title('Illustration of 120 Cycles/min')

f= k/(L*Ts);  %create frequency axis
X=(2/L)*abs(fft(data));  %obtains the spectrum

subplot(212)
plot(f, X);
xlabel('Frequency, Hz')
ylabel('Magnitude')
```

Hardware Components

The Hardware components used in this project are described in this section.

A. Ultrasonic Sensor

The type of ultrasonic sensor used in this project is a transceiver, which can both transmit and receive ultrasonic waves. The model of this sensor is HC-SR04. It is a 4-pin module, whose pin names are VCC, Trigger, Echo and Ground. The working mechanism of this ultrasonic sensor is shown in Figure 95.

Figure 91: Working of Ultrasonic Sensor

The speed of Ultrasonic wave is same as sound wave, which is 340 m/s, but this varies with temperature and humidity in air. The ultrasonic waves are also affected by temperature and humidity in air. To account for this variation, the temperature and humidity sensor is also used in this project.

The Ultrasonic transmitter transmits an ultrasonic wave that travels in air. When it gets obstructed by any material, it gets reflected back towards the sensor. This reflected wave is absorbed by the Ultrasonic receiver module as shown in Figure 104. The sensor works with the simple formula namely:

$$Distance = speed * Time$$

The speed of sound is 340 m/s. Time depends on placement and detection of obstacle. Using these values, distance is measured.

Advantages: Ultrasonic sensors can be used in the detection of an object. The parameters detected are:

- Presence
- Level
- Position
- Distance

Properties: Ultrasonic waves are independent of:

- Light
- Smoke
- Dust
- Colour
- Material (except for soft surfaces, i.e. wool, because the surface absorbs the ultrasonic sound waves and doesn't reflect sound.)

B. Temperature and Humidity Sensor

The DHT11 Temperature and Humidity Sensor is a very accurate calibrated digital sensor whose output consists of both temperature and humidity values. It consists of hygrometer for humidity measurement and NTC temperature sensor (thermistor) for temperature measurement.

C. Arduino UNO

Arduino is a microcontroller board that is most commonly used nowadays. Arduino family has different types of boards available in the market. The most common and extensively used microcontroller is Arduino UNO.

Arduino UNO is a microcontroller board that uses ATmega328P single-chip microcontroller. Arduino board has 14 digital input/output pins (of which 6 can be used as PWM outputs), 6 analogue input pins, 1 16 MHz quartz crystal, 1 USB connection, 1 power jack, 1 ICSP header, and a reset button. It contains everything needed to support the ATmega328P microcontroller. The Arduino UNO board is shown in Figure 116 in Appendix E. Interfacing I2C with Arduino board is given in Appendix F.

Distance Measuring Ultrasound Sensors – MINI-A and HC-SR04

A. Principle behind Distance / Range Measurement using Ultrasonic Sensors

The ultrasonic distance sensor is capable of measuring distances between 2 cm to 400 cm, i.e. the distance between the sensor and the object with sensitivity measuring as less than a millimetre. It is a low current device and hence is suitable for battery powered devices. It is also suitable for portable devices which are also the objective of this project (Micropik, n.d.).

Ultrasonic distance sensors use pulses of ultrasonic sound (sound above the range of human hearing) to detect the distance between them and nearby solid objects while some ultrasonic sensors have the capabilities to detect water level. The sensors consist of two main components namely (DroneBotWorkshop, 2017):

Ultrasonic Transmitter – This transmits the ultrasonic sound pulses. It operates at 40 KHz.

Ultrasonic Receiver – The receiver listens for the transmitted pulses. If it receives them, it produces an output pulse whose width can be used to determine the distance the pulse travelled.

There are many applications, such as: level measurement, proximity detection, presence detection, robotics, educational products etc.

B. MINI-A Ultrasonic Sensor

The MINI-A sensor shown in Figure 96 provides a total system in a compact package, which contains an ultra-sensitive electrostatic transducer and the supporting circuitry to provide a 0 to +5 VDC (or 0 to +10 VDC) output with fully independent zero and span adjustments over the entire operating range of detecting a target from 1-12 inches, 6"-40' away. The MINI-A can be externally triggered or can continually sense at a 10 Hz rate. (SensComp Global Components, 2004).
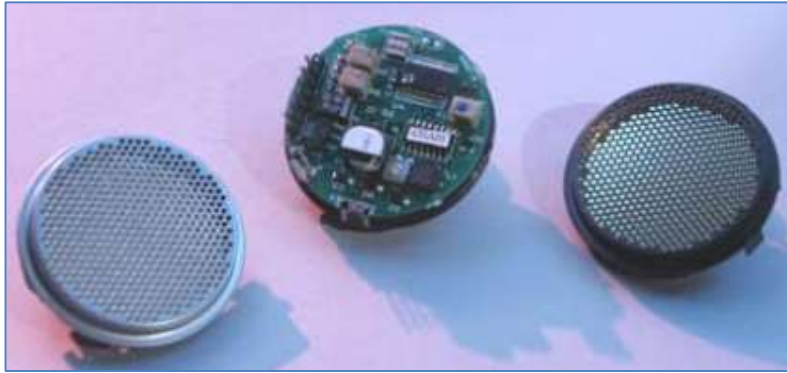
Figure 92: Mini-A Sensor (Senscomp, 2005)

MINI-A Ultrasound sensor's features

The features of this sensor are stated below:

- 50 kHz electrostatic transducer with integrated Surface Mount Technology (SMT) and electronic circuitry.

  o SMT is preferred because the wires that had traditionally been used for connections were not actually needed for printed circuit board construction. Rather than having leads placed through holes, the components could be soldered onto pads on the board instead.

  o As the components were mounted on the surface of the board, rather than having connections that went through holes in the board, the new technology was called SMT and the devices used were surface mount devices, Surface Mount Devices (SMDs). (Poole, 2013).

  o This technology is used because they are low in cost, highly efficient, quick to manufacture and safe to use.

- Ranges from 1" to 12", 6" to 20" or from 12" to 40".

  o Accuracy of a sensor depends on the distance between it and the target.

- Analogue Output from 0 to 5 VDC or from 0 to 10 VDC.

- Independent Push-Button Settable Zero and Span Adjustment of Analogue Output.

- Range Window LED Indication.

- Analogue Output Temperature Compensated.

MINI-A Ultrasound sensor setup instruction

Figure 97 illustrates the MINI-A US pinout.
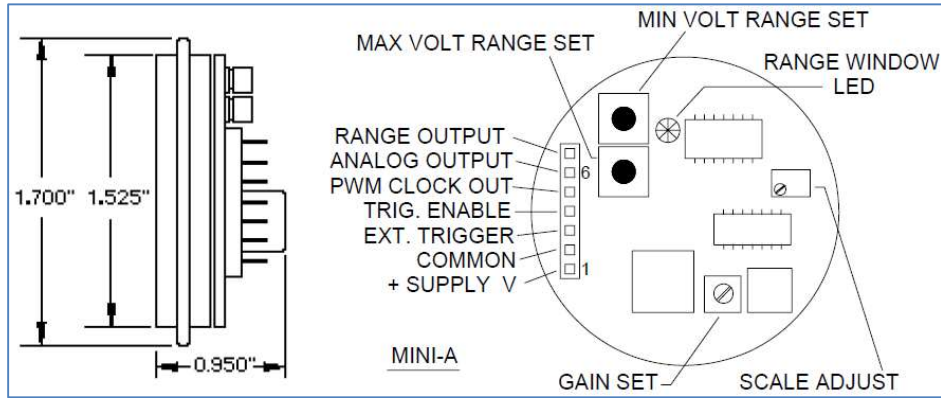
Figure 93: Mini-A US Sensor Pinout (Senscomp Global Components, 2004)

Overall Hardware Connection

This subsection will list out all the hardware connections and wiring of the whole ultrasound sensors system. Figure 97 and Figure 98 show the typical pinning for MINI-A ultrasound sensor.

The overall connection of the whole system only involved wiring of two digital signal pins for triggering MINI-A sensor, two analogue signal pins for collecting the output voltage from MINI-A sensor, power supply source wiring, external trigger enabled pins for both sensors and ground (GND), and pin connection of myDAQ device to the negative of power supply source.
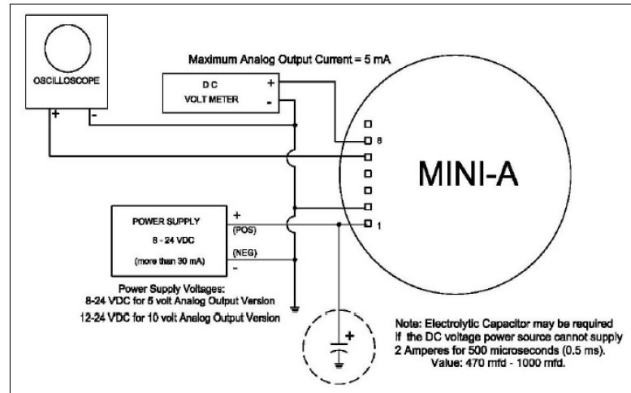
FIGURE 94: MINI-A US Sensor Connection Diagram (Senscomp Global Components, 2004)

As the ultrasound sends a 'ping' and waits to hear an echo, sound waves propagate from the transmitter and bounce off objects, returning an echo to the receiver. If the speed of sound is known, the distance to an object can be calculated from the time delay between the emitted and reflected sounds.

While the principle of calculating distance from the time of travel is simple, there are many limiting factors to consider. Sound diverges very rapidly, so the transducer must be carefully designed to produce a beam as small as possible. While some applications require a wide beam, a narrow beam improves the range and reduces background interference as this is going to be the main focus of accomplishment. There is a direct relationship between beam width and target surface angle: the wider the beam, the greater the possible angle between the transducer and the surface. When the angle is too great (>12 degrees), the reflected beam misses the transducer. While some surfaces may produce scattered diffuse reflections, these are much weaker and are not used for distance measuring purposes leading to inaccuracy.

Furthermore, humidity alters the attenuation of sound in air, which determines the maximum range of an ultrasonic device. Attenuation is also related to the frequency of the emitted sound. Higher frequencies improve the sampling resolution but attenuate more thereby reducing the range.

The stated possible limitations that could introduce inaccuracy to the experiment would have to be properly addressed, to achieve the aim and objects of this project.
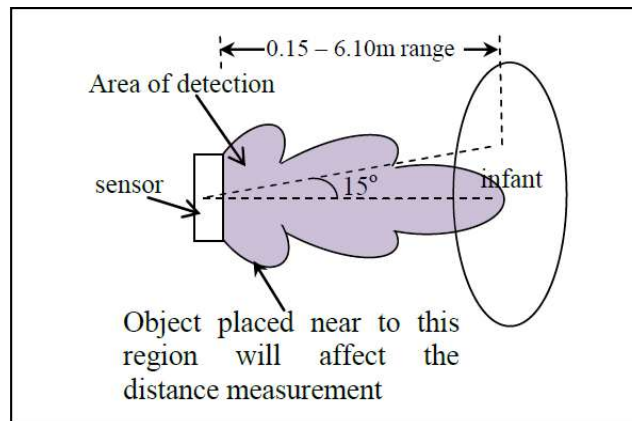
Figure 95: Mini-A Ultrasound effective measurement area (Senscomp, 2005)

Any object placed within the area shown as in Figure 99 will cause echo pulse above the MINI-A's threshold voltage of 2V. As shown in Figure 100, the MINI-A transducer has a Pulse Width Modulated (PWM) clock output that provides TTL-compatible digital waveform to measure time of flight (TOF) of echo pulse signal between the sensor and the target.

The ultrasound transmitter of MINI-A sensor will act as the receiver for the echo pulse. When the MINI-A transducer is triggered, the PWM clock will change from logic '0' to logic '1'. Any detected echo pulse above 2V threshold voltage will stop this clock.
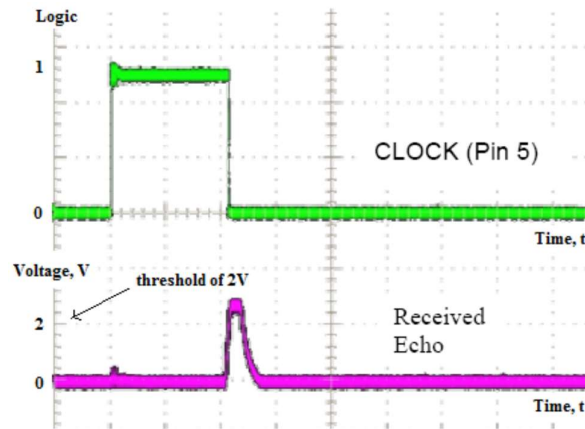
Figure 96: Mini-A Sensor's PWM Clocking with respect to echo pulse (Senscomp, 2005)

The measured time, t, is to be utilised to determine the distance of object where distance $L = Vt/2$. V is the constant speed of pulse transmitted and t is the PWM time.

The corresponding output voltage for distance is to be obtained, then processed internally by MINI-A sensor using equation 14:

$$V_{out}=0.9V_{new}+0.1V_{old}. \text{ (SENSCOMP, 2005)} \qquad (14)$$

EQUATION 9: OUTPUT VOLTAGE V_{OUT}

Typical demonstration of output voltage and the corresponding measured distance are shown in Figure 101.
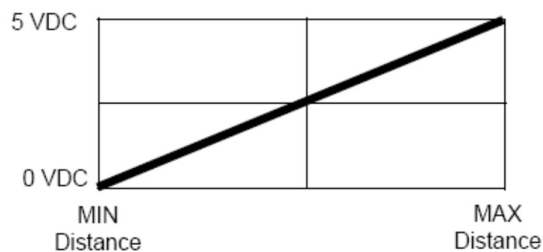
Figure 97: Characteristic of Mini-A Sensor's Output Voltage with respect to distance (Senscomp, 2005)

The distance of baby's chest wall is to be monitored for specific period of time. During inhaling, the chest will expand and the distance measured will be reduced. When exhaling, the chest will inflate and the distance between sensor and baby's chest wall will increase.

Figure 102 shows the method of determining inhaling and exhaling process of breathing. The values obtained during breathing are to be used to determine the breathing count (inhaling and exhaling cycle).
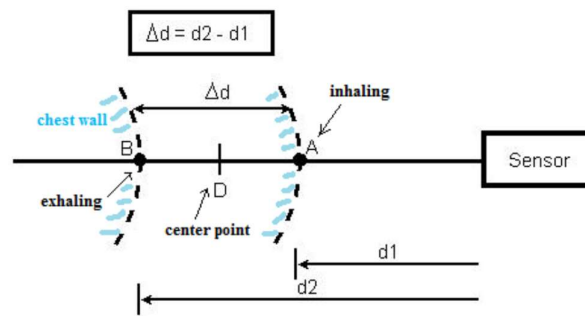
Figure 98: Measuring distance of chest wall during inhaling and exhaling
(Senscomp 2005)

Ultrasound beam pattern
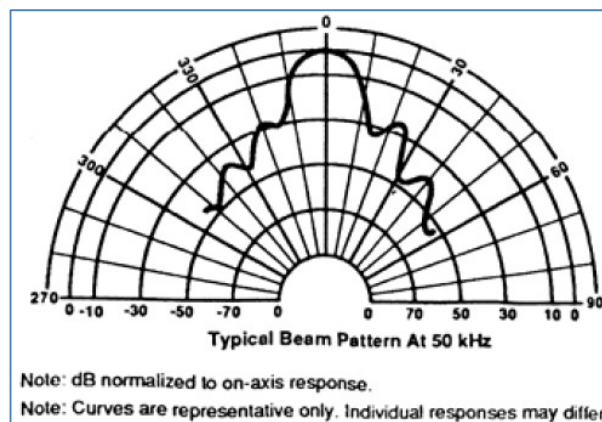
Figure 99: Beam Pattern (Mimrod, 2005)

As a beam of ultrasound travels outwards from the surface of the transducer, the spreading of the ultrasonic energy undergoes change in area. The phrase "ultrasound beam shape" usually refers to this relation. Generally, ultrasound beam suffers from divergence, as it moves away from the transducer (Nimrod, 2005).

The beam pattern shown in Figure 103 actually shows the performance of the sensor, particularly at a certain frequency, with its angular position, by which the beam is moving around the target. It predicts how adjacent, parallel, opposed-mode sensor pairs can be placed next to each other, without generating optical crosstalk (iKnow Sensors, 2003).

Benefits of Mini-A Sensor

- Self-Contained Compact Design.
- Can be triggered internally or externally.
- Excellent Receiving Sensitivity.
- Push Button Range Settings for Quick and Easy Set-Up.
- Works with almost any surface type
- Resistant to vibration, radiation, background light and noise
- Unaffected by dust, dirt or high humidity
- Facilitation to further research
- Low cost

Ultrasound Sensor precision

Despite the devise datasheet, an experiment is carried out to establish the actual precision of the US sensor. This will indicate how accurately the sensor can receive the ultrasound wave after hitting a target.

The sensor's output pin was connected to a voltmeter. The target was set at 200 mm roughly and observed by varying the distance of the sensor.
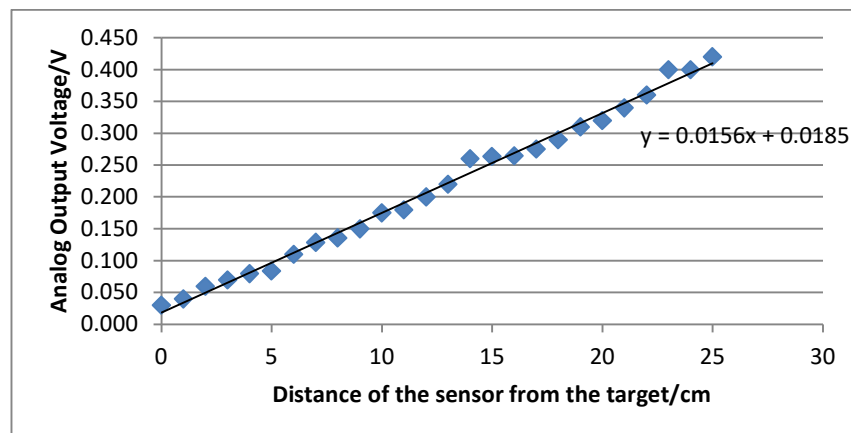
Figure 100: Sensor Precision (iKnow Sensors, 2003)

142

Figure 104 demonstrates the accuracy of the sensor. Looking at the line of best fit, it can be seen that the sensor would deliver precise result as it keeps its level of accuracy throughout, even after the increasing the distance. The US sensor would be a good way to start the experiment to gain knowledge of this research.

C. Distance Measuring Sensor - HC-SR04

The HC-SR04 Ultrasonic Distance Sensor is used to measure the distance of an object from itself. It is an inexpensive device that is very useful for robotics and test equipment projects. Also to demonstrate the overall objectives of this investigation for a viable contactless respiration rate monitoring system. The sensor is used to measure the distance of the baby in the incubator. HC-SR04 can be hooked directly to an Arduino or other microcontroller (Micropik, n.d.).

The Electric parameters of HC-SR04 is shown in Table 6.

Table 6: Electric Parameters for HC-SR04 Ultrasonic Sensor (Micropik, n.d.)

Parameter	Rating
Working Voltage	DC 5 V
Working Current	15 mA
Working Frequency	40 Hz
Max Range	4 m
Min Range	2 cm
Measuring Angle	15 degrees
Trigger Input Signal	10 μs TTL pulse
Echo Output Signal Input	TTL lever signal and the range in proportion
Dimension	45*20*15 mm

The HC-SR04 has the following four connections as shown in Table 7.

Table 7: Connections for HC-SR04 Ultrasonic Sensor (Micropik, n.d.)

Pin	Description
VCC	This is the 5 Volt positive power supply
Trig	This is the "Trigger" pin, the one driven to send the ultrasonic pulses
Echo	This is the pin that produces a pulse when the reflected signal is received. The length of the pulse is proportional to the time it took for the transmitted signal to be detected
GND	This is the Ground pin

The ultrasonic sensor operates at a 5V pulse with at least 10 μs in duration where it is then applied to the Trigger pin for initiation of the device. The US sensor thereby responds by transmitting a burst of 8 pulses at 40 KHz. The 8-pulse pattern, which is also known as a signature unique that allows the receiver to distinguish between the unrelated signals it receives, one being the classification of the transmitted pattern and the other being the alternative surrounding noise and so forth (Micropik, n.d.).

The ECHO pin triggers to a high state to start forming the beginning of the echo-back signal. When the burst of pulses is triggered and no data is received as there is no detected object in series for the pulse to reflect back, the receiving signal, i.e. the echo signal, will get timed-out after 38 ms, resulting in a low signal. A 38 ms pulse is then produced which would indicate no obstruction within the range of the sensor (DroneBot Workshop, 2017).

Conversely, the ECHO pin is set to a low state when the signal is received, i.e. when the pulse is reflected back due to the existence of an object causing the signal reflecting/echoing back to the receiving pin. Upon receiving of the pulse, it produces a pulse with the width that fluctuates between 150 μs to 25 ms, depending on the time it took for the signal to be received (DroneBot Workshop, 2017).

As a result, the width of the received pulse is used to calculate the distance to the reflected object. All in all, to achieve the correct distance, as the pulse indicates the time it took for the signal to be sent out and reflected back, the result requires to be divided by 2 (DroneBot Workshop, 2017). The HC-SR04 timing diagrams without and with object detection are shown in figures 105 and 106 respectively. Dimensions of HC-

SR04 sensor are presented in Figure 107. Its effective angle of operation is shown in Figure 108.
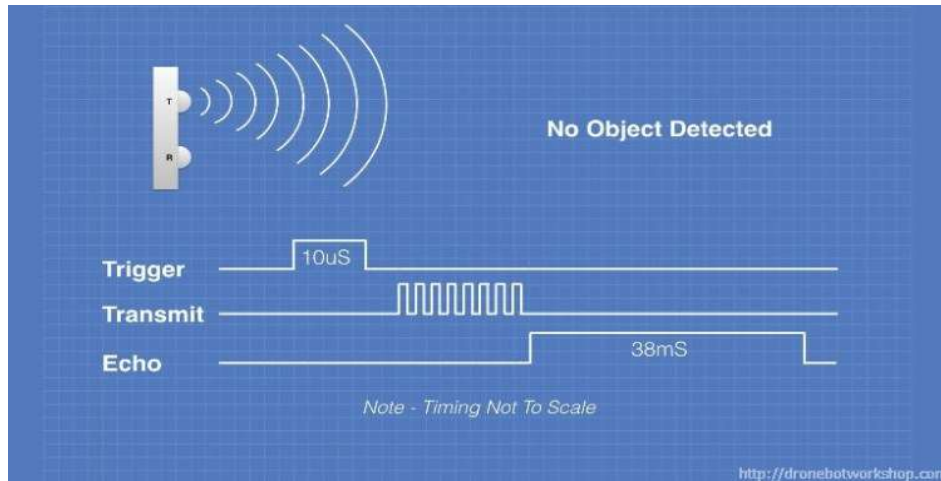
Figure 101: Illustration of HC-SR04 timing diagram with no object being detected (DroneBot Workshop, 2017)
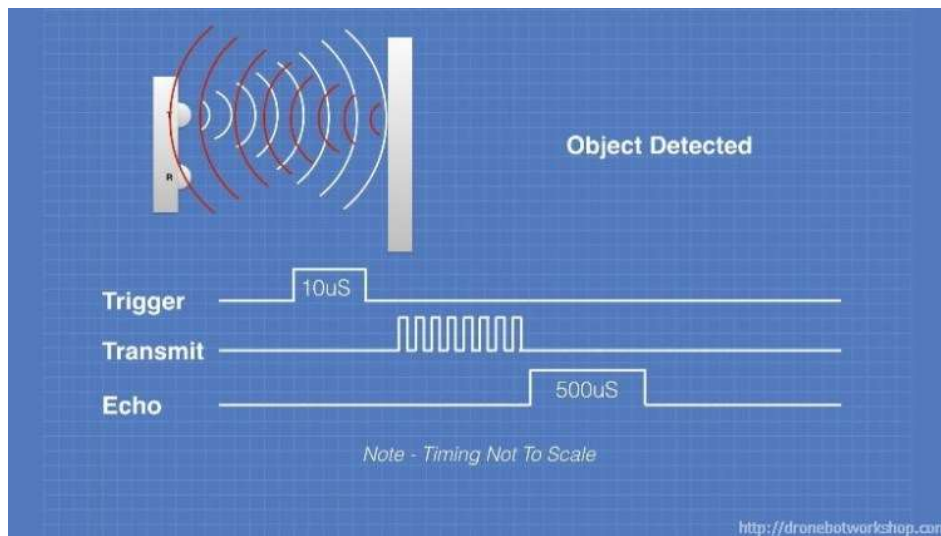
Figure 102: Illustration of HC-SR04 timing diagram with object being detected (DroneBot Workshop, 2017)
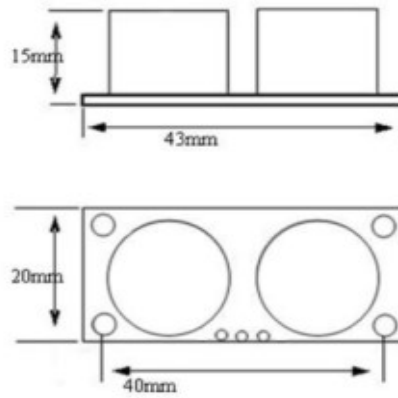
Figure 103: Illustration of the dimensions of the US sensor (DroneBot Workshop, 2017)

Practical test of performance,
Best in 30 degree angle
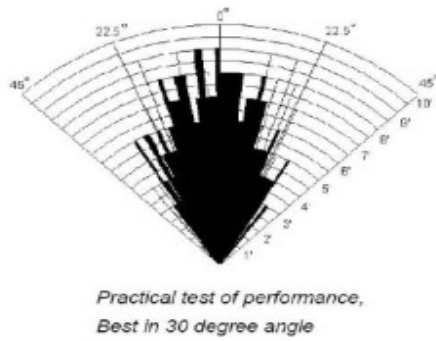
Figure 104: Demonstration of the effective angle of operation (DroneBot Workshop, 2017)

Interfacing Ultrasonic Sensor with Arduino Board

A. Arduino UNO

The Arduino UNO board is shown in Figure 109.
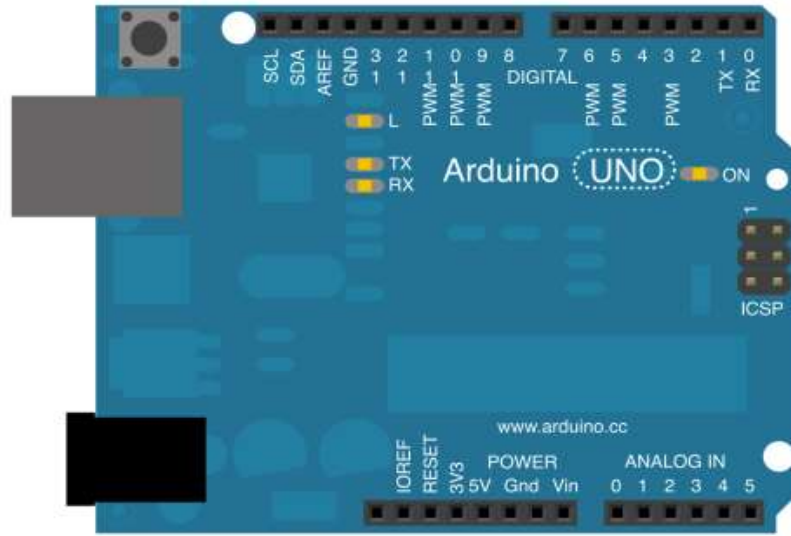
Figure 105: Arduino UNO (Ardunio, 2018)

The power pins of the Arduino board are (Ardunio, 2018):

-   VIN. The input voltage to the Arduino board when it is using an external power source (as opposed to 5 volts from the USB connection or other regulated power source). You can supply voltage through this pin, or, if supplying voltage via the power jack, access it through this pin.

-   5V. This pin gives an output of regulated 5V from the regulator on the board. The board can be supplied with power either from the DC power jack (7 - 12V), the USB connector (5V), or the VIN pin of the board (7-12V). Supplying voltage via the 5V or 3.3V pins, bypasses the regulator, and can damage your board. This is not advisable.

-   3V3. A 3.3 volt supply generated by the on-board regulator. Maximum current draw is 50 mA.

-   GND. Ground pins.

- IOREF. This pin on the Arduino/Genuino board provides the voltage reference with which the microcontroller operates. A properly configured shield can read the IOREF pin voltage and select the appropriate power source or enable voltage translators on the output to work with 5V or 3.3V pins.

B. Ultrasonic Sensor

The ultrasonic sensor is shown in Figure 110.

Figure 106: Ultrasonic Sensor

The four main pins in the ultrasonic sensor are:

- Vcc (5V supply)
- Gnd (Ground)
- Trig (Trigger)
- Echo (Receive)

C. Connection

- Ultrasonic sensor has four pins (GND, VCC, TRIG, ECHO).
- It works under 5V power supply. Connect VCC pin of sensor to Arduino 5V.
- GND pin of ultrasonic is connected to GND of Arduino
- Interface Trig pin of sensor is connected to 6th pin of Arduino
- Interface Echo pin of sensor is connected to 7th pin of Arduino

D. Connection Diagram
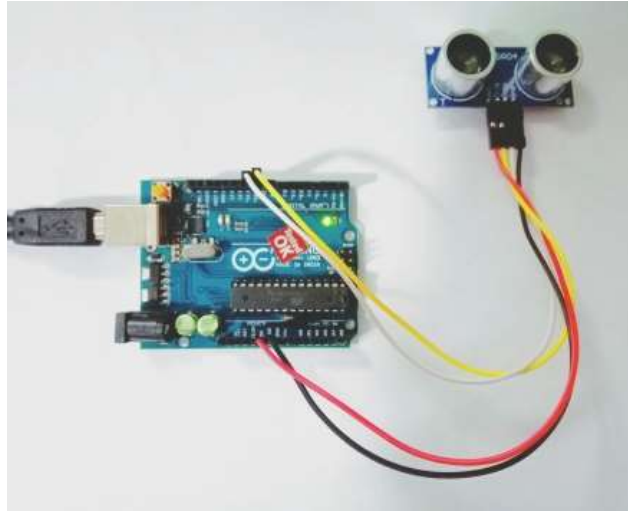
Figure 107: Interfacing Ultrasonic Sensor with Arduino Board

Connection of one ultrasonic sensor to Arduino board is shown in Figure 111. All four ultrasonic sensors are connected in a similar fashion.

Interfacing I2C LCD with Arduino

A. I2C LCD

The front and back view of I2C LCD is shown in Figure 112.
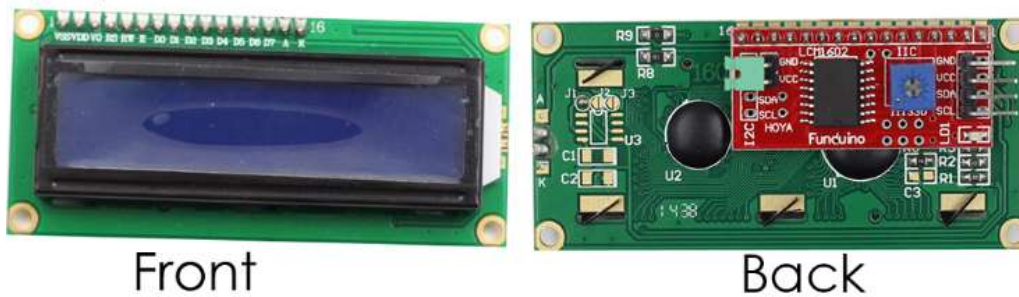
Figure 108: I2C LCD

There are four pins in I2C LCD namely:

• Vcc (5V supply)

• Gnd (Ground)

• SCL (Serial clock line)

• SDA (Serial data line)

B. Connection

• Connect VCC pin of LCD with Arduino 5V supply

• GND pin of LCD is connected to GND of Arduino

• SDA pin of LCD is connected to SDA / A4 pin of Arduino

• SCL pin of LCD is connected to SCL / A5 pin of Arduino

C. Connection Diagram

Connection diagram of I2C LCD is shown in Figure 113.
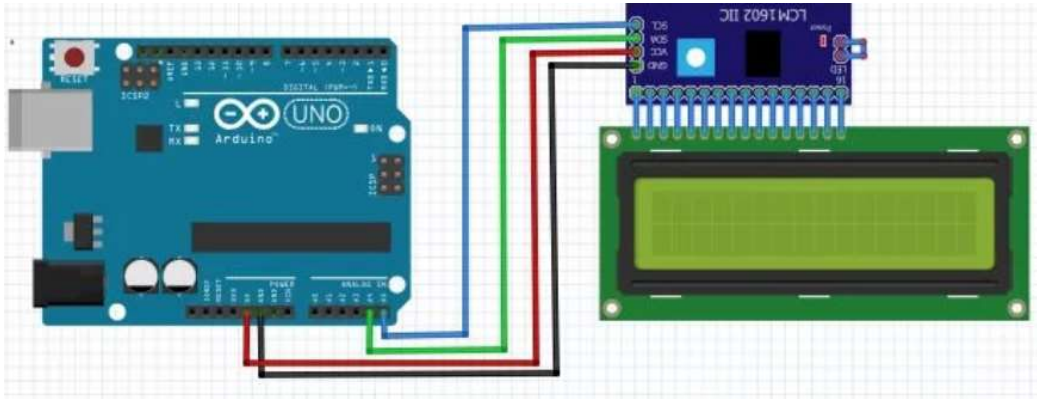
Figure 109: Interfacing I2C LCD with Arduino UNO

Instructions:

Make sure that I2C LCD library is installed in Arduino IDE.

You should have prior knowledge of I2C addresses of I2C LCD.

DHT22 – Temperature and Humidity Sensor

Since the speed of sound factors into the HC-SR04 distance calculation as this would affect the reading if the temperature was not taken into consideration, the use of DHT22 sensor is utilised to factor in the temperature and the humidity.

Measurement accuracy of an ultrasonic sensor depends on several parameters like air temperature, humidity, air pressure, air currents, external noise, and types of gas. In this case, the sensor is placed in an incubator working at controlled temperature, humidity, and air pressure. Speed of sound is 340 meters per second in air. Speed of ultrasonic signal increases with increase in temperature. (Pepperl & Fuchs, 2018).

Sensor is placed within 1-meter distance from the baby in the incubator. Since sound travels at a speed of 340 meters per second and the distance here is less than 1 meter, in a controlled temperature, temperature effect is very negligible on sound.

A. DHT22 Sensor

Figure 114 shows the wiring depiction of the DHT22 sensor with the Ultrasonic sensor and the Arduino Uno board.
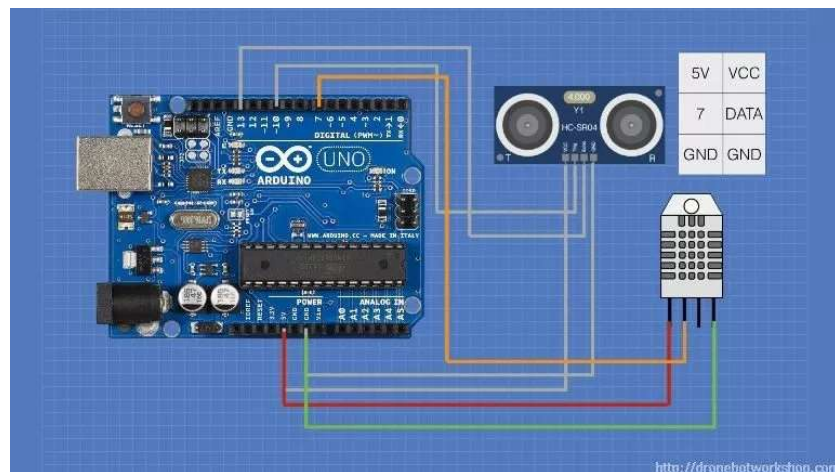
Figure 110: DHT22 Pinout and Wiring (Dronebot Workshop, 2017)

Wiring in this figure represents:

- Red wire – power of 5V recommended
- Orange wire – data out

- No wire - no connection
- Green - ground

In order to get DHT22 to function correctly, it requires a couple of code libraries from Adafruit. Two libraries, Adafruit AM2315 library and Adafruit Unified Sensor library, are installed directly within the Arduino IDE using the Library Manager, to provide the correct functionality of the sensor (Dronebotworkshop, 2017). An example of the results is shown in Figure 115.
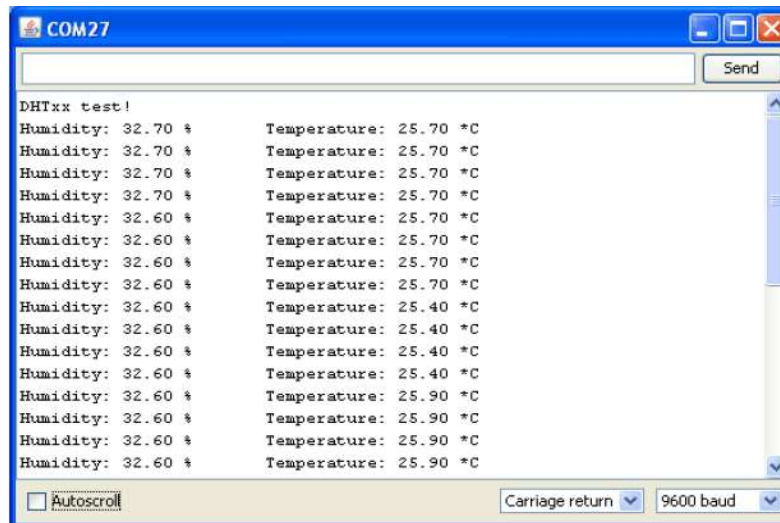
Figure 111: Temperature and Humidity (Lady Ada, 2018)

B. DHT22 Characteristics

Characteristics of DHT22 Sensor are (Lady Ada, 2012):

- Low cost
- 3 to 5V power and I/O
- 2.5mA max current use during conversion (while requesting data)
- Good for 0-100% humidity readings with 2-5% accuracy
- Good for -40 to 80°C temperature readings ±0.5°C accuracy
- No more than 0.5 Hz sampling rate (once every 2 seconds)
- Body size 15.1mm x 25mm x 7.7mm
- 4 pins with 0.1" spacing

C. Summary

The use of the DHT22 sensor would ideally be beneficial to the accuracy of the ultrasonic wave signals whilst taking into consideration the factors of the speed of

sound in air varying with temperature, air pressure, and humidity. This method provides a relatively inexpensive but very accurate, and efficient technique to the overall system accuracy.

ESP8266 Wi-Fi adapter

A. Hardware Connections

The connection of the module is considerably straight-forward. However, there are factors that needs to be considered in relation to input power (Rancidbacon, 2018):

- The ESP8266 requires 3.3V power
- The ESP8266 needs to communicate via serial at 3.3V

The connections available on the ESP8266 Wi-Fi module are shown in Figure 116.
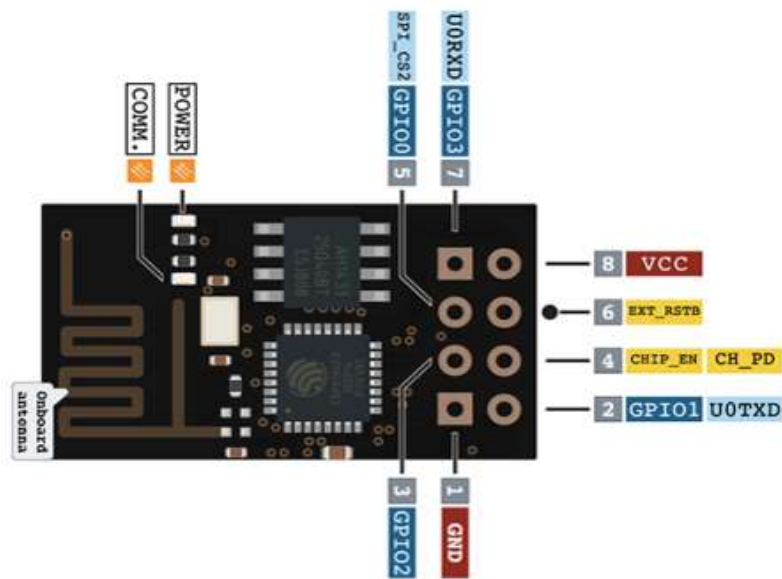
Figure 112: ESP8266 Pinout ("ESP8266 Pin Diagram", 2016)

Red power light turns on and the blue serial indicator light flickers briefly when power is applied to the module. This infers that the device is properly powered.

B. Applications of ESP8266

Some of the applications where ESP8266 US is used are (Espressif systems, 2013):

- Smart Power Plug
- Home Automation
- Mesh network
- Industrial wireless control
- Baby Monitor

- Network Camera

- Sensor networks

- Wearable electronics

- Wireless location-aware devices

- Security ID tag

- Wireless positioning system signals

- IoT

C. Ultra-Low Power Technology of ESP8266

The ESP8266 device consumes very little power whilst designed for mobile, wearable electronics. The main reason this device brings interest to the overall concept is for Internet of Things (IoT) applications. There are primarily three modes when it comes to its power saving architecture operation, namely active, sleep and deep sleep mode.

One of the many advantages of the ESP8266 device is that it consumes less than 12 uA in sleep mode and less than 1.0 mW (DTIM=3) or less than 0.5mW (DTIM=10) to stay connected to the wireless access point (Espressif systems, 2013).

Looking at the sleep mode feature, only the calibrated real-time clock and watchdog stays active. Wherein the real-time clock could be programmed should one would want to wake-up the ESP8266 device at any required interval. Additionally, it can be programmed to wake-up when a specific condition is met or detected. The "minimal wake-up time" feature of the ESP8266 is useful for mobile device SOCs, where this US would ideally allow them to stay in low-power standby mode until Wi-Fi is needed (Espressif systems, 2013).

ESP8266 device can be programmed to reduce the power output of the PA to fit various application profiles by trading off its range for power consumption. This feature is needed to satisfy the power demand of mobile and wearable electronics. Connection of ESP8266 with Arduino board is shown in Figure 117.
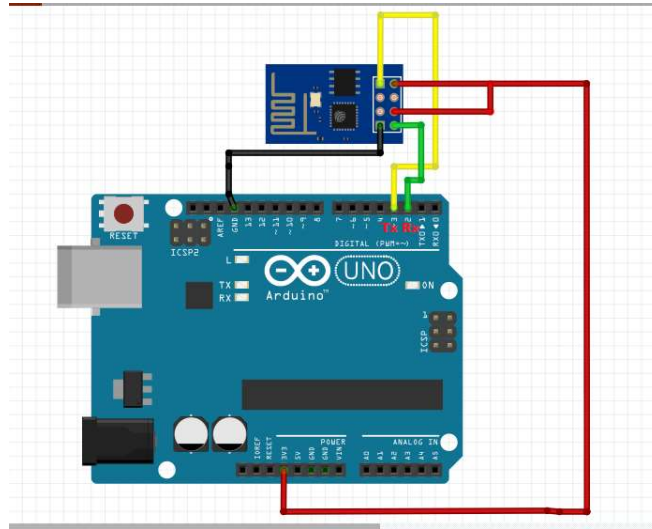
Figure 113: ESP8266 Connection with Arduino Board (Myelectronicslab, 2016)

D. Medical Standard for Transmission of Wireless Signals in Hospitals

Medical practice is using medical electrical and electronics equipment for observation and treatment of patients. Electromagnetic interference (EMI) between wireless transmitters and medical equipment is an issue in healthcare industry. The effects of EMI are unexpected automatic shutdown, automatic restart, and waveform distortion of sensitive medical devices connected to patients. These lead to wrong data presentation and hence patient's prognosis cannot be judged correctly. They may also directly affect the patient's treatment also. Hence these devices and also devices like ESP8266 Wi-Fi Adapter need to have a minimum level of immunity to EMI interference. These are defined by International Electro -technical Commission (IEC) 60601-1-2 standard. Immunity level is the minimum electric field at which the performance of the device degrades (IEC 60601-1-2:2014, 2018).

E. Summary

The connectivity to the cloud using the IoT phenomenon is made possible with the use of a ESP8266 Wi-Fi adapter. The respiration rate data transferred over the cloud can be manipulated in many ways. For example, system/machine/pattern learning, predictive and preventative maintenance, stream analytics, dash boarding, and lastly for reporting purposes. The Wi-Fi adapter is controlled programmatically via Arduino sketches from Arduino libraries, thereby making it a feasible module to be utilised as a means of data transportation device.

Analytics

Analytics is very important for any project to make good decisions. The practice of analytics is to support better decision making by providing the relevant facts to get fruitful and accurate results.

The root of any statistical analysis is probability in mathematics. There are a number of branches in probability that are used according to requirements and need. This project uses "Combination" approach in probability.

Explanation of logic:

The key logic used for integration of all four ultrasonic sensors is **"Combination"** approach in probability, which is a statistical technique in Mathematics.

A combination is a selection of all or part of a set of objects, without regards to the order in which the objects are selected. For example, there is a set of three letters namely A, B, and C. The user is interested in knowing the number of ways 2 letters are selected from that set. Each possible selection would be an example of a combination.

Similarly, the four ultrasonic sensors are considered as objects of a set. All possible combinations of this set should be used to get maximum results. For a set having 4 elements, there are 16 possible combinations or subsets. All these combinations are used in this project.

Arduino Code

The Arduino code used in the project and its explanation are presented in this section.

First, LCD library is added as shown in the code below.

```
1
2 // include the library code:
3
4 #include <Wire.h>
5 #include <LiquidCrystal_I2C.h>
6 LiquidCrystal_I2C lcd(0x27, 20,4);
7
```

The temperature and humidity sensor library is added.

```
7
8 #include "DHT.h" // library for DHT22
9 #define DHTPIN A0
10 #define DHTTYPE DHT22
11 DHT dht(DHTPIN, DHTTYPE);
12
```

Several different data types and variables are used in the script. Some variables are declared and initialised for use in the rest of the code.

```
13
14 // Definition of some variables
15 unsigned long duration_1, duration_2, duration_3, duration_4, st ;
16 unsigned int C_1=0, C_2=0, C_3=0, C_4=0, pause=0, t, x;
17 float s;
18
```

The Arduino pins against each sensor are declared.

```
18
19 // Definition of ultransonic sensors pins
20
21 const int trig_1 = 0; // Trigger Pin of Ultrasonic Sensor 1
22 const int echo_1 = 1; // Echo Pin of Ultrasonic Sensor 1
23
24 const int trig_2 = 2; // Trigger Pin of Ultrasonic Sensor 2
25 const int echo_2 = 3; // Echo Pin of Ultrasonic Sensor 2
26
27 const int trig_3 = 4; // Trigger Pin of Ultrasonic Sensor 3
28 const int echo_3 = 5; // Echo Pin of Ultrasonic Sensor 3
29
30 const int trig_4 = 6; // Trigger Pin of Ultrasonic Sensor 4
31 const int echo_4 = 7; // Echo Pin of Ultrasonic Sensor 4
32
```

In Arduino programming there are two main loops in every code.

> void setup (for pins initialisation)

> void loop (main program)

In void setup, Serial Monitor, LCD, LED, Buzzer, temperature and humidity sensor, and ultrasonic sensor pin modes are initialised and defined. The baud rate for Serial Monitor is 9600, which is declared in the code.

```
32
33  void setup()
34  {
35    Serial.begin(9600);
36    Serial.println(" Please wait");
37    Serial.println(" Results... ");
38
39    lcd.init();                    // initialize the lcd
40    lcd.backlight();
41
42    lcd.clear();
43    lcd.setCursor(0, 0);
44    lcd.print(" Please wait");
45    lcd.setCursor(0, 1);
46    lcd.print(" Results... ");
47
48
49
50    dht.begin();         // initialize the temprature and humidity sensor
51
52
53    pinMode(13, OUTPUT); // pin number 13 for buzzer
54    pinMode(12, OUTPUT); // pin number 12 for led blinking
55
56  // trigger pin of ultrasonic sensor used as an output for transmitting ultrasonic signal
57  //  and echopin as an input for receiving ultrasonic signal
58
59      //1st ultrasonic sensor
60      pinMode(trig_1, OUTPUT);
61      pinMode(echo_1, INPUT);
62
63      //2nd ultrasonic sensor
64      pinMode(trig_2, OUTPUT);
65      pinMode(echo_2, INPUT);
66
67      //3rd ultrasonic sensor
68      pinMode(trig_3, OUTPUT);
69      pinMode(echo_3, INPUT);
70
71    //4th ultrasonic sensor
72      pinMode(trig_4, OUTPUT);
73      pinMode(echo_4, INPUT);
74  }
75
```

In void loop, various computations are done. First, temperature and humidity of environment is calculated.

```
76 void loop()
77 {
78
79   float hum = dht.readHumidity();
80   float tem = dht.readTemperature();
81
```

Then, a pulse of eight cycles is transmitted using all four ultrasonic sensors. For this, initially, "trig" pin is set to low to erase any bug (voltage) in it. Then an ultrasonic signal having eight cycles is transmitted for only ten microseconds. Then, this pin is set to low (zero voltage) again.

For sensor 1, it is shown as

```
83  //*********************** 1st ************************ //
84  // Sending an Ultrasonic signal
85  digitalWrite(trig_1, LOW);
86  delayMicroseconds(2);
87  digitalWrite(trig_1, HIGH);
88  delayMicroseconds(10);
89  digitalWrite(trig_1, LOW);
90
```

This pulse / transmitted signal bounces back, if it hits any obstacle.

In Arduino programming, a (pulseIn) function exists which gives the time in microseconds for the pulse to reach and bounce back again to the source.

By using the time and speed of sound, the distance of the obstacle from the sensor is calculated. The speed of sound is 340m/sec. The distance computation is shown in the following programming part.

```
91  // Receiving of ultrasonic signal
92  duration_1 = pulseIn(echo_1, HIGH, 25000);
93  duration_1 = duration_1*0.034/2;
94
```

The transmitting and receiving of signals for sensor 2 is as below:

```
95    //*************************** 2nd *********************************** //
96
97  // Sending an Ultrasonic signal
98    digitalWrite(trig_2, LOW);
99    delayMicroseconds(2);
100   digitalWrite(trig_2, HIGH);
101   delayMicroseconds(10);
102   digitalWrite(trig_2, LOW);
103
104   // Receiving of ultrasonic signal
105   duration_2 = pulseIn(echo_2, HIGH, 25000);
106   duration_2 = duration_2*0.034/2;
107
```

The transmitting and receiving of signals for sensor 3 is as below:

```
108 //*************************** 3rd *********************************** //
109
110 // Sending an Ultrasonic signal
111   digitalWrite(trig_3, LOW);
112   delayMicroseconds(2);
113   digitalWrite(trig_3, HIGH);
114   delayMicroseconds(10);
115   digitalWrite(trig_3, LOW);
116
117   // Receiving of ultrasonic signal
118   duration_3 = pulseIn(echo_3, HIGH, 25000);
119   duration_3 = duration_3*0.034/2;
120
```

Similarly, the transmitting and receiving of signals for sensor 4 is as below:

```
121   //*************************** 4th *********************************** //
122
123 // Sending an Ultrasonic signal
124   digitalWrite(trig_4, LOW);
125   delayMicroseconds(2);
126   digitalWrite(trig_4, HIGH);
127   delayMicroseconds(10);
128   digitalWrite(trig_4, LOW);
129
130   // Receiving of ultrasonic signal
131   duration_4 = pulseIn(echo_4, HIGH, 25000);
132   duration_4 = duration_4*0.034/2;
133
```

When ultrasonic signal bounces back, it produces ripple in the desired range (10 cm to 50 cm). So this should be counted and LED should blink. Depicted as per the following:

```
137  // Checking of desired conditions to meet the results
138      if ( duration_1 > 10 && duration_1 < 30 )
139          { C_1 = C_1 + 1;
140          digitalWrite(12, HIGH);
141          }
142
143      if ( duration_2 > 10 && duration_2 < 30 )
144          { C_2 = C_2 + 1;
145          digitalWrite(12, HIGH);
146          }
147
148      if ( duration_3 > 10 && duration_3 < 30 )
149          { C_3 = C_3 + 1;
150          digitalWrite(12, HIGH);
151          }
152
153      if ( duration_4 > 10 && duration_4 < 30 )
154          { C_4 = C_4 + 1;
155          digitalWrite(12, HIGH);
156          }
157
```

If no detection occurs by any of the four sensors till 10 seconds, then it will be considered as pause. For pause detection, the buzzer should go ON. This behaviour is represented in the code below:

```
int k = (duration_1==0 && duration_2==0 && duration_3==0 && duration_4==0);
/* check that if all the sensors have no output means equal to 1 the it shows that
no ripple exist and a pause is occur*/
if(k==1)
    {
      pause++;
      digitalWrite(12, LOW);
    }
```

When Arduino board is switched ON or RESET, it will consume ten seconds for data computation and results visualisation. This part is of the following:

```
170     st = millis();
171 st = st/1000;
172 s = st /10;
173 if ( s >= 1){
```

After 10 seconds, the values of temperature and humidity will be shown in the Serial Monitor. If no computation is done due to sensor non-availability or any other problem in sensor, it will show as "Failed to read from DHT11".

```
174  //************************** temperature and humidity **************************
175
176  if (isnan(tem) || isnan(hum))
177    {
178      Serial.println("Failed to read from Dht11");
179    }
180
181    else {
182
183  Serial.println("Temp: " + String(tem)      );
184  Serial.println("Humdity: " + String(hum));
185
186    }
```

Then, if pause occurs for less than 10 secs and greater than 0 sec, then it will show as "NOR" = Normal in both the LCD and Serial Monitor.

```
188 //************************** Pause visualization **************************//
189              if(pause > 0 && pause < 10) {
190
191              lcd.setCursor(0, 0);
192
193                Serial.println("Pause:NOR");
194                  lcd.print("Pause: NOR          ");
195                      }
```

If pause occurs for greater than 10 secs, then it is shown as "ABNOR" = Abnormal followed by the number of seconds within brackets on both LCD and Serial Monitor. The buzzer also goes ON.

```
197              else if (pause > 10 && k == 1)
198                {
199                  lcd.setCursor(0, 0);
200                    Serial.println("  Pause:ABNOR( " + String(pause) + ")");
201                    lcd.print("Pause:ABNOR(" + String(pause) +")         ");
202                    digitalWrite(13,HIGH);
203                }
```

Again, when pause becomes normal, the buzzer goes OFF.

```
207              if ( pause > 0 && k == 0)
208                {
209                    pause = 0;
210                    digitalWrite(13,LOW);
211                }
212
```

Let us suppose that a minute or 60 seconds has elapsed. The ripple status should be reviewed. a variable "t" is used for elapsed time measurements.

If elapsed time is 60 seconds, then a function named "myfun" will be called for ripple status estimation.

```
215  // check wether the time elapsed is 60 second or not
216  x = millis();
217  x = x/1000;
218  t= x % 60 ;
219
220    if(t==0)
221  {
222    myfun(C_1, C_2, C_3, C_4); // funtion calling
223  }
224
```

In "myfun" function, all possible combinations of the four ultrasonic sensors are used according to combinations in probabilistic statistical approach.

1st Combination:

```
234  // if no detection is occured by any sensor
235  if(var_1==0 && var_2==0 && var_3==0 && var_4==0)
236  {
237    rip = 0;
238  }
---
```

2nd Combination:

```
240    // if detection is by only sensor 1
241  else if(var_1 > 0 && var_2==0 && var_3==0 && var_4==0)
242  {
243    rip = var_1;
244  }
```

3rd Combination:

```
246    // if detection is by only sensor 2
247    else if(var_1 == 0 && var_2 > 0 && var_3==0 && var_4==0)
248  {
249    rip = var_2;
250  }
```

4th Combination:

```
252   // if detection is by only sensor 3
253   else if(var_1 == 0 && var_2==0 && var_3 > 0 && var_4==0)
254   {
255     rip = var_3;
256   }
---
```

5th Combination:

```
258   // if detection is by only sensor 4
259   else if(var_1 == 0 && var_2 == 0 && var_3 == 0 && var_4 > 0)
260   {
261     rip = var_4;
262   }
263
```

6th Combination:

```
264   // if detection is by sensor 1 & 2
265   else if(var_1 > 0 && var_2 > 0 && var_3 == 0 && var_4 == 0)
266   {
267     rip = (var_1 + var_2)/2;
268   }
269
```

7th Combination:

```
270   // if detection is by sensor 1 & 3
271   else if(var_1 > 0 && var_2 == 0 && var_3 > 0 && var_4 == 0)
272   {
273     rip = (var_1 + var_3)/2;
274   }
```

8th Combination:

```
276   // if detection is by sensor 1 & 4
277   else if(var_1 > 0 && var_2 == 0 && var_3 == 0 && var_4 > 0)
278   {
279     rip = (var_1 + var_4)/2;
280   }
281
```

9th Combination:

```
282 | // if detection is by sensor 2 & 3
283 | else if(var_1 == 0 && var_2 > 0 && var_3 > 0 && var_4 == 0)
284 | {
285 |    rip = (var_2 + var_3)/2;
286 | }
287 |
```

10th Combination:

```
288 | // if detection is by sensor 2 & 4
289 | else if(var_1 == 0 && var_2 > 0 && var_3 == 0 && var_4 > 0)
290 | {
291 |    rip = (var_2 + var_4)/2;
292 | }
293 |
```

11th Combination:

```
294 | // if detection is by sensor 3 & 4
295 | else if(var_1 == 0 && var_2 == 0 && var_3 > 0 && var_4 > 0)
296 | {
297 |    rip = (var_3 + var_4)/2;
298 | }
299 |
```

12th Combination:

```
300 | // if detection is by sensor 1,2 & 3
301 | else if(var_1 > 0 && var_2 > 0 && var_3 > 0 && var_4 == 0)
302 | {
303 |    rip = (var_1 + var_2 + var_3)/3;
304 | }
```

13th Combination:

```
306 | // if detection is by sensor 1,2 & 4
307 | else if(var_1 > 0 && var_2 > 0 && var_3 == 0 && var_4 > 0)
308 | {
309 |    rip = (var_1 + var_2 + var_4)/3;
310 | }
```

14th Combination:

```
312   // if detection is by sensor 1,3 & 4
313   else if(var_1 > 0 && var_2 == 0 && var_3 > 0 && var_4 > 0)
314   {
315     rip = (var_1 + var_3 + var_4)/3;
316   }
317
```

15th Combination:

```
317
318   // if detection is by sensor 2,3 & 4
319   else if(var_1 == 0 && var_2 > 0 && var_3 > 0 && var_4 > 0)
320   {
321     rip = (var_2 + var_3 + var_4)/3;
322   }
323
```

16th Combination:

```
323
324   // if detection is by all sensors (1,2,3,4)
325   else if(var_1 > 0 && var_2 > 0 && var_3 > 0 && var_4 > 0)
326   {
327     rip = ( var_1 + var_2 + var_3 + var_4)/4;
328   }
```

Now if ripple value is less than 29 or greater than 79, it is considered as abnormal value.
The results are shown as Rip: ABNOR (25) and buzzer will go ON.

```
332   lcd.setCursor(0, 1);
333
334   if(rip < 29 || rip > 79)
335   {
336   Serial.println("Rip:ABNOR ( " + String(rip) + " )   ");
337   lcd.print("Rip:ABNOR (" + String(rip) + ")           ");
338    digitalWrite(13,HIGH);
339   }
```

Contrarily, if ripple value is between 29 and 79, then it is considered as normal value.
The results are shown as Rip: NOR (50).

```
340   else {
341   Serial.println("Rip:NOR ( " + String(rip) + " )      ");
342   lcd.print("Rip:NOR (" + String(rip) + ")            ");
343   }
344
```

After 60 seconds has elapsed, the ripple count value for each sensor will be reset to zero for next ripple count of 60 seconds.

```
344     .
345   C_1 = 0, C_2 = 0, C_3 = 0, C_4 = 0 ;
346 }
```

The Arduino code for pause detection and ripple count of a sine wave is presented above.

MATLAB code for raw data analysis from Sine wave

Raw data from sine wave is analysed using MATLAB code. The MATLAB code and its explanation is given in this appendix.

All recorded data is imported into MATLAB. This recorded data can be of any file format like .txt, .xml, etc. In this case, it is in .txt file format.

```
% Import Raw_Data into matlab
x = load('1_min.txt');
```

The main task here is data analysis. There are different approaches for data analysis. Each approach has its own limitations and conditions to apply to a data set.

A self-designed filter is used to meet desired objectives and goal.

The following MATLAB code shows how to extract the abnormal pause from recorded data.

```
% **** Abnormal Pause Status ******

a_pause = x; % raw_data stored into another variable

d=0;
% a designed filter to extract abnormal pause from the raw data
for i =1:length(a_pause)
if( a_pause(i)== 0);
    d=d+1;
    if(d>=10)
        for j = i-9:1:i
            a_pause(j)=1;
        end
    end
else
    d=0;
    a_pause(i)=0;

end
end
```

For abnormal Ripple count extraction, the following filter / MATLAB code is used.

```
% ***** Abnormal Ripple Count ****

 a_ripple = x; % raw_data stored into another variable

 % a designed filter to extract abnormal ripple_count
 % past sixty from the raw data

for i =1:length(x)
 if((x(i) < 29 && x(i) > 1) || x(i) >79);
   % do nothing
 else
     a_ripple(i)=0;
  end
 end
```

A filter is designed similarly for normal Ripple count according to predefined parameters. This is shown in the following line of codes.

```
% **** Normal Ripple count *****

 n_ripple = x; % raw_data stored into another variable

 % a designed filter to extract normal ripple_count
 % per past sixty seconds from the raw data

for i =1:length(x)
 if(x(i) > 29 && x(i) < 79);
   % do nothing
 else
     n_ripple(i)=0;
  end
 end
```

At the end, the results are shown with the following line of MATLAB code.

```matlab
figure, bar(x,'b')
hold on
bar(a_pause,'r')
bar(a_ripple,'g')
bar(n_ripple,'m')

title('1-Minute Data Analysis');
legend('','Abnormal Pause','Abnormal Ripple','Normal Ripple');
xlabel('Number of Samples');
ylabel('Number of Ripples');
```

To calculate the length of this calculated data magnitude, the following code is used.

```matlab
num_bins = length(x_mag);
```

All the calculated data results are shown to the user by using the following line of codes.

```matlab
subplot(221)
bar(x,'g')
xlabel('Number of Samples');
ylabel('Number of Ripples');
title('( 1-Min) Raw Data in time domain')
```

```matlab
subplot(224)
% normalized frequency calculation
bar([0:1/(num_bins/2 -1):1],x_mag(1:num_bins/2),'g')
xlabel('Normalized frequency (\pi rads/samples)')
ylabel('Magnitude');
title('Magnitude of fft')
```

NodeMcu (ESP-12)

NodeMcu ESP8266 is a firmware based open source development board. It is an open source IoT platform. The firmware runs on ESP8266 WIFI chip and hardware which is based on the ESP-12 module. It is basically a SoC (System on Chip) with an integrated circuit that integrates all components of a computer or other electronic systems (Shakunthala et al. 2018).

NodeMcu ESP8266 is used for IoT (Internet of Things) projects like Home Automation, Innovative School and College Projects.

Interfacing Ultrasonic Sensor with NodeMcu

The NodeMcu (12-E) is shown in the Figure.118.
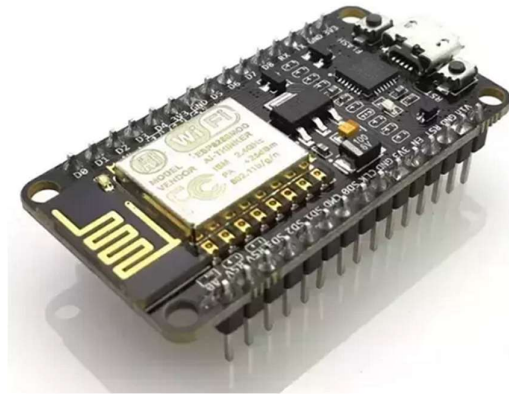
Figure 114: NODEMCU 12-E (ESP8266 MODULE)

The Ultrasonic sensor is shown in the following Figure 119.

Figure 115: Ultrasonic Sensor

There are Four Pins on the ultrasonic sensor. They are:

- Vcc (3.3V to 5V supply)
- Gnd (Ground)
- Trig (Trigger)
- Echo (Receive)

Connection

- Ultrasonic Sensor have four pins (GND, VCC, TRIG, and ECHO).

- Connect VCC pin of sensor with Positive lead of 5V DC power supply.
- Connect GND pin of sensor with Negative lead of 5V DC power supply
- Interface Trig pin of sensor to 6th digital pin (D6) of NodeMcu
- Interface Echo pin of sensor to the 7th digital pin (D7) of NodeMcu

Connection Diagram

Connection diagram of Ultrasonic sensor with NodeMCU is shown in Figure 120.
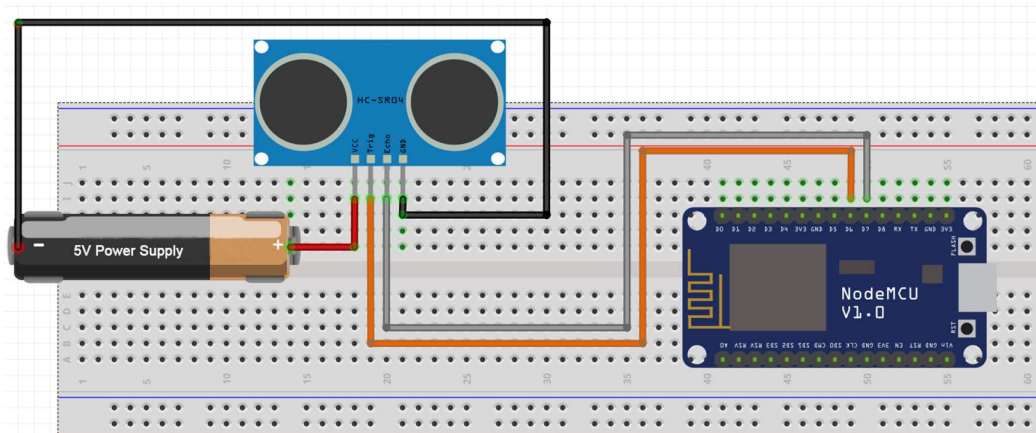
Figure 116: Interfacing of Ultrasonic Sensor with NODEMCU

APPENDIX N CLOUD – THINKSPEAK IOT ANALYTICS PLATFORM

ThingSpeak is an IoT analytics platform. It provides services of data aggregation, data analytics using MATLAB and data visualisation in cloud with free of cost.

ThingSpeak Channel

ThingSpeak allows a user to create a Channel like YouTube or Television channel. This channel can be public or private depending upon user desire or requirements. Each channel has a particular "Channel ID" and its own specific Write and Read API keys, which are used to send or receive data from ThingSpeak. When a channel has been created, a user can clear its fields multiple times regardless of creating multiple channels.

ThingSpeak Channel Fields

Each channel contains eight fields. A user wants to transmit three sensors outputs to ThingSpeak simultaneously, say, temperature, humidity and air pressure. Three fields will be used for this requirement and each will have one output.

ThingSpeak Analysis and Visualisation

After data accumulation, analysis can be performed using this data in cloud. For data analysis MATLAB coding will be used. During MATLAB analysis, a user must code that which channel and fields are going to be used.

Accumulated data can be visualised using different coding options available in MATLAB.

The Arduino code and its explanation are of the following.

NodeMcu is used to transmit data to ThingSpeak. NodeMcu connects an active wireless network for data transmission to ThingSpeak Channel. To fulfil this requirement, a user can use its own WIFI connection network.

- As data transmission is done using ESP8266 chip available on NodeMcu. So, for this purpose in NodeMcu code, first ESP8266 library is added.
- As the transmission also need WIFI connection. So, for this requirement WIFI client library is added.
- As data is transmitted to ThingSpeak Channel, therefore ThingSpeak library is added in NodeMcu code.

```
// nodemcu : send data to thingspeak

#include <ESP8266WiFi.h>;

#include <WiFiClient.h>;

#include <ThingSpeak.h>;
```

The following lines of code are very important in any NodeMcu code. Here a user has to write its own wireless connections specifications. SSID means wireless network name. Password means Secrets characters and numbers which prove authentication and gives access to connect wireless connection.

```
const char* ssid = "wifi"; // your Network SSID

const char* password = "95917301"; // Your Password

WiFiClient client;
```

The Next important step is to enter the ThingSpeak Channel number and read, write API keys. The following lines of code contain the ThingSpeak Channel number and write API key. As here data is transmitted to ThingSpeak Channel.

177

```
unsigned long myChannelNumber  =   970452; // Your Channel Numnber (wothout Brackets)

const char * myWriteAPIKey = "DGCMRTLTCJX3RV26"; // Channel Write API Key
```

There are some variables declarations that used for saving information.

```
// Definition of some variables
int y;
unsigned long duration_1, x ;
unsigned int C_1=0, pause=0,t;
float s;
```

This is Ultrasonic sensor pins declaration.

```
// Definition of ultransonic sensors pins

const int trig_1 = D6; // Trigger Pin of Ultrasonic Sensor 1
const int echo_1 = D7; // Echo Pin of Ultrasonic Sensor 1
```

The following lines of codes shows the wireless connection start-up.

```
void setup()

{
  Serial.begin(115200);

  delay(10);

    // Connect to Wifi Network

    WiFi.begin (ssid, password);

      while (WiFi.status() != WL_CONNECTED)
      {
      delay(500);
      Serial.print(".");
       }
      Serial.println (" ");
      Serial.println ("WiFi Connected!");
```

The following lines states that ThingSpeak starts as client.

```
// ThingSpeak Connetion startup
  ThingSpeak.begin(client);
```

The NodeMcu pins declaration, which are used for ultrasonic sensor.

```
// NodeMcu Pins Declaration
  pinMode(LED_BUILTIN, OUTPUT); // Builtin led blinks incase of detection

  //1st ultrasonic sensor
    pinMode(trig_1, OUTPUT);
    pinMode(echo_1, INPUT);
}
```

The ultrasonic sensor starts work by emittance of ultrasonic rays and receives upon bouncing back.

```
// Sending an Ultrasonic signal
digitalWrite(trig_1, LOW);
delayMicroseconds(2);
digitalWrite(trig_1, HIGH);
delayMicroseconds(10);
digitalWrite(trig_1, LOW);

// Receiving of ultrasonic signal
duration_1 = pulseIn(echo_1, HIGH, 25000);
duration_1 = duration_1*0.034/2;
```

If the ripples are present between 10 cm to 50 cm (distance from ultrasonic sensor), then detection occurs and ripples are counted, otherwise it is considered as no ripple is present.

```
// Checking of desired conditions to meet the results
  if (duration_1 > 10 && duration_1 < 40 )
    { C_1++;
    digitalWrite(LED_BUILTIN, HIGH);
    }
```

As data transmitted to ThingSpeak after every 15 seconds. The time is checked by using the following lines of codes.

```
// check wether the time elapsed is 15 second or not
x = millis();
x = x/1000;
t= x % 15;
```

If time is elapsed fifteen seconds, then the data transmit to ThingSpeak Channel.

```
y = C_1;

ThingSpeak.setField(1, y);              // send value to thingspeak

ThingSpeak.writeFields(myChannelNumber, myWriteAPIKey);
```

The ThingSpeak MATLAB code and its explanation is given below.

First, transmitted data set is imported into ThingSpeak MATLAB environment. There are several ways to import data into ThingSpeak analysis environment like previous 100 entries, previous 5-minute data, specific dates interval data, etc. But each has its own pros and cons.

Pause Analysis

Here the following specific features having data is imported in ThingSpeak analysis environment.

✓ Channel ID: 936270
✓ Filed: 1
✓ Previous number of points / entries: 50

Name

Pause Analysis

MATLAB Code

```
1 %% Importing ThingSpeak data into Matlab |
2
3 [sensor_data,timestamps]=thingSpeakRead(936270,'Fields',1,'NumPoints',50);
4
```

For Pause analysis time is seperated using the following code:

```
11 %% Brief Analysis
12
13 tm = minute(timestamps);
14 ts = second(timestamps);
15 pause = zeros(size(ts));
16
```

The Pause analysis is done using the following lines of code. The time interval having no ripple detection till 15 seconds or more is considered as Pause here.

```
18
19 for i = 1:length(tm)-1
20
21     if tm(i) == tm(i+1)
22         t = ts(i+1) - ts(i);
23      else
24         t = ( 60 - ts(i)) + ts(i+1);
25     end
26
27 %     % Abnormal Pause Analysis
28
29     if (t > 15)
30         pause(i) = 0.75;
31     end
32
33 end
34
```

As pause is time interval having no ripples but to visualise it to user a value 0.75 is used (0.75 value of amplitude shows pause). The following lines of codes are used to visualise the pause detection to user.

```
35          % Data Visulaization
36
37              bar(timestamps, pause,'b');
38              legend('Abnormal Pause')
39
40          xlabel('Time');
41          ylabel('Sensor Ripples');
42          title('Pause Analysis');
```

Ripples Analysis:

For ripple analysis same data will be used as in pause analysis.

Name

Ripple Analysis

MATLAB Code

```
1 clc, clear all, warning off;
2
3 %% Importing ThingSpeak data into Matlab
4
5 [sensor_data,timestamps]=thingSpeakRead(936270,'Fields',1,'NumPoints',50);
6
```

The following lines of code separate the time from timestamps variable that consist of specific date and time, when data was accumulated to ThingSpeak.

```
12
13 %% time filteration
14
15 tm = minute(timestamps);
16 ts = second(timestamps);
17 d = zeros(size(sensor_data));
```

The ripple detected over past 60 seconds are counted using the following lines of code.

```
18
19 % Ripple Count over past 60 seconds
20
21 for i = 1:length(tm)
22
23     % Ripple Count
24     if ( rem(i,4) == 0 )
25         rip_count = sensor_data(i) + sensor_data(i-1) + sensor_data(i-2) + sensor_data(i-3);
26         d(i) = rip_count;
27     end
28
29 end
```

After ripple count over past sixty seconds, ripple analysis is performed either ripple count is normal or abnormal according to predefined conditions. This is done using the following lines of code.

```
30
31 %% Ripple Analysis
32
33         % Normal
34
35 n_ripple = d;
36    for i = 1:length(d)
37         if (d(i) > 29 && d(i) < 79 )
38
39            else
40              n_ripple(i) = 0;
41         end
42    end
43
44         % Abnormal
45
46    a_ripple = d;
47    for i = 1:length(d)
48         if ((d(i) < 29 && d(i) > 1) || d(i) > 79 )
49
50            else
51             a_ripple(i) = 0;
52         end
53    end
54
```

The ripple count analysis is visualised to user by the following lines of code.

```
55
56          bar(timestamps, a_ripple,'r');
57          hold on
58          bar(timestamps, n_ripple,'g');
59          legend('Abormal Ripple Count','Normal Ripple Count')
60
61      xlabel('Time');
62      ylabel('Ripples');
63      title('Ripples Analysis ');
64
65
```

Things to remember when using ThingSpeak Channel

When a user wants to transmit data to ThingSpeak Channel, the following are taken into consideration:

A user may have to change the following parameters:

- Wireless Connection   (highlighted using black open block
- ThingSpeak Channel ID   (highlighted using Red open block
- Channel Field ID   (highlighted using Red open block)

{Choose the desired Channel filed ID, where transmitted data will be saved}

```
const char* ssid = "wifi"; // your Network SSID
const char* password = "95917301"; // Your Password

WiFiClient client;

unsigned long myChannelNumber =   971899; // Your Channel Numnber (wothout Brackets)

const char * myWriteAPIKey = "DOZVCWDNK3T9B780"; // Channel Write API Key


  ThingSpeak.setField(1, y);          // send value to thingspeak
```

Similarly, in ThingSpeak analysis, a user will have to change the Channel ID, Read API key, Field ID and number of samples / entries (or custom range data) according to MATLAB Code.

```
%% Importing ThingSpeak data into Matlab
;tamps]=thingSpeakRead(971899,'Fields',1,'NumPoints',60,'ReadKey','I0AXT8UHLIL7AB42');
```

Channel ID
Channel Field ID Number
number of entries
Channel Read API key

For ripple detection, desired ripple focus area (distance between the object and the sensor) has been chosen, but a user will have to change it accordingly to the desired range.

For example: your focused area (center point) of an object is far way, for example, 50 cm from ultrasonic sensor, then you will have to change the following the lines of codes.

```
// Checking of desired conditions to meet the results

    if (duration_1 > 10 && duration_1 < 40 )
```

[I have used the ripple detection range 10 cm to 40 cm from base point of ultrasonic sensor placement]

If you want to make it as 10 cm to 50 cm, you will have to change it accordingly as in the following figure

```
// Checking of desired conditions to meet the results

    if (duration_1 > 10 && duration_1 < 50 )
```

Ultrasound based Respiration Rate Monitoring System – IoMT Practical setup is shown in Figure 121 and Figure 122.
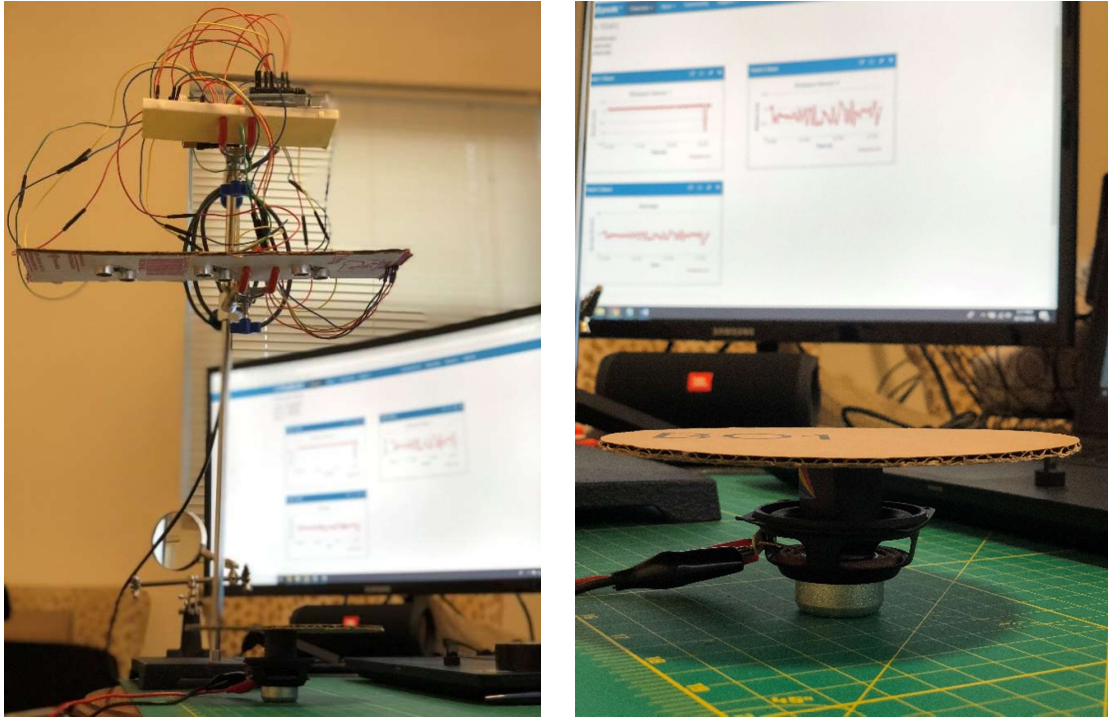

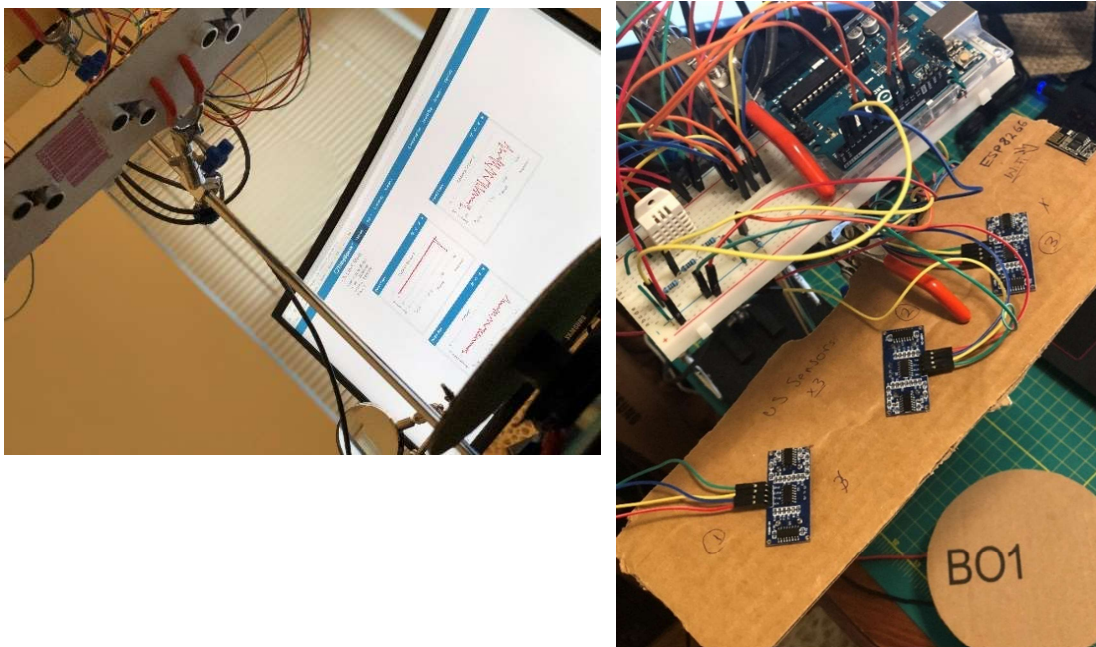Figure 117: US-Based Respiration Rate Monitoring System – IoMT Practical Setup

Figure 118: IoMT Practical Setup

$$Vout = Vref * (1 + \frac{R2}{R1}) \qquad\qquad (7)$$

EQUATION 10: V_{OUT} CALCULATION

where *Vref* = 1.23V.

As *Vout* = 10V, the value of R_2 must be 7.1 kΩ. The rest of the components are chosen with the following characteristic of the circuit: V_{out} = 10V, $V_{in(max)}$ = 12V and I_{LOAD} = 2A (maximum current pulled by the sensor corresponding to the moment when the ultrasound pulses are transmitted).

L_1 = 15 µH

C_{out} = 330 µF/25V

C_{FF} = 330 µF/25V

C_{in} = 680 µF

D_1, Schottky diode 1N5824

Practical Calculation and Results:

Respiration Actual as given in equation 9 is calculated as:

$$rA = f * 60 \tag{9}$$

EQUATION 11: RESPIRATION ACTUAL

$$rA = 0.397 * 60$$

$$rA = 23.82 \text{ cycle/min}$$

Period is calculated from equation 10 as:

$$T = X2 - X1 \tag{10}$$

EQUATION 12: PERIOD CALCULATION

$$T = 29.95 - 27.45$$

$$T = 2.5 \text{ seconds}$$

Frequency is calculated from equation 11 as:

$$f = 1/T \tag{11}$$

EQUATION 13: FREQUENCY CALCULATION

$$f = 1/ 2.5$$

$$f = 0.4 \text{ Hz}$$

Respiration calculated is computed as in equation 12

$$rC = f * 60 \tag{12}$$

EQUATION 14: CALCULATED RESPIRATION

$$rC = 0.4 * 60$$

$$rC = 24 \text{ cycles/min}$$